Supplementary Notes

A community computational challenge to predict the activity of pairs of compounds

Mukesh Bansal[1,2,18], Jichen Yang[3,18], Charles Karan[4,18], Michael P Menden[5], James C Costello[6,61], Hao Tang[3], Guanghua Xiao[3], Yajuan Li[7], Jeffrey Allen[3,7], Rui Zhong[3], Beibei Chen[3], Minsoo Kim[3,8], Tao Wang[3], Laura M Heiser[9], Ronald Realubit[4], Michela Mattioli[10], Mariano J Alvarez[1,2], Yao Shen[1,2], NCI-DREAM community[11], Daniel Gallahan[12], Dinah Singer[12], Julio Saez-Rodriguez[5], Yang Xie[3,8], Gustavo Stolovitzky[13] & Andrea Califano[1,2,14–17]

[1]Department of Systems Biology, Columbia University, New York, New York, USA. [2]Center for Computational Biology and Bioinformatics, Columbia University, New York, New York, USA. [3]Quantitative Biomedical Research Center, Department of Clinical Sciences, University of Texas Southwestern Medical Center, Dallas, Texas, USA. [4]Columbia Genome Center, High Throughput Screening Facility, Columbia University, New York, New York, USA. [5]European Molecular Biology Laboratory, European Bioinformatics Institute, UK. Wellcome Trust Genome Campus, Hinxton, Cambridge, UK. [6]Howard Hughes Medical Institute, Department of Biomedical Engineering and Center of Synthetic Biology, Boston University, Boston, Massachusetts, USA. [7]Department of Immunology, University of Texas, Texas, USA. [8]Simmons Comprehensive Cancer Center, University of Texas Southwestern Medical Center, Texas, USA. [9]Department of Biomedical Engineering, Oregon Health and Science University, Portland, Oregon, USA. [10]Center for Genomic Science of IIT@SEMM, Fondazione Istituto Italiano di Tecnologia (IIT), Milan, Italy. [11]Full lists of members and affiliations appear below.. [12]Division of Cancer Biology, National Cancer Institute, Bethesda, Maryland, USA. [13]IBM Computational Biology Center, IBM, T.J. Watson Research Center, Yorktown Heights, New York, USA. [14]Department of Biomedical Informatics, Columbia University, New York, New York, USA. [15]Department of Biochemistry and Molecular Biophysics, Columbia University, New York, New York, USA. [16]Institute for Cancer Genetics, Columbia University, New York, New York, USA. [17]Herbert Irving Comprehensive Cancer Center, Columbia University, New York, New York, USA. [18]These authors contributed equally to the work

Table of Contents: Supplementary Note

Nature Biotechnology doi:10.1038/nbt.3052

Supplementary Note 1: Scoring using probabilistic c-index

We used the concordance index (c-index) that computes the proportion of concordance between the predicted and observed ranks of compound-pairs to quantify the quality of ranking of all predictions. Let us first rank the 91 compound pairs according to the average over experimental replicates of the experimentally determined *EOB*, from the most synergistic to the most antagonistic. Denote the rank of compound pair i (with $1 \leq i \leq 91$) as o_i and the rank predicted for that pair by a given team as p_i. For example if compound pair k was observed to be the most synergistic, then $o_k = 1$. Note that if $i \neq j$ then $o_i \neq o_j$ and $p_i \neq p_j$. For $i \neq j$, we define a score s_{ij} as follows

$$s_{ij} = \begin{cases} 1, & if\ (o_i > o_j\ \&\ p_i > p_j \text{ or } o_i < o_j\ \&\ p_i < p_j) \\ 0, & if\ (o_i > o_j\ \&\ p_i < p_j \text{ or } o_i < o_j\ \&\ p_i > p_j) \end{cases}$$

The concordance index is defined as

$$c\text{-}index = \frac{2}{91 \times 90} \sum_{\substack{i=1\ldots90 \\ j=i+1\ldots91}} s_{ij}$$

Quantification using c-index assumes that there is no ambiguity in the observed rankings, and therefore both the prize and penalty for concordance and discordance is extreme. Due to experimental noise in the observation of synergy between any compound pair, there is an uncertainty in ranking compound pairs from most synergistic to most antagonistic. To incorporate uncertainties in the observed ranking we modified the c-index so that we have a reliable scoring of all participants. To compute the probabilistic c-index (PC-index) we calculated, for all $i \neq j$, a score $sp_{ij}\ as$

$$\mathrm{sp}_{ij} = \begin{cases} \frac{1}{2} + \frac{1}{2}\,\mathrm{erf}\left(\frac{EOB_i - EOB_j}{\sqrt{sem_{EOB_i}^2 + sem_{EOB_j}^2}} \right) & \text{if } p_i < p_j \\ \frac{1}{2} - \frac{1}{2}\,\mathrm{erf}\left(\frac{EOB_i - EOB_j}{\sqrt{sem_{EOB_i}^2 + sem_{EOB_j}^2}} \right) & \text{if } p_i > p_j \end{cases}$$

where 'erf' is the error function defined as $\mathrm{erf}(x) = \frac{2}{\sqrt{\pi}} \int_0^x e^{-t^2}\,\mathrm{d}t$, and we denote by EOB_i the average over experimental replicates of the experimentally determined *EOB* for compound pair *i*, and by sem_{EOB_i} is the standard error of the mean of the *EOB* for compound pair *i*. Suppose compound pair i is on average more synergistic than compound pair j, that is $EOB_i > EOB_j$. Then the argument of the erf function is positive which makes the erf term positive. Therefore, if pair *i* is predicted to be more synergistic than pair *j*, then $p_i < p_j$ and $\mathrm{sp}_{ij} > \frac{1}{2}$. If, however, pair i is predicted to be less synergistic than *j*, then $p_i > p_j$ and $\mathrm{sp}_{ij} < \frac{1}{2}$. The opposite occurs if $EOB_i < EOB_j$. It follows that if the prediction is concordant with the gold standard then the score sp_{ij} returns a value between 0.5 and 1, and conversely if prediction and measurement are dis-concordant then sp_{ij} returns a value between 0 and 0.5. The probabilistic concordance index is thus defined as:

Nature Biotechnology doi:10.1038/nbt.3052

$$PC\text{-}index = \frac{2}{91\times 90} \sum_{\substack{i=1\ldots 90 \\ j=i+1\ldots 91}} sp_{ij}$$

The maximum score for the c-index, when both predicted and observed list of compound pairs are concordant is 1, but due to noise in the data, the maximum PC-index is less than 1 even for the average experimentally measured *EOB*. In this dataset, the maximum PC-index (PC_{max}) is found to be 0.90. The minimum PC-index (PC_{min}) corresponds to a prediction with exactly the opposite order compared to the average experimentally measured *EOB*, and is therefore 0.10. The normalized PC-index is defined as

$$PC\text{-}index_{norm} = \frac{PC\text{-}index - PC_{min}}{PC_{max} - PC_{min}}$$

Supplementary Note 2: NCI-DREAM Drug Synergy Prediction Methods

RANK 1 & 3

Synergy/Antagonism Prediction by Drug Induced Genomic Residual Effect

Jichen Yang[1], Hao Tang[1], Guanghua Xiao[1], Yajuan Li[2], Jeffrey Allen[1], Rui Zhong[1], Beibei Chen[1], Minsoo Kim[1], Tao Wang[1], Yang Xie[1]

1. Quantitative Biomedical Research Center, Department of Clinical Sciences, University of Texas

2. Department of Immunology, University of Texas

Summary Sentence: Drug Induced Genomic Residual Effect (DIGRE) model.

Introduction

Our basic hypothesis is that the combinatorial drug effect for compounds A and B result from the residual genomic changes induced by one of the drugs prior to the application of the second. In another word, if we assume the cells were treated with compounds A and B sequentially, the genomic changes induced by compound A will further contribute to the effect induced by compound B, the one that was applied later.

Methods

DIGRE model contains three major steps (**Figure 1**): (1) comparing the transcriptional changes induced by individual drugs to derive the similarity scores between drug pairs. (2) Estimating the effects of drug induced genomic/transcriptional changes on cell survival based on the similarity scores. (3) Finally estimating a drug combination score.

Nature Biotechnology doi:10.1038/nbt.3052

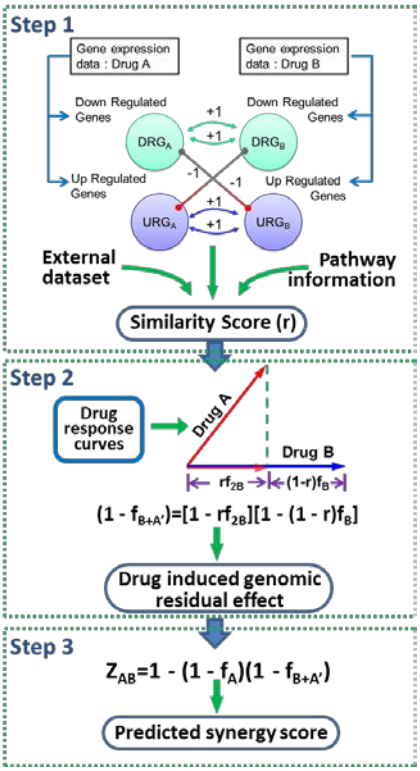

Figure 1: Work flow for DIGRE.

Estimation of similarities between two compounds

The similarity score consists of two components: one is contributed from the overlapping genes between the up-regulated genes (URGs) and down-regulated genes (DRGs), and the other is contributed from the non-overlapping genes.

In component 1 of the analysis, if a gene is up-regulated or down-regulated by both compounds A and B in the same direction, and it is included in the 8 cell growth related KEGG pathways (CGP), then it will contribute one positive point for the similarity score. On the other hand, if a gene is regulated by compound A and compound B in different direction, and belongs to CGP, then it will contribute one negative point for the score. The CGP was built using pathways empirically selected from KEGG pathway database based on our knowledge firstly, and then refined by a small drug combination training dataset [1]. In particular, we selected 12 pathways which were highly related to cell growth. Then we remove one of the 12 pathways each time and merged the remaining to build a CGP with which we applied our approach to the external training dataset. Based on the results, we screened out 8 pathways that contributed mostly to the performance and merged them to build final CGP. The 8 KEGG pathways are: aminoacyl-tRNA biosynthesis, MAPK signaling pathway, NF-kappa B signaling pathway, Cell Cycle, p53 signaling pathway, Apoptosis, TGF-beta signaling pathway, Cancer pathway.

The process to calculate contribution from component 2 includes two steps. The first step is to identify the genes that belong to CGP (i.e. related to cell growth) and are in up-regulated genes for compound A (URG_A) or down-regulated genes for compound A

Nature Biotechnology doi:10.1038/nbt.3052

(DRG_A) but did not contribute to score component 1. The next step is to identify the upstream genes (defined in the next paragraph) of the gene set identified in the previous step. If any upstream genes are differentially-regulated following compound B treatment (URG_B or DRG_B), but were not used to score in component 1, then they will contribute 1 point for the scoring of component 2. The sign of the point is determined by the sign of differential regulation of both genes as well as the direction of the interaction. In the second step, we repeat the same analysis for the genes that belong to CGP and are differentially expressed for compound B but did not contribute to score component 1. Therefore, a positive contribution would be either from in the intersection between: genes in URG_B with genes with positive interaction to URG_A, or genes in DRG_B with genes with positive interaction to DRG_A, or genes in URG_B with genes negative interaction to DRG_A, or genes in DRG_B with genes with negative interaction to URG_A.

The upstream genes used in component 2 analysis were predefined by 32 KEGG global pathways (GP). In particular, we selected KEGG pathways belonging to genetic information processing, environmental information processing, cellular processing, and cancer disease. From this set of selected pathways we removed any pathway with fewer than 10 edges. Finally we merged the remaining 32 KEGG pathways into a global pathway (GP) which included 11642 interactions among 2322 genes.

Finally, we normalized the similarity scores by the number of differentially expressed genes induced by the compound. The similarity score for compound A treatment followed by compound B is:
$r_{B+A'} = contribution\ (component\ 1 + component\ 2)/(URG_B + DRG_B)$,

and the similarity score for compound B treatment followed by compound A is:
$r_{A+B'} = contribution(component\ 1 + component\ 2)/(URG_A + DRG_A)$

Estimation of combinatorial effect based on compounds' similarities
The combinatorial effect of the drug pairs depends on the sequence of compound treatment. In our estimation of induced cell death from compound combination, we used the averaged cell death from both possible sequences of compound treatment. Particularly, we set $f_{B+A'}$ is the percentage of cell death after drug B treatment when cells have genomic/transcriptional changes induced by drug A. Then
$(1 - f_{B+A'}) = (1 - r_{B+A'} f_{2B})[1 - (1 - r_{B+A'}) f_B]$.
where $(1 - r_{B+A'} f_{2B})$ accounts for the contribution from compound B that are similar to compound A. $(1 - r_{B+A'}) f_B$ accounts for the contribution from compound B that are dissimilar to compound A, and assumed to be independent to compound B. The cell death for compound B treatment followed by compound A treatment, $Z_{B+A'}$, is estimated as
$Z_{B+A'} = 1 - (1 - f_A)(1 - f_{B+A'}) = 1 - (1 - f_A)[1 - r_{B+A'} f_{2B}][1 - (1 - r_{B+A'}) f_B]$
Similarly, the induced cell death for compound A treatment followed by compound B treatment, $Z_{A+B'}$, is estimated as
$Z_{A+B'} = 1 - (1 - f_B)[1 - r_{A+B'} f_{2A}][1 - (1 - r_{A+B'}) f_A]$
The final cell death, also defined as synergistic score, is estimated as
$Z = (Z_{B+A'} + Z_{A+B'})/2$.

Nature Biotechnology doi:10.1038/nbt.3052

Analysis of different feature

To better investigate how different factors contribute to the overall prediction, we compared the results from different variations of the model by individually removing one factor at a time. Firstly, we remove the "residual effect" hypothesis, and assume that the similarity scores between drug pairs have monotonic relationship with the drug-drug interaction scores. Specifically, we calculated the similarity score $r_{AB} = (r_{A+B'} + r_{B+A'})/2$ for the drug pair A and B, where $r_{B+A'}$ and $r_{A+B'}$ were calculated using the same formula described above. If we rank the drug pairs based on the decreasing order of the similarity scores for the synergetic effects, i.e. assuming that the pairs with higher similar scores would be more synergistic, the *PC-index* decreased to 0.49. If we ranked the similarity scores in the increasing order, i.e. assuming the synergism was brought by dissimilarity, the result was also much worse than DIGRE. Secondly, we removed the "focus view" or the "global view" from DIGRE, the *PC-indexes* degraded to 0.603 and 0.597, respectively, compared to the full model performance. Performance after removing some of the other features (i.e. Mathematical modelling and dose-response dynamics) could not be tested due to the implicit nature of those in the model.

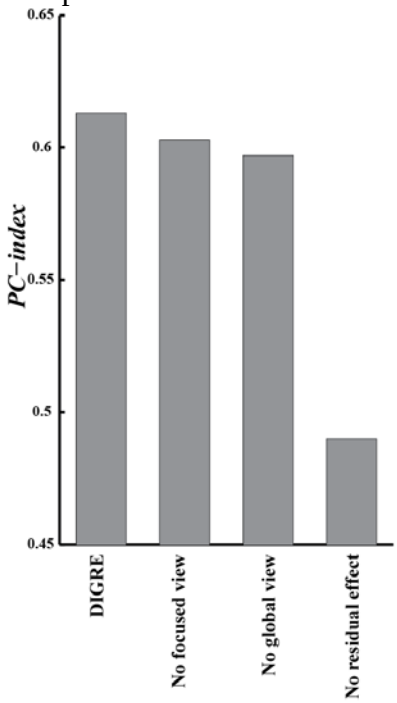

Figure 2: DIGRE's performance after removing some of the features from the method.

Conclusion

We believe that the following factors contributed to the performance of the DIGRE model: (1) It is based on a biologically motivated hypothesis for drug synergistic effects. (2) The relationship between the drug response and genomic profiles changes were explicitly modeled. (3) The information from the dose-response curves were explicitly incorporated in the model. (4) To model the similarity of the genomic profiles between two drugs, only the relevant genes were included (focused view). (5) Pathway and gene-

Nature Biotechnology doi:10.1038/nbt.3052

gene interaction information were incorporated into the model. (6) Existing biological knowledge and external datasets were used to optimize the model.

References

1. Jin G, Zhao H, Zhou X, Wong ST: *An enhanced Petri-net model to predict synergistic effects of pairwise drug combinations from gene microarray data*. Bioinformatics 2011, 27(13):i310-316.

RANK 2

Predicting compound combinations that have a synergistic effect in reducing viability of a DLBCL cell line

Chirayu Pankaj Goswami and Lang Li
Center for Computational Biology and Bioinformatics, IU School of Medicine, Indianapolis IN USA

Summary Sentence: Drug activity synergism prediction is derived by comparing the effect of drug treatment on a subset of genes identified as responsible for drug treatment effect from genomic analysis.

Background for Methodology

In our method, drug activity synergism prediction is derived by comparing the effect of drug treatment on a subset of genes identified as responsible for drug treatment effect from genomic analysis. Gene expression profiles of cells change upon treatment with external compounds. We believe that the most informative 'direct' changes in gene expression profile are brought about immediately after treatment of cells with compounds. We also believe that drug activity in treated samples is produced by change in expression of a particular group of genes, and higher or lower efficacy of drugs can be attributed to change in a common subset of genes specific for higher and lower efficacy drugs. The set of genes which are responsible for higher efficacy of drugs (IC_{20} at 48 hrs) are most meaningful genes to predict drug interactions in our method.

Methods

Data

Gene expression profiling data for DLBCL cell line was downloaded from Dream Consortium website. The data was in form of raw cel files. Data was imported to Partek Genomics Suite software. RMA background correction was performed using Partek GS. We kept samples treated with drugs for least amount of time only (6 hrs) and discarded the rest of the samples. DMSO treated samples were used as control samples (also treated for 6 hrs only).

Nature Biotechnology doi:10.1038/nbt.3052

Identification of core subset of genes responsible for higher efficacy (IC_{20} at 48 hrs) of compounds

To identify the subset of genes we believe is responsible for higher efficacy of drugs, we identified differentially expressed genes for each drug treatment by comparing drug treated samples (IC_{20} at 48 hrs, 6 hrs) with control (DMSO) samples. This was done for all drugs. We combined all the genes differentially expressed with a significant p value (P<=0.05) in each IC_{20} at 48 hrs drug treatment and selected the unique genes from this combined list to create a list of genes specific to low IC_{20} activity. This forms the core gene list. This step is explained in Figure 1.

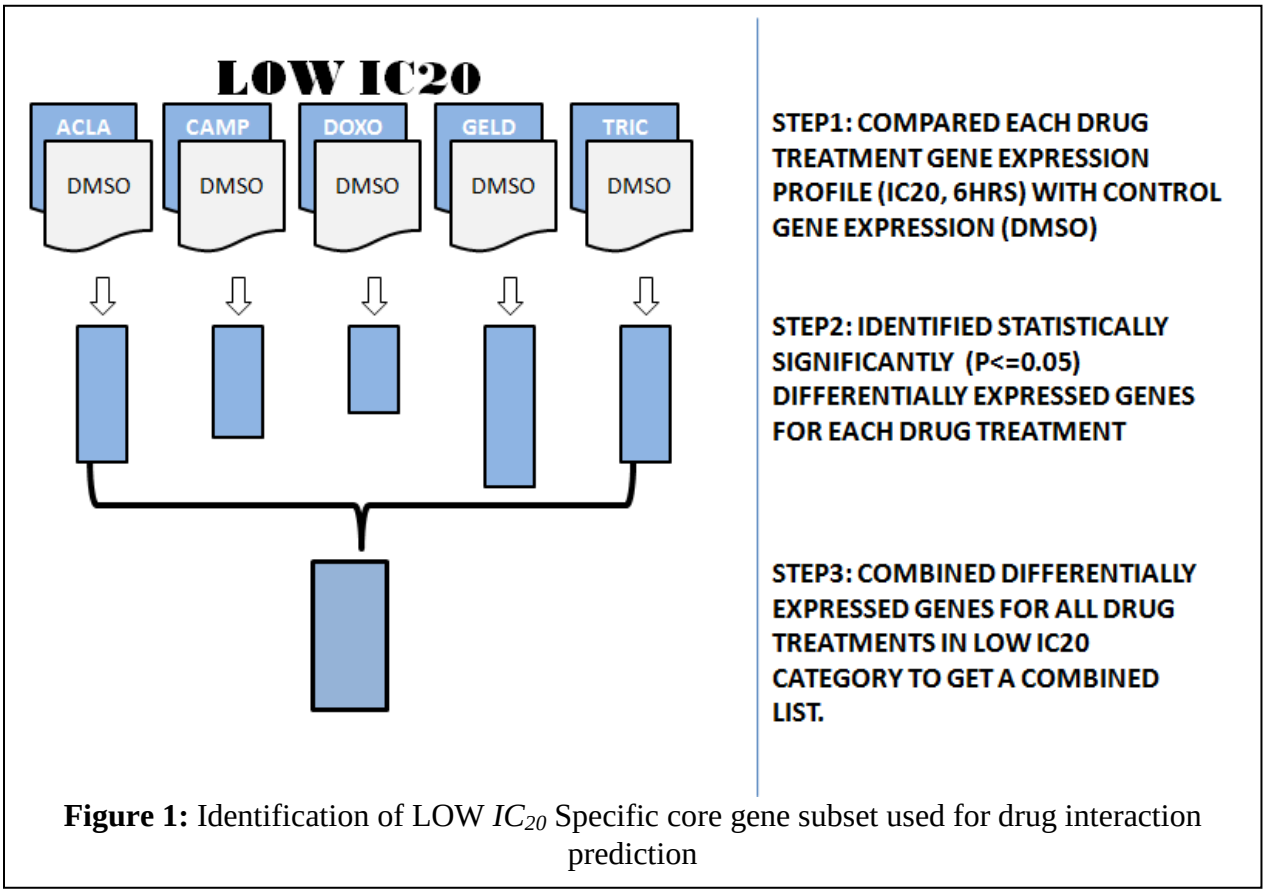

Figure 1: Identification of LOW IC_{20} Specific core gene subset used for drug interaction prediction

Prediction of drug combination synergistic effect using the core subset

We made predictions of synergism of drug combinations using the core gene list in step 1. Within a drug pair, synergistic genes were defined as genes from the core list which were significantly differentially expressed ($p < 0.05$) in both drugs compared to normal controls and were regulated in the same direction (Fold Change). On the other hand, antagonistic genes were identified as genes that were significantly differentially expressed in both drugs but their direction of regulation was opposite. Using the number of synergistic and antagonistic genes per drug combination an Interaction score was calculated using the following formula

Nature Biotechnology doi:10.1038/nbt.3052

$$\text{Interaction Score} = \frac{n_{syn} - n_{ant}}{n_{core}}$$

where,
n_{syn} = # of genes from the core list that were significantly differentially expressed for both drugs and were regulated in the same direction
n_{ant} = # of genes from the core list that were significantly differentially expressed for both drugs and were regulated in the opposite direction
n_{core} = total number of genes in the core subset

Results
Interaction Score was calculated for each drug pair, and ranks were assigned to drug pairs using this score. Scores ranged from +10.62 (most synergistic) to -0.85 (most antagonistic). For drug combinations having same score, higher ranking was given to the drug pair that has greater number of genes affected by the drugs in combination.

RANK 4

A differential expression analysis strategy for predicting synergistic effects of drug combinations

Summary Sentence: Apply differential expression analysis and correlation analysis to ranking synergistic and antagonistic effect of drug combinations.

Introduction
With the development of biotechnology, drug combinatorial therapy has become a promising strategy for treating complex diseases in recent years. There has been a category of methods to predict effective drug combinations from molecular or/and pharmacological data [1-4]. The current study belongs to this category. Traditionally, the common strategy for predicting synergistic affects from gene microarray data [5, 6] is to compare the drug effects derived from microarray data treated by a drug combination with those from the microarray data treated by two drugs separately. However, it becomes a more challenging task due to the absence of gene expression data for drug combinations in current study. In particular, we will only use the baseline expression profile and those expression profiles treated by each individual drug/compound with limited number of conditions and replicates to predict synergistic effects of drug/compound combinations.
The basic assumption of our method is that expression properties of differential expressed genes obtained by comparing the expression profile of a cell line before and after treatment with a drug reflect the effect of this drug to this cell line. We further assume that the correlation of expression profiles of differential expressed gene set of two drugs will imply the synergistic and antagonistic effect of these two drugs.

Methods

Nature Biotechnology doi:10.1038/nbt.3052

We collected the gene expression profiles of Ly3 cell lines treated with each of the 14 DMSO diluted compounds at concentration IC_{20} at three different time points, and the profiles at the same time points after administration of DMSO vehicle only. We found that the gene expression profiles of multiple replicates are highly correlated with each other (r>0.99), so we used the average expression profiles of multiple replicates (after normalization) as the unified profile of each drug. We employed the following procedure to achieve the final goal (Figure 1):

Step 1 We regarded the gene expression profile after administration of DMSO vehicle only as the baseline profile and used it to compute the differential expression score (the absolute value of difference between case and control) at 3 different time points respectively for each drug.

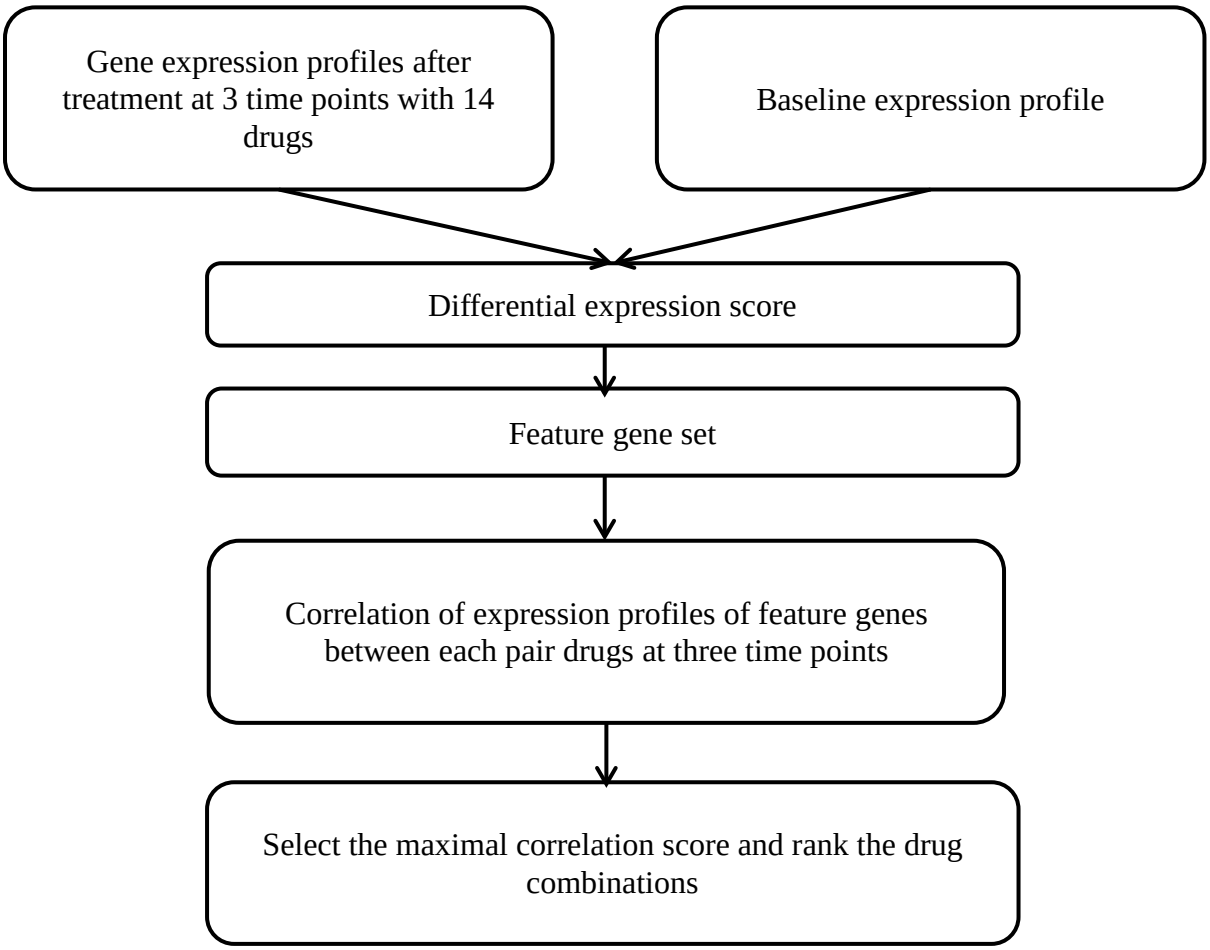

Figure 1: The flowchart of our method.

Step 2 At each time point, we selected the top 100 genes with the highest differential expression score for each drug and combine these genes of all drugs together as feature genes. In total, we obtained 1140, 1148, 1005 genes for the three time points respectively.

Step 3 We calculated the pairwise Pearson correlation coefficient of expression profiles between any two drugs. We then selected the one with the maximal absolute value among

Nature Biotechnology doi:10.1038/nbt.3052

the three correlation values corresponding to the three time points as the synergistic score for each pair of drugs and ranked the drug pairs according to this score.
Step 4 We calculated the distribution of synergistic scores and select the score closest to the dramatic change point (as shown by the red line in Figure 2) as the position indicating the additive effect of drug combination.

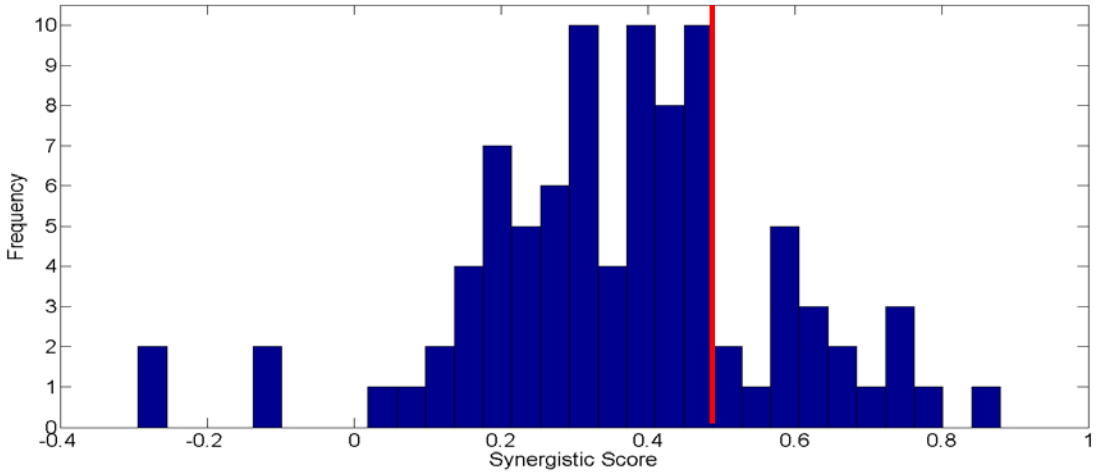

Figure 2: Histogram of the synergistic scores of 91 drug combinations. The red line indicates the dramatic change point which is used to select the drug combination as demarcation for additive effects.

Conclusion/Discussion
Predicting the synergistic effect of drug/compound combinations from gene expression profiles is a challenging task. In the current study, the absence of the treated expression profiles of drug combinations makes it more difficult. Here we tried to define the affected gene set of all drugs using differential expression analysis and calculate the correlations of those affected genes to predict the synergistic effect of drug/compound combinations. The method presented here is very simple and the predictive ability can be potentially improved in several aspects: (1) using mutation information to filter feature genes; (2) integrating pathway or network information to screen feature genes; (3) generating treated expression profiles of cell lines with drug combinations and building model to compare them with those of each drug; (4) increasing the sample number and time point number.

References

1. Zhao, X. M., Iskar, M., Zeller, G., Kuhn, M., van Noort, V., & Bork, P. (2011). Prediction of drug combinations by integrating molecular and pharmacological data. Plos Computational Biology, 7(12), e1002323.
2. Jia, J., Zhu, F., Ma, X., Cao, Z. W., Li, Y. X., & Chen, Y. Z. (2009). Mechanisms of drug combinations: interaction and network perspectives. Nature Reviews Drug Discovery, 8(2), 111-128.
3. Borisy, A.A., et al., Systematic discovery of multicomponent therapeutics. Proceedings of the National Academy of Sciences 100(13):7977-7982, (2003).

Nature Biotechnology doi:10.1038/nbt.3052

4. Santoro, A., Bonadonna, G., Bonfante, V., & Valagussa, P. (1982). Alternating drug combinations in the treatment of advanced Hodgkin's disease. The New England journal of medicine, 306(13), 770.
5. Jin, G., Zhao, H., Zhou, X., & Wong, S. T. (2011). An enhanced Petri-net model to predict synergistic effects of pairwise drug combinations from gene microarray data. Bioinformatics, 27(13), i310-i316.
6. Wu, Z., & Chen, L. (2009). A Network-based Approach for Identifying Effective Drug Combination. In The Third International Symposium on Optimization and Systems Biology (OSB 09), pp. 207-213.

RANK 5

Predicting drug synergy using distance between gene sets

Summary Sentence: Ranked drug pairs on the basis of a metric describing distance between perturbed pathways.

Introduction

This was not a textbook prediction task because no examples of multi-drug treatment responses were provided. Our strategy was to focus on predicting additive effects, assuming that ranking within the additive range of the responses would be the main determinant of the challenge winner. Gene set enrichment analysis (GSEA) [1] was the foundation of our method.

Methods

We hypothesized that differential gene expression at 24 hours compared to DMSO revealed perturbed molecular pathways. We assumed that additive responses might be predicted when cells are treated with two drugs that perturb different pathways--i.e., complementary perturbed pathways. We quantified "pathway perturbation" using GSEA on a high-level cut of the gene ontology (GO). We selected gene sets that were significantly perturbed at false discovery rate < 0.05. We computed Manhattan distance between pathway perturbation vectors. Distant pathways were deemed complementary and therefore additive/synergistic. We ranked drug pairs from distant (presumed synergistic) to close (presumed antagonistic) using the distance metric.

Discussion

This rudimentary strategy resulted in statistically significant non-random performance. The simplistic assumption that pathway distance is correlated with synergy / antagonism is clearly insufficient for accurate prediction.

References

1. A. Subramanian, P. Tamayo, V. K. Mootha, S. Mukherjee, B. L. Ebert, M. A. Gillette, A. Paulovich, S. L. Pomeroy, T. R. Golub, E. S. Lander, and J. P. Mesirov. Gene set enrichment analysis: a knowledge-based approach for interpreting genome-

Nature Biotechnology doi:10.1038/nbt.3052

wide expression profiles. Proc Natl Acad Sci U S A, 102(43):15545– 15550, Oct 2005.

RANK 6

Prediction of Drug Synergism from Expression Data

Summary Sentence: Designed a geometry-based score to predict the synergistic effect of drugs.

Motivation

This challenge is to predict the activity of pairs of compounds in the DLBCL LY3 cell line, from expression profiles acquired after treatment of the cell line with each of 14 individual compounds, based on the measured IC_{20} (20% viability reduction) at 24h induced by each compound in isolation. There are many possible reasons for drug synergism. For example, if both drugs target at the same pathway or the same gene, the combination of them may not be synergistic. If one drug can help the delivery of another drug, it is very possible that they are synergistic.

In this work, we aimed at design a simple but universal algorithm that can be widely applied to similar tasks. Thus we only used 24hr IC_{20} values and gene expression value at that time point. We did not use any other external or disease/drug-related information. Given that we do not fully understand the actual effect of each drug in the transcriptome, we need to develop a mathematical representation for their actions. Intuitively, if two drugs suppress the same set of genes, their joint effect might be additive. If they suppress different disease-related pathways, it is likely that their combination could be synergistic. So the main idea is to represent each drug's action on expression levels as a vector and then use a geometric method to calculate their joint and exclusive actions. With their joint and exclusive actions, we can evaluate the synergism of drug pairs.

Methods

Preprocessing

Considering that all drugs are used for treating B-cell lymphoma cancer, all drugs tend to suppress many B-cell lymphoma cancer-related pathways/genes, such as those involved in cell proliferation. As a result the control in the dataset is not quite useful to identify the specific action for each drug. So we used the average expression levels of 14 drugs as the 'real' control. For each drug, we took the 24h expression profile and calculated the average expression levels over samples at concentration = IC_{20}. We calculated the average expression levels over all 14 drugs. This can be also seen as the average action of drugs. We then find the differentially expressed probes (fold change greater than 1.5 or less than 2/3) for each drug. We use **DEP_i** to denote the set of differentially expressed probes for drug **i**.

Weighting Scheme

Nature Biotechnology doi:10.1038/nbt.3052

Since the task is to predict the drug effect at 60h after treatment, we extrapolated the IC_{20} values to 60h for each drug, by fitting an exponential function. These IC_{20} values measure the concentration or sensitivity of each drug to suppress 20% viability of the cell line. We use them to reweight each drug. The sensitivity weight can be calculated as **W_i = -log(IC_{20}) + 2.1** for drug **i**, where 2.1 is chosen to make sure all weights are positive.

Joint Effect of Drugs

We calculated the overlapping score for each drug pair **(i,j)** as

V_ij = | Intersect(DEP_i, DEP_j) | /min(|DEP_i |, | DEP_j |),

where, |X| denotes the size of set X.

The higher **V_ij**, the more likely that drug **i** and **j** have the similar effect on expression. If **V_ij**=1, drug i and j should perform almost the same action to treat the cell line.

Synergistic Effect of Drugs

Opposed to joint effect, two drugs might be complementary to each other if they can enhance each other's actions. So we compare the expression changes of two drugs on their differential expressed probes.

1. We calculated the fold changes of all probes for drug **i** and **j**, and stored them in two vectors **D_i** and **D_j**.
2. We then calculate the correlation between **D_i** and **D_j** on the subset **DEP_i** and **DEP_j** respectively, as **C_ij** and C_ji. We also calculate projected vector norm **L_ij** from **D_i** and **D_j** on probe set **DEP_j**, and projected norm **L_ji** from **D_j** and **D_i** on probe set **DEP_i.**
   R_ij = C_ij*L_ij and **R_ji = C_ji*L_ji** then represent whether a drug have the similar action to another.

We want to capture the complementary effect but exclude joint effect of two drugs. So we finally compose the score as **(1-V_ij)(R_ij*W_i + R_ji*W_j)** as the synergism of drug **i** and **j**. A zero score means additive effect. A positive score means synergistic.

Discussion

This method performed pretty well although it did not include any disease-related or drug-related information. We expect to improve the algorithm by incorporating drug-specific information, such as their expected target genes, into account.

RANK 7

Drug Synergy Prediction using Genetic Sensitivity and Gene Expression Profiles

Summary Sentence: Predicted synergy between anti-cancer drugs based on a systematic study of synergy between fungicidal drugs leveraging the drug's chemical properties, chemogenomic profiling and gene-expression data.

Nature Biotechnology doi:10.1038/nbt.3052

Background/Introduction

Although combined therapies can provide potentially better clinical potency [Fitzgerald 2006], systematic large-scale assays of drug interactions have been scarce until recently [Cokol 2011]. We approached the problem of synergy prediction as a machine-learning problem in which we trained Support Vector Machines (SVMs) based on a systematic study of the synergy between 200 pairs of antifungal compounds [Cokol 2011]. In addition to two basic features – chemical similarity and known chemical-protein interactions [Kuhn et al., 2008], we devised a novel feature that integrated measurements of growth-inhibition after drug treatment (in yeast deletion strains) [Hillenmeyer, 2008] with gene expression changes after drug treatment (in human cancer cell lines) [Lamb, 2006].

Methods

We trained SVMs with radial kernels on fungicidal drug combinations and applied the model to predict the ranking of the compound pairs presented in the challenge. We used the set of drug-synergy-specific features described below as input and synergy measurements from [Cokol 2011] as training standard to evaluate the prediction of synergy between drug pairs. Missing values were imputed with zeros and the CARET R package [Kuhn, 2008] was utilized for training. The features are described in detail below.

Chemical Similarity. We used the Indigo toolkit [Pavlov 2011] to compute a measure of chemical similarity between pairs of compounds. We created fingerprints from the SMILES string of each compound and used the Tanimoto-coefficient of two fingerprints as a measure of similarity between compounds.

Chemical Interactions. We used the STITCH database [Kuhn et al., 2008] to retrieve known chemical interactions for compound pairs. When a pair of compounds did not have any known interaction but was still present in STITCH, we used the topological overlap measure [Ravasz 2002] over the drugs' first-degree neighbours to get a proxy interaction score.

Nature Biotechnology doi:10.1038/nbt.3052

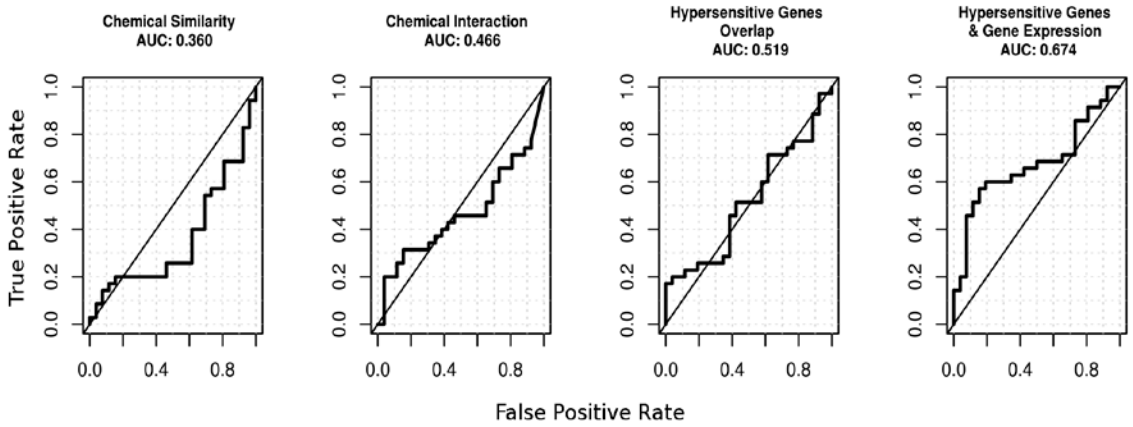

Figure 1: Classification performance of different features. Each of the input features was used to classify drug pairs into synergistic or non-synergistic pairs. Chemical similarity and the combination of hypersensitive gene sets with gene expression data appear to be informative to predict synergy or antagonism.

Hypersensitive gene sets and drug induced gene expression changes. Hillenmeyer et al. screened yeast-deletion strains with a large number of compounds to identify genes which when deleted made the cells hypersensitive to each compound [Hillenmeyer 2008]. Jansen et al. proposed to use the overlap of the hypersensitive gene sets for a pair of compounds as a measure of synergy between the compounds [Jansen 2009]. We included these scores as features when available. However, in evaluation based on experimental measurements, this feature did not offer a biologically meaningful interpretation of synergy.

Therefore, we defined a novel measure that combined the Hillenmeyer et al. hypersensitivity data with large-scale gene expression changes measured upon drug treatment. The motivation behind this approach is as follows: if the deletion of certain genes leads to a strong growth defect when treated with one drug, and another drug represses these genes, the two drugs are likely to be synergistic. We analyzed the raw expression data from the CMAP compendium [Lamb 2006] to obtain differential gene-expression profile per drug. After mapping the fitness-defect scores from yeast ORFs to human genes we then calculated a score for a pair of drugs equal to the correlation between one drug's hypersensitivity profile and the other's differential-expression profile.

We used an SVM classifier with radial kernels to learn a model for synergy using all the features described above. After parameter selection and evaluation, we predicted pairwise synergy scores for the drugs in the challenge and used these scores to produce our final ranking.

Conclusion/Discussion

Nature Biotechnology doi:10.1038/nbt.3052

Before learning a collective model, we evaluated each of our features for their ability to classify the drug pairs into synergistic and antagonistic combinations (Fig. 1). The chemical similarity of compounds was surprisingly informative for the dataset of fungicidal drugs, with compounds that were chemically similar being less likely to interact synergistically (AUC=0.36). We also found that sharing targets made a pair of compounds slightly less likely to be synergistic (AUC=0.46). The third feature – the overlap of hypersensitive genes of two drugs – has been proposed earlier as a measure of synergy for fungicidal drugs [Jansen 2009], but in our evaluation, we found this feature to not be informative (AUC=0.51). However, our novel feature combining the sensitivity scores with differential-expression was significantly informative (AUC=0.67).

It is worth noting that classifying drug pairs into synergistic versus non-synergistic is much easier than predicting the specific amount of synergy between two drugs, a formidable problem even when using methods as diverse as SVMs with radial kernels, elastic-net regression or kNN. The utter lack of appropriate training data is yet another gap that hinders a more accurate study of synergy. In this study, we trained on fungicidal drugs tested on yeast and predicted on anti-cancer drugs tested on human cells, potentially an extraordinary leap of knowledge that is expected to yield a loss in accuracy. More drug-drug interaction studies and systematic large-scale experiments with human cells will alleviate this situation and allow a more realistic computational prediction framework.

References

1. Cokol, M., Chua, H. N., Tasan, M., Mutlu, B., Weinstein, Z. B., Suzuki, Y., Nergiz, M. E., et al. (2011). Systematic exploration of synergistic drug pairs. *Molecular systems biology*, *7*(544), 544. doi:10.1038/msb.2011.71
2. Fitzgerald, J. B., Schoeberl, B., Nielsen, U. B., Sorger, P. K. (2006) Systems biology and combination therapy in the quest for clinical efficacy. Nature Chemical Biology, 2(9), 458.doi:10.1038/nchembio817
3. Hillenmeyer, M. E., Fung, E., Wildenhain, J., Pierce, S. E., Hoon, S., Lee, W., Proctor, M., et al. (2008). The chemical genomic portrait of yeast: uncovering a phenotype for all genes. *Science*, *320*(5874), 362–5. doi:10.1126/science.1150021
4. Jansen, G., Lee, A. Y., Epp, E., Fredette, A., Surprenant, J., Harcus, D., Scott, M., et al. (2009). Chemogenomic profiling predicts antifungal synergies. *Molecular systems biology*, *5*(338), 338. doi:10.1038/msb.2009.95
5. Kuhn, Max. (2008). Building Predictive Models in R Using the caret Package. *Journal of Statistical Software*, *28*(5).
6. Kuhn, Michael, von Mering, C., Campillos, M., Jensen, L. J., & Bork, P. (2008). STITCH: interaction networks of chemicals and proteins. *Nucleic acids research*, *36*(Database issue), D684–8. doi:10.1093/nar/gkm795

7. Lamb, J., Crawford, E., Peck, D., Modell, J. W., Blat, I. C., Wrobel, M. J., Lerner, J., et al. (2006). The Connectivity Map: using gene-expression signatures to connect small molecules, genes, and disease. *Science*, *313*, 1929–1935.
8. Pavlov, D., Rybalkin, M., Karulin, B., Kozhevnikov, M., Savelyev, a, & Churinov, a. (2011). Indigo: universal cheminformatics API. *Journal of Cheminformatics*, *3*(Suppl 1), P4. doi:10.1186/1758-2946-3-S1-P4
9. Ravasz E, Somera AL, Mongru DA, Oltvai ZN, Barabasi AL (2002) Hierarchical organization of modularity in metabolic networks. Science, 297:1551–1555.

RANK 8

Combination drug effect prediction model using score function based on molecular data

Summary Sentence: The score function utilizes transporter gene information, T-scores, and differently expressed gene (DEG) sets of drugs. The method is based on the following 2 assumptions: 1) if 2 drugs regulate the same targets, then they will show similar DEG sets, and 2) synergistic and antagonistic effects occur only if 2 drugs regulate the same targets, or 1 drug affects the transporter gene of another.

Background/Introduction

Combination drugs are said to have synergistic effects if they interact with each other to enhance the effects of individual drugs. On the other hand, combination drugs are said to have antagonistic effects if they interact with each other to inhibit the effects of individual drugs. In addition, combination drugs are said to have additive effects if they do not interact with each other and instead act independently.

In this challenge, we provide cell line information, gene expression data obtained at several time points, and drug names. We also propose a new scoring function to measure synergistic/antagonistic effects to rank a given drug combinations.

Methods

The complete workflow of our method is illustrated in Figure 1. The whole experiment can be divided into 3 parts: t-test, Filter, and Scoring.

Nature Biotechnology doi:10.1038/nbt.3052

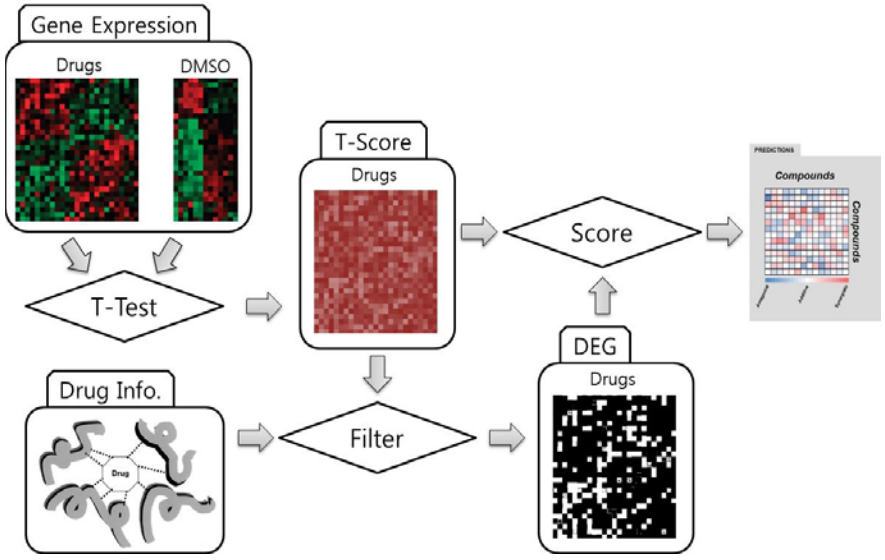

Figure 1: Complete workflow

T-test

We performed t-test using the gene expression data of drugs and dimethyl sulfoxide (DMSO) at 24 h time point. As a result, we obtained T-scores that represent how gene expressions of drugs are different from those of DMSO.

Filter

In the filtering process, we filtered out the expressions of DEGs from the T-score results using drug information from external databases. From DrugBank (http://www.drugbank.ca/) and PubChem (http://pubchem.ncbi.nlm.nih.gov/), we gathered target and transporter information for the given drugs.

The filtering process can be divided into 3 steps. First, we filtered out genes with false discovery rate (FDR) values larger than 0.1. This step eliminated genes showing no difference in expression and significantly and differentially expressed genes remained. Through this step, we obtained significant gene sets for each drug. Second, we filtered out genes that exist in 2 or less significant gene sets, and genes from drugs with IC_{20} value of 100 μM were not included. In this process, we selected genes that significantly affect the viability of cell lines, and we excluded genes from drugs with IC_{20} value of 100 μM for the same reason. Third, we included target genes of drugs in their DEG set. The target gene information is gathered from external databases. As a result, we could get significant DEG sets, including target genes for each drug.

Score

In the scoring process, we scored drug synergistic effects for all the drug combinations. There exist many previous scoring functions, but most of them are dependent on viability results in response to drugs. As the task is to predict viability, these functions cannot be used. Therefore, we propose a new scoring function for determining drug synergistic effects using transporter gene information from external databases, T-scores, and DEG sets of drugs:

Nature Biotechnology doi:10.1038/nbt.3052

$$\text{Synergy}_{AB} = \frac{\frac{\sum_{i}^{G_{AB}}(T_{Ai} \times T_{Bi})}{N_{AB}} - \frac{\sum_{j}^{G_{trA}}\left(\text{sign}(T_{Bj}) \times (T_{Bj})^2\right) + \sum_{k}^{G_{trB}}(\text{sign}(T_{Ak}) \times (T_{Ak})^2)}{N_{trA} + N_{trB}}}{\frac{N_A - N_{AB}/2}{N_A} + \frac{N_B - N_{AB}/2}{N_B}}$$

where,

G_{AB} = Common genes from DEG sets of drug A and B,
G_{trA}/G_{trB} = Transporter genes of drug A/B,
T_{Ai}/T_{Bi} = T − score of gene i on drug A/B,
N_{AB} = Number of common genes from DEG sets of drug A and B,
N_A/N_B = Number of genes from DEG sets of drug A/B, and
N_{trA}/N_{trB} = Number of transporter genes of drug A/B.

We have 2 assumptions for this scoring function:

- If 2 drugs have common targets, then they will show similar DEG sets[1].
- The synergistic and antagonistic effects occur only if (i) 2 drugs have common targets, or (ii) 1 drug affects the transporter gene of another[2].

The denominator part of the fraction represents the commonality of the DEG sets of drugs. From the above assumption, we can infer that if 2 drugs have synergistic/antagonistic effects, then they will have many common targets and if they have additive effects, then they will have only a few common targets. Therefore, we defined the denominator such that 'higher the number of common DEGs between the 2 drugs, the larger the denominator value.' This will make the absolute value of the whole score larger, if the 2 drugs have synergistic or antagonistic effects. We divided N_{AB} into 2 to limit the range of the denominator.

The first part of the numerator of the fraction is related to the directionality of the T-scores of drugs. We assumed that if T-scores of the common DEGs of drugs show the same directionality, then the 2 drugs will have synergistic effects, and if T-scores show different directionality, then the 2 drugs will have antagonistic effects. Therefore, we averaged the multiplied value of T-scores of the common DEGs of drugs.

The second part of the numerator of the fraction is related to the drug transporter. If 1 drug affects the gene expression of another drug's transporter, it will produce synergistic or antagonistic effects. If drug A increased the gene expression of the transporter of drug B, then it will increase the clearance of drug B, which results in antagonism and vice versa. We squared the T-score to make the dimension the same as that of the first part of the numerator.

The score becomes larger for positive values, if 2 drugs show synergistic effects. On the other hand, the score becomes smaller for negative values, if 2 drugs show antagonistic effects. If the score nears zero, it indicates that the 2 drugs have additive effects.

Conclusion/Discussion

Using the proposed scoring function, we could rank all drug combinations according to their synergistic effects. The statistical significance of these results is represented with probabilistic c-index, p-value, and FDR. Our results showed a probabilistic c-index of 0.551, a p-value of 6.12E-02, and FDR of 2.37E-01. Our assumptions about the synergistic and antagonistic effects are limited. If we consider a wider range of synergistic and antagonistic drugs to further test, we could obtain more reliable results.

References

Nature Biotechnology doi:10.1038/nbt.3052

1. Gottlieb, A., Stein, G.Y., Ruppin, E. & Sharan, R. PREDICT: a method for inferring novel drug indications with application to personalized medicine. *Molecular systems biology* **7**, 496 (2011).
2. Jia, J. et al. Mechanisms of drug combinations: interaction and network perspectives. *Nature reviews. Drug discovery* **8**, 111-128 (2009).

RANK 9

Rank Aggregation Method for Predicting Drug Synergy

Summary Sentence: We used rank-aggregation method to combine the results of many prediction methods to find the most commonly ranked synergy ordering.

Background/Introduction

The goal of the problem is to rank the extent of synergy between pairs of drugs when co-administered to the LY3 lymphoma cell-line using time-course microarray data for each drug along with the copy-number variation data for the LY3 cell-line. We attempted to use methods that encompassed both the *a priori* knowledge of cancer biology and modern predictive techniques. To incorporate *a priori* knowledge we used Gene Set Enrichment Analysis to relate our feature sets to biologically relevant processes. In the absence of synergy data, our methodology can only capture consistently ranked data but not necessarily the true rankings.

Methods

For this challenge, we developed a set of 'Hypotheses' and then aggregated the results of each hypothesis.

Hypothesis 1: Drugs that cause correlated changes in gene expression will have synergistic effects

We used the time-course microarray data to find the fold-change and RankProduct [3] associated p-value between the controls (DMSO and Media) and the drug treated cell line. We grouped these by time-point that resulted in three evaluations for each drug and considered only the high-concentration dataset. Considering each drug treatment as a vector in N-dimensional space, with the value being the fold-change between control and treated experiments, we found the angle between each pair of vectors considering only the genes with p-values < 0.01. Pairs of drugs were ranked by their included angle with the most synergistic angle being 0 degrees. This produced three ranked lists, one for each time-point.

Hypothesis 2: Drugs which cause differential regulation of similar pathways will have synergistic effects

Using the p-values calculated above we found the statistically enriched KEGG Pathways, GO Molecular Functions and GO Biological Processes for each comparison. We considered annotation term as significant if its minimum Benjamini p-value [4], across all time-points, was below 0.01. We then used the hypergeometric test to determine the likelihood of the observed overlap between each pair of drugs with low likelihoods being

Nature Biotechnology doi:10.1038/nbt.3052

indicative of synergy. This produced three ranked lists, one for each of the annotation types.

Hypothesis 3: Drugs that interact with the same genes will have synergistic effects

Using the ChEMBL database [5] we determined the genes which interact with a drug. We used the hypergeometric test to determine the significance of the overlap. The pairs were ranked with those sharing no genes were ranked at the bottom. This produced one ranked list.

Hypothesis 4: Drugs that interact with the significantly altered genes of another drug will have synergistic effects

Using the ChEMBL data gathered in H3 and the p-values calculated in H1 we used the hypergeometric test to determine the likelihood of overlap between the genes bound by Drug-A and the significantly altered genes in Drug-B. Since this test is not symmetric we used the mean of the two p-values. The pairs were ranked and those which shared no genes in common were ranked at the bottom.

Hypothesis 5: Drugs that are mentioned in the same clinical trial articles will have synergistic effects

This method relies on the idea that drugs with similar effects are likely to be studied at the same time and that the publication bias will enrich for 'positive' effects. We used a pubmed query to find the number of clinical trial articles which mention both each pair of drugs. We used a hypergeometric test to rank the pairs by the likelihood of their overlap.

Final Aggregation

We used a simple mean rank aggregation method [6] to join all of the lists. We looked at the Kendall's Tau and its associated p-value between each pair of ranked lists. We found that they are all positively correlated with each other and many pairs have p-values < 0.1. However, this only tells us that we are getting consistent results, we have no way of evaluating whether they are consistently right or consistently wrong.

Conclusion/Discussion

Our main pitfall in this challenge was not finding more training data to test our hypotheses in other systems. Without such training data to evaluate our predictions virtually all machine-learning methods become useless. In its place, we developed a set of hypotheses from our biological knowledge and found pairs that consistently agreed.

References

1. Pedregosa F, Varoquaux G, Gramfort A, Michel V, Thirion B, et al. (2011) Scikit-learn: Machine Learning in Python. Journal of Machine Learning Research 12: 2825-2830.

2. Guyon I, Weston J, Barnhill S, Vapnik V (2002) Gene selection for cancer classification using support vector machines. Machine learning 46: 389-422.

3. Hong F, Wittner B, Breitling R (2009) RankProd: Rank Product method for identifying differentially expressed genes with application in meta-analysis. R version 2.

4. Dennis G, Jr., Sherman BT, Hosack DA, Yang J, Gao W, et al. (2003) DAVID: Database for Annotation, Visualization, and Integrated Discovery. Genome Biol 4: P3.

5. Gaulton A, Bellis LJ, Bento AP, Chambers J, Davies M, et al. (2012) ChEMBL: a large-scale bioactivity database for drug discovery. Nucleic acids research 40: D1100-D1107.

Nature Biotechnology doi:10.1038/nbt.3052

6. Fagin R, Kumar R, Sivakumar D. Efficient similarity search and classification via rank aggregation; 2003. ACM. pp. 301-312.

RANK 10 & 23

Inferring cell line drug sensitivity from patient survival data

Summary Sentence: Tested the possibility to directly infer cell line viability from patient survival data via shared gene expression patterns of patients and compound effects.

Background/Introduction

Cell lines are regularly used as models to understand tumor cells in human patients. Usually it is reasoned that if a compound is capable of reducing the viability of model cell lines, then the same compound should also have potential for increasing patient survival.

This motivates the question: Can this link also be reversed and utilized for the prediction of effects of combined compounds or for the effects of the same compound when applied to other cell lines? When exploring gene expression data of patients, one can usually identify many genes that are significantly correlated with patient survival, for example in a "higher expression is worse" pattern. In this example the assumption of the reversed reasoning would be: Any compound that is capable of decreasing the expression of these "bad genes" will also have potential to reduce viability of the tumor cell lines.

In this report a prototype algorithm is presented that uses assumptions like these to connect the information known about single compounds for the Ly3 cell line with gene expressions in order to the make predictions about the effect of combined compounds on the same cell line.

Methods

Information on the patient side was learned from the GSE10846 study [1]; more precisely, from the normalized $\log_2(\text{ratio})s\ M_{i,j}$ before treatment for all available genes I and for all available patients J in both the CHOP and RCHOP treated subsets (downloaded from Gene Expression Omnibus; accession: GSE10846).

Based on the follow-up information of disease-specific overall survival (or progression-free survival, if available) genes were identified whose expressions were significantly correlated with survival of DLBCL patients. These genes were partitioned in correlated genes $I^+ \subset I$ (showing a "higher is better" pattern) and anticorrelated genes $I^- \subset I$ ("lower is better"). Genes without significant correlation ($\alpha = 0.05$) were excluded.

As information based on a single gene is rather uncertain, hierarchical clustering of the gene expressions was used, separately for both identified gene partitions and based on the correlation metric with Ward linkage. Several signatures of co-regulated genes $G_k^+ \subset I^+$ and $G_k^- \subset I^-$ were defined manually by visual inspection of and selecting clusters in the resulting dendrograms. Clearly, this is a non-deterministic step of this prototype algorithm that should be consolidated. Only well-separated clusters were selected for further analysis.

Nature Biotechnology doi:10.1038/nbt.3052

For each identified gene signature again a survival analysis for the average signature expression was conducted. In these survival analyses also survival slopes $s_k^{\pm}$ were calculated for every signature, defined as the expected linear increase (or decrease) in survival per difference in the signature's average gene expression. This encodes the information by how much a higher expression of a particular set of co-regulated genes G_k^+ is better (or worse for G_k^-) from patient's perspective.

Now the dual information is required: How strongly does a compound decrease or increase the expression of the same genes $G_k^{\pm}$ in Ly3 and how does this change correlate with the viability of Ly3?

Ideally, one would have measurement data before and after treatment for many cell lines and compounds to estimate the compound effects on gene expression level and viability level robustly. In this challenge normalized GEP data $\widetilde{M}_{\text{before},i,n}$ and $\widetilde{M}_{\text{after},i,n,c}$ for before and after compound administration for genes I and for compounds n administered with concentration c were available, but only for the single DLBCL cell line Ly3. Let

$$d_{\text{before}\to\text{after},k,n} := -\overline{\widetilde{M}_{\text{before}}\left(G_k^{\pm}, n\right)} + \overline{\widetilde{M}_{\text{after}}\left(G_k^{\pm}, n, C\right)}$$

be the average signature change of $G_k^{\pm}$ from before to after administering compound n (weighted average over all concentrations $c \in C$). For a pair of compounds (n_1, n_2) a simple additive model was applied on GEP level:

$$d_{\text{before}\to\text{after},k,(n_1,n_2)} := d_{\text{before}\to\text{after},k,n_1} + d_{\text{before}\to\text{after},k,n_2}$$

Then an interpretation ansatz for the following four categories of genes was made:

$d_{\text{before}\to\text{after},k,n}$	$s_k^{\pm}$	**Interpretation**
Inhibition	Lower is better	Compound works by inhibiting "high is bad" genes
Inhibition	Higher is better	Cell line counter-reacts by downregulating "low is bad" genes in order to survive
Overexpression	Lower is better	Cell line counter-reacts by upregulating "high is bad" genes in order to survive
Overexpression	Higher is better	Compound works by expressing "low is bad" genes

The predictive signed weights $w_{i,n}$ of each gene and for any compound n were defined for every single gene to be proportional to the following information:

- based on cell line gene expression data:
  - gene expression difference $d_{\text{before}\to\text{after},k,n}$ before and after treatment (relative log2(ratio) of the gene versus the average log2(ratio) of its gene cluster)
  - one minus the p value of this gene expression difference (using a two-sample t-test between arrays after treatment (all durations, all concentrations) versus the DMSO arrays)
- based on patient gene expression data:
  - survival difference between the partial cohort with gene expression below versus above the median for the average expression of $G_k^{\pm}$
  - one minus the p value of the previous survival difference (Kaplan-Meier, log rank)

Nature Biotechnology doi:10.1038/nbt.3052

The response information was available in form of the decrease in viability v_n after administration of each single compound n. This information had to be "distributed" over the genes in order to connect with the predictive gene weights $w_{i,n}$. For the first submission a simple model was used that associated every gene with the same constant observed viability decrease (averaged over the IC_{20}@24h and IC_{20}@48h concentrations), i.e. $v_{i,n} \coloneqq v_n$. For the second submission an extrapolation was used based on the graphically available titration curves: The nonlinear decrease of viability visible therein when increasing the concentration of the compound was taken into account as follows: If a gene's $\log_2$(ratio) was two times the $\log_2$(ratio) of another gene, then it was associated with a viability decrease at two times the IC_{20} concentration in the titration curve which typically decreases rapidly in a nonlinear way.
Then the Bliss independence model [2] was used to predict the contributions of every gene to the viability decrease caused by a compound pair (n_1, n_2):

$$v_{i,(n_1,n_2)} \coloneqq 100\% - \left(\left(100\% - v_{i,n_1}\right)^{|w_{i,n_1}|} \cdot \left(100\% - v_{i,n_2}\right)^{|w_{i,n_2}|}\right)^{\frac{2}{|w_{i,n_1}|+|w_{i,n_2}|}}$$

Let $w_{i,(n_1,n_2)} = w_{i,n_1} + w_{i,n_2}$ be the gene weights specific for a compound pair (n_1, n_2). Note that due to the signed weights, the $w_{i,(n_1,n_2)}$ are zero for genes with neutralizing compound effects, i.e. for $d_{\text{before}\rightarrow\text{after},k,n_1} = -d_{\text{before}\rightarrow\text{after},k,n_2}$. The total decrease of viability due to the compound pair was finally predicted as

$$v_{(n_1,n_2)} \coloneqq \sum_i w_{i,(n_1,n_2)} v_{i,(n_1,n_2)} \Big/ \sum_i w_{i,(n_1,n_2)}$$

These predictions were used to rank the compound pairs from the most synergistic to the most antagonistic.

Conclusion/Discussion

With the help of this challenge it was possible to test the conjecture that it is possible to quantitatively infer the decrease in cell line viability for pairs of compounds from gene expression patterns associated with patient survival and the inhibition or overexpression effects of single compounds thereon.
Although more data was provided, only the gene expression and viability data (the titration curves) were used in order to specifically test the conjecture.
The predicted sensitivity rankings of the compound pairs were not significant.
As explained in the method section, the $v_{i,n}$ were assumed to be constant for all genes and equal to the observed viability decrease v_n in the first submission. A second submission took into account the nonlinear decrease of viability over concentration. As these titration curves were only provided as graphics and not in numbers, the decrease-in-viability-over-concentration function had to be extracted visually, which was not ideal. Therefore, also in the second submission, this nonlinear information was used only with a weight of 50% (i.e. the extrapolations were mixed with v_n 1:1). Interestingly, the second submission produced a more than two-fold better (albeit still insignificant) p-value of 0.181. This suggests that the nonlinearity in the titration curves is important to correctly model synergistic effects. It should be investigated whether the predictions could be

Nature Biotechnology doi:10.1038/nbt.3052

further improved by determining $v_{i,n}$ solely by this information and on the basis of precise numeric values for the titration curves.
Possible pitfalls of the presented prototype algorithm that should be revised are the visually defined gene clusters, the visually extracted viability-over-concentration functions and the weighting scheme that allows for negative weights. Additionally it should be tried to apply the weighting not on single gene level, but only on gene clusters level to gain more robust predictions.
Although this model did not predict significant rankings, a model based on a similar conjecture was used in the sister challenge about breast cancer in order to predict effects of compounds on so far untested cell lines. This model was able to produce significant predictions. Taking both results together, it is probable that we can learn something new about the tested conjecture:
Gene clusters $G_k^{\pm}$ that are relevant for patient survival can indeed be used to transfer the information about compound effects to a new cell line, but only if these gene clusters were stratified by weights based on the consistency of the compound effects on many cell lines of the disease. If their weights are only determined by experiments with different compounds but the identical cell line, then predictions of the effects of combinations of compounds on the same cell line are not possible. Maybe this can be explained as follows: For a single cell line, several of the $G_k^{\pm}$ that were identified based on patient survival are not applicable, since the cell line is only representative for a specific subtype of the disease. This is especially true for diseases like DLBCL that are known to be genetically heterogeneous. Additionally, a single compound only affects the gene expressions of a specific subset of genes and the overlap with the $G_k^{\pm}$ might be small for most of the tested compounds. Taking both facts together there might simply not be enough information to robustly define the weights for the $G_k^{\pm}$ in the "single cell line, multiple compounds" scenario.
Clearly, from an analysis point of view it would be ideal if one had GEP measurements before and after compound administration like in this challenge, but for many cell lines of the disease like in the breast cancer sub-challenge. Then it would be possible to combine both weighting schemes which should result in a self-stabilizing effect and might also allow predicting the effects of pairs of compounds based on patient survival (not just for a single cell line but for all used in the training phase plus new ones).

References

1. Lenz et al. "Stromal gene signatures in large-B-cell lymphomas. ", N Engl J Med 2008, Nov 27;359(22):2313-23. PMID: 19038878
2. Borisy, A.A., et al. "Systematic discovery of multicomponent therapeutics.", Proceedings of the National Academy of Sciences, 2003. 100(13): p. 7977-7982.

RANK 11

Pathway Based Prediction of Drug Synergisms

Nature Biotechnology doi:10.1038/nbt.3052

Summary Sentence: Drug pairs synergisms were predicted on the basis of activation of biological pathways in response to single drug administration.

Background/Introduction

The data we used to address the challenge are:

- The gene expression profiles corresponding to a set of 14 perturbations (14 compounds), at three time points (6h, 12h, and 24h), at two concentrations (one corresponding to the IC_{20} of the compound at 24 hours and one corresponding to the IC_{20} at 48 hours).
- the gene expression profiles of cells exposed to DMSO in 8 replicates
- the drug dose-response data from which the IC_{20} were calculated

Since a training set was not available for this challenge, we based our prediction on the synergistic/antagonistic effects observed on pathways activation, calculated assuming that the expression of genes in cells treated with a compound pair is equal to the sum of the expression of genes treated with single compounds (assuming superimposition of the effects).

In our analysis, we did not considered the entire set of genes but only those that resulted differentially expressed in at least one time point (treated cells vs. DMSO) for at least one drug concentration (SAM [1] and False Discovery Rate threshold = 0.05 were used) and that were annotated in KEGG database.

Methods

Our ranking was based on the ordered list of estimated viability reduction, i.e. the percentage of dead cells with respect to the total cell sample, when compounds *i* and *j* are simultaneously administred. The estimate of viability reduction for each pair of compounds *i* and *j* is computed on the basis of five main steps: 1) calculation of pathway activation for each pathway *p* in response to each compound *i*, singularly administred; 2) pathway filtering; 3) calculation of pathway activation for each pathway *p* in response to the simultaneous administration of compounds *i* and *j*; 4) calculation of equivalent concentrations of drugs *i* and *j* that should be administred singularly to obtain the same effect of the compound pair (*i*, *j*); 5) calculation of the corresponding viability reduction. The five steps are explained in details in what follows.

Step1

Let us indicate with D_{iH} and D_{iL} the concentrations of drug *i* corresponding to IC_{20} at 24 (high dose) and 48 hours (low dose), respectively. For each pathway *p* in KEGG, we used gene expression data at 24h corresponding to D_{iH} and D_{iL} to compute pathway *p* activations $A_p(D_{iH})$ and $A_p(D_{iL})$. In particular, we used the bioconductor package *graphite* [2] to propagate pathway connections through chemical compounds and to run the Signaling Pathway Impact Analysis (*SPIA*) which uses the list of differentially expressed genes and their log fold changes together with the signaling pathways topology, to assign an activation score to each pathway [3]. This score can also be negative, meaning that an inhibition of the pathway, rather than an activation, occurs.

Step2

For each drug *i*, we then filtered out pathways for which $A_p(D_{iH})$ and $A_p(D_{iL})$ are not consistent. The rationale is that if a pathway is activated at low compound dose, it must be equally or greatly activated at high dose; on the opposite, if a pathway is inhibited at

Nature Biotechnology doi:10.1038/nbt.3052

low compound dose, it must be equally or greatly inhibited at high dose; i.e. for a pathway *p* to be retained, one of the following conditions must hold:

$$\begin{cases} A_p(D_{iH}) \geq A_p(D_{iL}) \geq 0 \\ A_p(D_{iH}) \leq A_p(D_{iL}) \leq 0 \end{cases}$$

Step3

We summed the log fold change (treated cells vs. DMSO) data measured for two drugs *i* and *j* at 24 hours in response to treatments with D_{iH} and D_{jH} (only high concentration is considered) and used *graphite* and *SPIA*, as described in step 2, to compute pathway *p* activation $A_p(D_{iH}+ D_{jH})$.

Step 4

We plotted on a Cartesian plane the points with coordinates $(D_{iL}, A_p(D_{iL}))$; $(D_{iH}, A_p(D_{iH}))$; $(D_{jL}, A_p(D_{jL}))$; $(D_{jH}, A_p(D_{jH}))$ (Figure 1, left panel, dotted gray and black lines) and extrapolated the virtual concentrations $Đ_{ip}$ and $Đ_{jp}$ that would be necessary to obtain an effect $A_p(D_{iH}+ D_{jH})$ on pathway *p*, administring drug *i* and *j* singularly (Figure 1, left panel, dotted blue lines). We then took the median of $Đ_{ip}$ and $Đ_{jp}$ values across all KEGG pathways that passed the filter at step 3, obtaining values $Đ_i$ and $Đ_j$ for drugs *i* and *j*, respectively.

Step 5

We used the drug dose-response data of drugs *i* and *j* from which the IC_{20} at 24 hours was calculated to approximate a piece-linear dose-response curve and extrapolate the viability reduction EVR_i and EVR_j of drugs *i* and *j*, correspondingly to $Đ_i$ and $Đ_j$ respectively. Figure 1, right panel, shows one of the dose-response data pictures available to the challenge participants, to which we have superimposed a dotted blue line which summarizes the extrapolation of the viability reduction EVR_i for drug *i*, starting from its virtual concentration $Đ_i$. We finally averaged the estimated viability reductions of the two drugs to obtain an estimate of the viability reduction in response to simultaneous

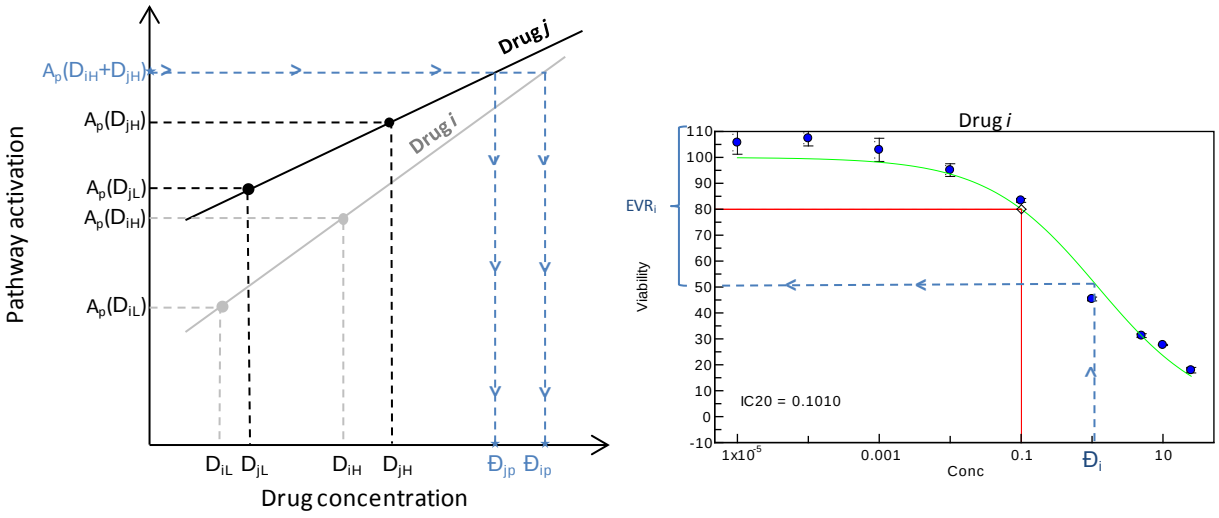

treatment with *i* and *j*.

Nature Biotechnology doi:10.1038/nbt.3052

Figure 1: Left panel: The concentrations of drugs *i* and *j* (D_{iL}, D_{iH}, D_{jL}, D_{jH}) and the corresponding activations on pathway *p* ($A_p(D_{iL})$, $A_p(D_{iH})$, $A_p(D_{jL})$, $A_p(D_{jH})$ are used to derive a straight line equation and to extrapolate the virtual concentrations $Ð_{ip}$ and $Ð_{jp}$ that would be necessary to obtain an effect $A_p(D_{iH}+ D_{jH})$ on pathway *p*, administring drug *i* and *j* singularly. Right panel: dose-response curve of drug i and extrapolation of the viability reduction EVR_i for drug *i*, starting from its virtual concentration $Ð_i$ (dotted blue line).

Conclusion/Discussion

Our method provides predictions of drug pairs synergism based on pathway activation, thus giving additional information on biological mechanisms underlying drug action. Since the challenge gold standard has now been released, it would be interesting to analyze which pathways are the most informative. Our preliminary analysis shows that performance of our method increases if we pre-select pathways based on prior knowledge rather than using them all. A future direction will be to assess if the pool of informative pathways is consistent across different drug pairs and if a part of the gold standard can be thus used as training set to learn which pathways should be selected.

Another direction we would like to explore consists in integrating selection, clustering, and functional annotation [4, 5] to find the main temporal patterns associated to functional groups of differentially expressed genes that respond to drug treatment. Groups of genes belonging to these main patterns could then be used in place of pathways to predict drug interaction.

References

1. Tusher VG, Tibshirani R, Chu G. Significance analysis of microarrays applied to the ionizing radiation response. Proc Natl Acad Sci U S A. 2001 Apr 24; 98(9):5116-21.
2. Sales G, Calura E, Cavalieri D, Romualdi C. graphite - a Bioconductor package to convert pathway topology to gene network. BMC Bioinformatics. 2012 Jan 31;13:20
3. Draghici S, Khatri P, Tarca AL, Amin K, Done A, Voichita C, Georgescu C, Romero R: A systems biology approach for pathway level analysis. Genome Research 2007, 17(10):1537-1545.
4. Di Camillo B, Toffolo G, Nair S.K, Greenlund L.J, Cobelli C. (2007). Significance analysis of microarray transcript levels in time series experiments. BMC Bioinformatics, vol. 8 suppl 1, p. 1-10,
5. Di Camillo B, Irving BA, Schimke J, Sanavia T, Toffolo G, Cobelli C, Nair KS (2012). Function-based discovery of significant transcriptional temporal patterns in insulin stimulated muscle cells. PLoS One. 2012;7(3):e32391

RANK 12

Predicting drug combination synergy based on gene expression signatures

Nature Biotechnology doi:10.1038/nbt.3052

Summary Sentence: Predict drug combination effects based on the overlaps of the gene expression signatures of individual drug treatments, using cell-line-specific genes derived from external datasets

Background/Introduction

Overlaps between cancer signatures and drug treatment signatures have been recently used to predict drug efficacy and to reposition drugs (Sirota et al., 2011; Shigemizu et al., 2012). We extend this approach to predict drug combination synergism and antagonism based on signature overlaps for a pair of drugs. Furthermore, we focus our approach on cell-line-specific genes. The underlying idea is that drugs that have overlapping signatures on important genes are more likely to interact, that is show either synergy or antagonism.

Methods

Method summary

1. Construct compound treatment signatures from the LY3 dataset provided for the challenge.
2. Construct cell line signatures using external data.
3. Predict drug pair synergism/antagonism based on the overlaps of the compound treatment and cell line signatures.

Compound treatment signatures

We constructed individual compound treatment signatures based on the given LY3 gene expression data set. We first computed the mean expression value for each gene over all probes related to that gene. We then discarded unreliable genes that had log2 ratio of DMSO vs. Media over 0.2. Finally, we computed differential expression at each time point for each drug as the log2 ratio of treatment vs. DMSO measurements. The compound-specific positive and negative gene signatures were then produced at each time point as the top and bottom 1000 differentially expressed genes, respectively.

LY3 signatures

To define the cell-line-specific gene signature for the LY3 cell line, we computed the fold change of the expression value of each gene on the LY3 cell line against a large panel of other cancer cell lines. All microarray samples included in this analysis are publicly available via the Gene Expression Omnibus GEO (accession numbers; GSE36133, GSE19495, GSE15947, GSE16924, GSE13218, GSE15481,GSE15903, GSE16798, GSE11118, GSE18866, GSE18913, GSE15400, GSE18476, GSE19203, GSE18571, GSE14879, GSE15520 and GSE18198), GSK Cancer Cell Line Genomic Profiling Data (George et al., 2008). The bulk of the gene expression data was acquired from the Cancer Cell Line Encyclopedia (GSE36133; Barretina et al., 2012). The positive and negative gene signatures for the LY3 cell line were produced as the genes with Tukey fold change value over 3 and under -3, respectively. This resulted in 662 and 510 genes in the positive and negative signatures.

Predicting drug pair synergism and antagonism

Notation used

Nature Biotechnology doi:10.1038/nbt.3052

- C.UP/C.DN: Cell line signature, i.e., set of up/down-regulated genes
- A.UP/DN, B.UP/DN: Drug signatures, i.e., set of up/down regulated genes for drugs A and B
- X ∩ Y: intersection of sets X and Y
- X∪ Y: union of sets X and Y
- X / Y: set difference of X and Y
- |X|: size of set X

Overlaps

- Reverse correlation overlaps, i.e. genes that show reverse expression patterns in the cell line signature and either of the drug signatures: REV.OL = {[C.UP ∩ (A.DN ∪ B.DN)] / [C.UP ∩ (A.DN ∩ B.DN)]} ∪ {[C.DN ∩ (A.UP ∪ B.UP)] / [C.DN ∩ (A.UP ∩ B.UP)]}
- Opposite overlaps, i.e., genes that show opposite expression for drugs A and B: OPP.OL = {C.UP ∩ [(A.DN ∩ B.UP) ∪ (A.UP ∩ B.DN)]} ∪ {C.DN ∩ [(A.DN ∩ B.UP) ∪ (A.UP ∩ B.DN)]}
- Direct correlation overlaps, i.e. genes that show similar expression patterns in the cell line signature and either of the drug signatures.
- DIR.OL = {[C.UP ∩ (A.UP ∪ B.UP)] / [C.UP ∩ (A.UP ∩ B.UP)]} ∪{[C.DN ∩ (A.DN ∪ B.DN)] / [C.DN ∩ (A.DN ∩ B.DN)]}

Final synergism-antagonism score

- The assumption behind the score is that reverse correlation overlaps indicate synergism, while opposite overlaps and direct correlation overlaps indicate antagonism.
- Score = |REV.OL| - |OPP.OL| - |DIR.OL|
- Final result was produced by computing the mean over the scores at each time point.

Properties of the score

- Score(drugA, drugA) = 0, i.e. combination of the same drug with itself is assumed to be additive.
- Scores above 0 indicate synergism, scores below 0 indicate antagonism. In practice scores close to 0 are treated as additive.

Conclusion/Discussion

Overall the task was very challenging, as seen from the poor prediction results of all methods. It remains to be seen whether gene expression data -driven methods really provide useful information for predicting drug combination effects. One key direction forward is to focus more only the important genes, chosen based on existing knowledge.

References

1. Barretina et al. (2012) The Cancer Cell Line Encyclopedia enables predictive modelling of anticancer drug sensitivity. Nature 483, 603-307.
2. George et al. (2007) Genome-wide analysis of neuroblastomas using high-density single nucleotide polymorphism arrays. PLoS ONE 2, e255.

Nature Biotechnology doi:10.1038/nbt.3052

3. Shigemizu et al. (2012) Using Functional Signatures to Identify Repositioned Drugs for Breast, Myelogenous Leukemia and Prostate Cancer. PLoS Computational Biology 8(2): e1002347.
4. Sirota et al. (2011) Discovery and Preclinical Validation of Drug Indications Using Compendia of Public Gene Expression Data. Science Translational Medicine 3, 96ra77.

RANK 13

Summary Sentence: The LY3 predictive virtual baseline was created based on the training data set provided for the effect of various compounds and this firmed up predictive system was then used to do predictions

Introduction

The Cellworks proprietary Tumor Cell Technology [1] has been used to predict the effect of the 91 possible pairs of 14 drugs ($^{14}C_2$ = 14*13/2). The predictive Tumor Cell Technology is a comprehensive integrated functional proteomics representation of the pathways converging on the key cancer phenotypes of proliferation, apoptosis, angiogenesis and metastasis. Tumor metabolism and nuances of tumor microenvironment are also incorporated. It is a dynamic network of pathways with inter- and intra-cellular crosstalk and associated autocrine and paracrine signaling. Such a system provides transparency to the maze of reactions within the cell. Any internal marker individually or in combination can be manipulated through specific percentage knockdown and over-expression and impact seen on the whole network. The predictive tumor cell based studies provide an insight into how a particular drug individually or in combination is impacting various cancer phenotypes across different tumor profiles representing patient sub-classes.

Methodology

Predictive Tumor Cell Platform

The Cellworks technology is a functional proteomics and metabolomics network representation *emulating* human physiology computationally and *predicting* clinical outcomes. The functional proteomics based platform allows execution of studies that *manipulate* targets and pathways with *quantitative assay* visibility and transparency into all phenotypes, pathways and biomarkers. The modeling of the time-dependent changes in the fluxes of the constituent pathways has been done utilizing modified ordinary differential equations (ODE).

The technology is implemented using a three-layered architecture. The top layer is a TUI/GUI (Text user interface/graphic user interface) driven user interface. The middle layer is the comprehensive representation of signalling and metabolic pathways covering all cancer phenotypes. The bottom layer is the computational back-plane which enables the system to be dynamic and computes all the mathematics in the middle layer. Figure 1A shows a snapshot of the Cellworks Predictive Tumor Cell Technology.

Nature Biotechnology doi:10.1038/nbt.3052

Cellworks Predictive Tumor Cell Technology is a *comprehensive* representation of signaling and metabolic pathway networks and integrates all cancer phenotypes and processes. A bottom-up approach was adopted to build the complete dynamic platform. Based on extensive literature search, each individual cellular process has been built as a standalone module and then functionally integrated to get the big picture. In case of inconsistent or unknown enzyme kinetic parameters, a trial and error method of optimization was followed to attain physiological enzyme behaviour. In such scenarios, data on experimental outcomes for a given set of inputs/perturbations has been used as alignment data set to reverse engineer the values of such parameters.

The tumor cell includes nearly 19127 cross talks and interactions among approximately 6500 molecules (including genes, proteins and metabolites). The platform currently includes representation of comprehensive signalling pathways such as growth factors like EGFR, PDGFRA, FGFR, c-MET, VEGFR and IGF-1R, cell cycle regulators, mTOR signalling, p53 signalling cascade, apoptotic machinery, DNA damage repair, cytokine pathways like IL1, IL4, IL6, IL12, TNF; lipid mediators and tumor metabolism, ER and Oxidative stress and others. [1-6]

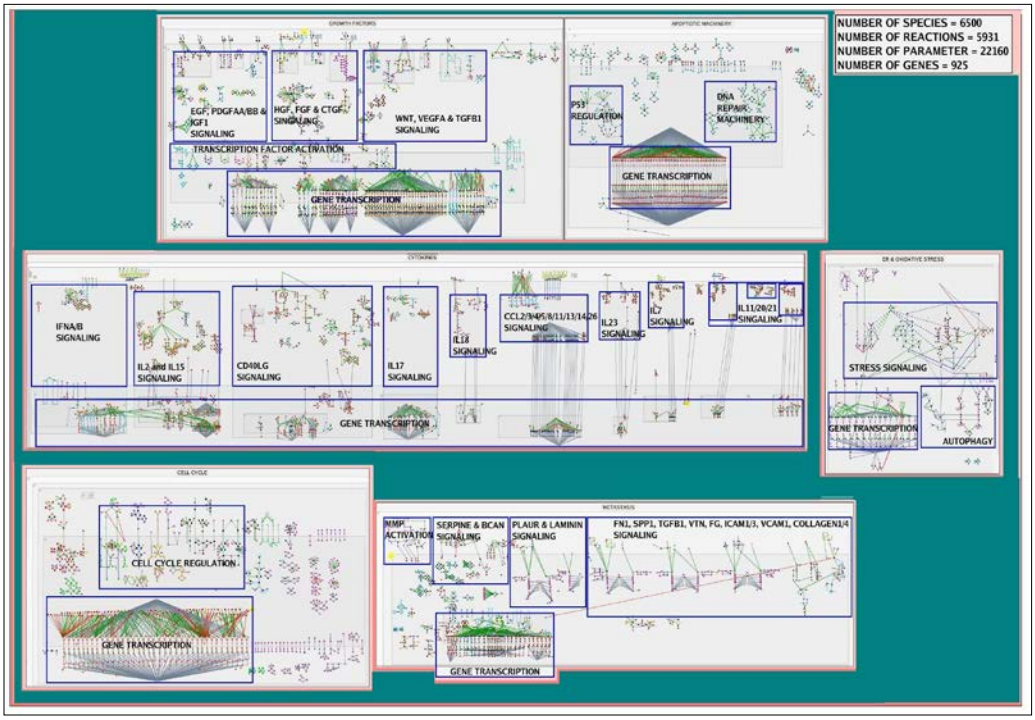

Figure 1A: A high level snapshot of the complex network of signalling pathways included in the predictive Tumor Cell Technology highlighting the key signalling blocks, secondary messengers, kinases, transcription factors etc.

The technology was extensively validated using more than 2000 studies and correlated with prospective and retrospective studies. Typical simulation based study time using this approach is 10-15 minutes of CPU time. The platform is constantly enhanced with on going incorporation of new published research and validations. Figure 1B shows a top

Nature Biotechnology doi:10.1038/nbt.3052

view of different interactions and cross talks between multiple pathways present in tumor cell platform.

A key assumption of the technology is, when a drug is introduced into the system, its concentration in the predictive experiment is explicitly assumed to be post ADME (Absorption, Distribution, Metabolism, and Excretion). The drug is assumed to be available at the site of action. In this kinetic based predictive tumor cell platform, there is no statistical variation in the outputs. The system provides predictive semi-quantitative trends visibility into all phenotypes and biomarkers.

Drug pair activity Prediction

The activity of given 14 pairs of compounds in the DLBCL LY3 cell line was predicted using Tumor Cell Technology platform. Figure 2 describes the process flow to conclude the drug combination prediction.

I. Creation of in silico equivalent of LY-3 cell lines

Tumor cell was customized to DLBCL LY-3 cell line based on different mutations, amplifications and deletions as given in the SNP data set. A basic assumption was made for the given data set, wherein, the normal cells were considered to have a copy no 2. Four class segments were considered abnormal segments based on their estimated copy number (C.N.)

- Single copy deletion (C.N. < 1.5)
- Double copy deletion (C.N. < 0.5)
- Gain of copy number (2.5 < C.N. < 3.5)
- Amplification (C.N. > 3.5)

Additionally a segment is called wild type, if (1.5 < C.N. < 2.5).

Nature Biotechnology doi:10.1038/nbt.3052

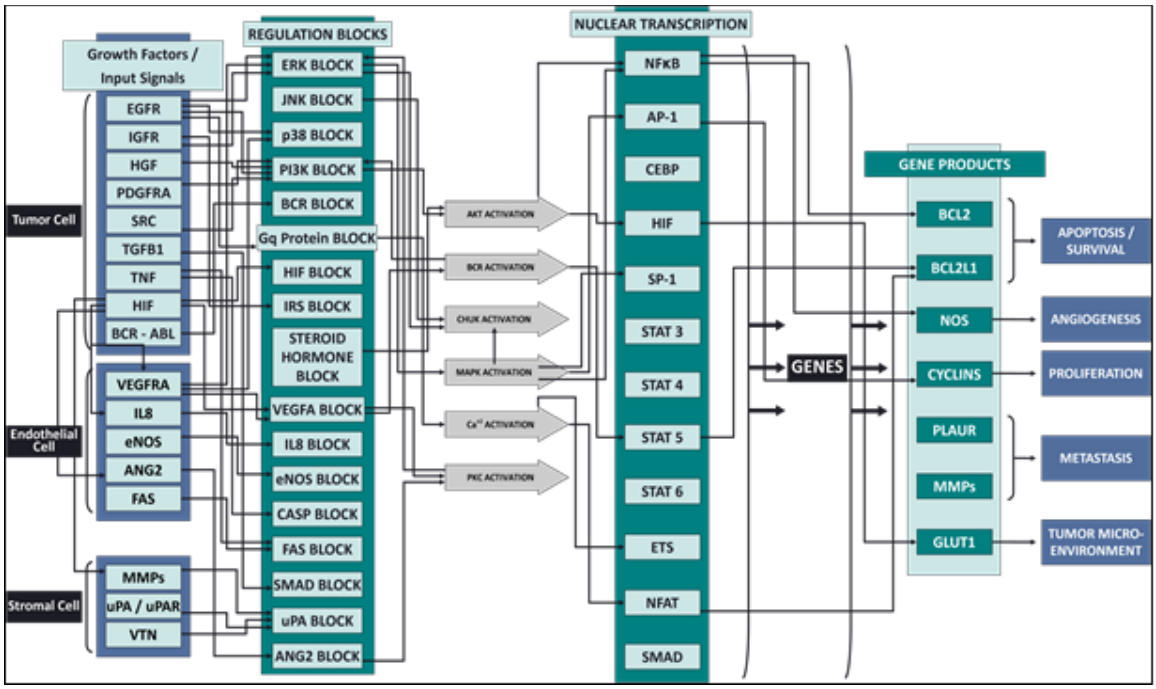

Figure 1B: A high-level view of the maze of interactions and cross-talks present in the Predictive Tumor Cell platform. The Cellworks Tumor Cell Technology on which predictive studies were conducted, is an integrated representation of the pathways in cancer that includes phenotypes of proliferation, apoptosis, angiogenesis, metastasis and conditions of tumor microenvironment such as tumor-associated inflammation.

Chromosome segments having double copy deletion and amplification are given more importance. Based on the above categorization, the final definition of DLBCL LY-3 cell line was shown to harbor mutations in the following genes -

NFkB (OE), MYD88 (OE), BCL2 (OE), IRF4 (OE), NFATC1 (OE), SRC (OE), CDKN2A (KD),CDKN2B (KD),PIM1 (OE), SMAD2 (OE), SMAD4 (OE), SMAD7 (OE), PIK3C3 (OE), PLCG1 (OE), PREX1 (OE), AURKA (OE), TP53 (Wild Type).

(OE – Over-expression; KD – Knockdown)

The predictive Tumor Cell Technology is simulated to control normal physiology state followed by overlaying the above mutations to dynamically transition to the cancer state that is aligned to the LY-3 profile.

Nature Biotechnology doi:10.1038/nbt.3052

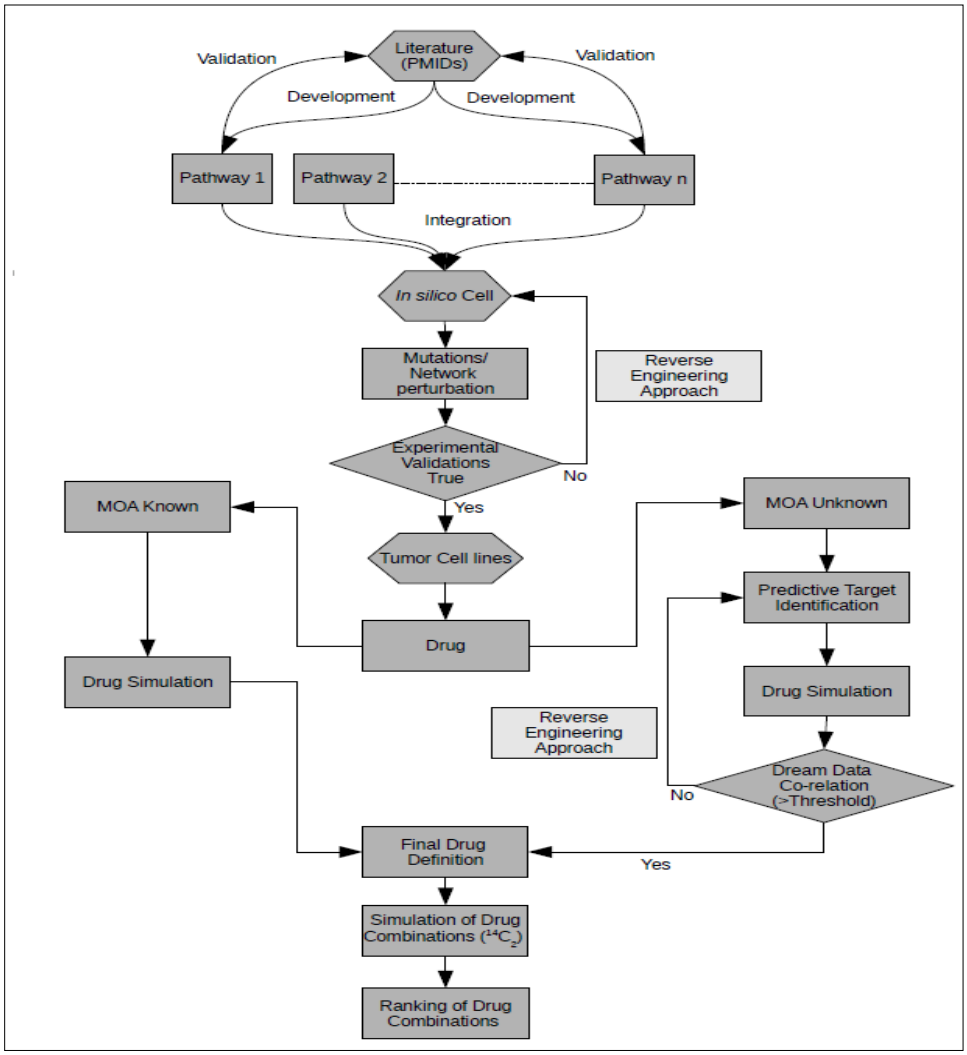

Figure 2: A high level schematic showing the process flow to predict the different drug combination effect using Cellworks Predictive Tumor Cell Technology.

II. Data Extraction and Normalization

From the list of ~20000 genes' compound treatment data set given as input, 482 genes were supported in the virtual Cellworks Tumor Cell system. The effect of compounds on these genes was extracted and compressed to a single entry by taking an average of values of replicates at 6, 12 and 24 hr respectively.

The expression of each gene was then normalized with respect to that in media treated cultures to arrive at percentage increase or decrease in each gene upon treatment with a particular drug. Now each gene had three entries in terms of percentage increase/decrease at IC_{20} drug concentration with respect to untreated at 6, 12 and 24 hr respectively. These three entries were filtered into a single entry. The one showing the maximum change in a particular gene was taken as the final data point for that gene. For eg: if for gene A, the data entry for 12 hrs was showing the maximum change, this data point was then considered for further analysis. So in the final normalized data set, each gene had single entry in terms of percentage increase/decrease at IC_{20} drug concentration.

Nature Biotechnology doi:10.1038/nbt.3052

III. Reverse Engineering Strategy to deduce Drug MOA

Customized LY-3 tumor cell line predictive system was trained for each of the 14 drugs at their IC_{20} drug concentration. Out of the 14 drugs, MOA for 2 drugs was relatively known - target therapy based drugs (Rapamycin and Geladinamycin) and these were put in the category of drugs with known MOA. These drugs were simulated at their IC_{20} concentration and used for further analysis. For rest 12 chemotherapeutic drugs where all targets of the compound were not known, basic definition of the drug was formulated based on the literature search for its targets and MOA. For instance, Aclacinomycin A is well reported to be a proteasome inhibitor, Camptothecin is a topoisomerase I/II inhibitor etc. Further refinement of the MOA of these drugs was done by reverse engineering the drug definition through iterative additions of most plausible targets to the initial drug definition and cross-checking the extent of correlation of experimentally determined gene expression data with that obtained in the simulation result for each version of drug definition, (where, drug definition is the collection of all molecules that are taken as direct targets of the drug and are consequently modified to mimic drug action). The correlation of simulation results with the experimental data was calculated in an automated manner where with simulation result corresponding to each version of the drug definition, the known experimental trends for the 452 genes were compared and percentage correlation was calculated. The drug definition achieving the best correlation percentage was frozen as the final definition. Here the threshold for acceptance was a minimum of at least 55% correlation. All the drugs defined in this way have been put in the final drug definition bucket at their IC_{20} concentration.

These drug definitions were further validated by comparing the dose-response of the drugs on viability with the experimentally determined compound titration curves shared by the DREAM team. IC_{20} values for different drugs predicted by the system were found to be in alignment with the experimentally determined IC_{20} at 48 hrs.

V. Synergy evaluation using the trained system

An in-house automated tool allows us to simulate all possible permutations and combinations for a given set of drugs where the best ones are filtered based on their effect on different phenotypes. The same was used to predict the combination effect of given 14 drugs on LY-3 tumor cell line system.

Effect of these combinations was checked on viability phenotype. Viability phenotype was defined in the system as the ratio of Survival and Apoptosis (Survival/Apoptosis). The survival phenotype has the key markers of survival pathways like AKT, BCL2 and BIRC5. Apoptosis phenotype includes the markers of extrinsic and intrinsic pathways of apoptosis like CASP3, BAX and PARP1.

The 91 combination pairs were ranked as synergistic, additive and antagonistic in accordance with the Bliss formula. The system predicted fractional inhibition induced by individual drugs and their combination. These fractional inhibitions were fitted in the Bliss formula and a value of c is determined ((c=A+B-A.B) where A and B are fractional inhibition by individual drugs) . Finally a Δ value was calculated ($\Delta = z - c$). Here z is the fractional inhibition by the combination. Combinations having Δ>1 were considered as synergistic. Δ<-1 were considered antagonistic and those between +1 and -1 were taken as additive.

References:

1. Cirstea, D., Hideshima, T., Rodig, S., Santo, L., Pozzi, S., Vallet, S., Ikeda, H., Perrone, G., Gorgun, G., Patel, K., Desai, N., Sportelli, P., Kaposi, S., Vila, S., Musketeer, S., Munster, N. C., Anderson, K. C., and Rae, N. (2010) Mo *Cancer Her* **9**, 963-975
2. Vila, S., Pahlavi, R., Kaposi, S., and Tatum, U. (2010) Cyst *Synch Biol* **4**, 25-33
3. Roy, K. R., Eddy, G. V., Maitreya, L., Agar, S., Achari, C., Vali, S., and Reddanna, P. (2010) *Cancer Chemother Pharmacol* **65**, 903-911
4. Rajendran, P., Ong, T. H., Chen, L., Li, F., Shanmugam, M. K., Vali, S., Abbasi, T., Kapoor, S., Sharma, A., Kumar, A. P., Hui, K. M., and Sethi, G. (2011) *Clin Cancer Res* **17**, 1425-1439
5. Shanmugam, M. K., Rajendran, P., Li, F., Nema, T., Vali, S., Abbasi, T., Kapoor, S., Sharma, A., Kumar, A. P., Ho, P. C., Hui, K. M., and Sethi, G. (2011) *J Mol Med (Berl)* **89**, 713-727
6. Kannaiyan, R., Hay, H. S., Rajendran, P., Li, F., Shanmugam, M. K., Vali, S., Abbasi, T., Kapoor, S., Sharma, A., Kumar, A. P., Chng, W. J., and Sethi, G. (2011) *Br J Pharmacol* **164**, 1506-1521

RANK 14

Inferring drug synergism via drug response pathways and publication co-occurrences

Summary Sentence: Inferring drug synergism via overlap of inferred drug response pathways and publication co-occurrences in PubMed.

Background/Introduction

A cell response to an external stimulus such as a small molecule or drug is assumed to initiate from its direct targets and mediated via a cascade of interacting proteins and expressed genes. The main assumption underlying our method is that the effect of two drugs affecting unrelated pathways is an additive one, while drugs affecting the same or cross-talking pathways will have a augmenting or inhibiting effect, depending on the relative expression direction of the genes shared by the two pathways (i.e. both regulated in the same – augmenting or opposite – inhibiting - directions).

To this end, we constructed drug response pathways connecting known drug targets with drug response gene expression signatures over a protein-protein and protein-DNA interaction networks. We then ranked the effect of two drugs based on the relative overlap of the two pathways and the expression direction of the genes included within them. Last, we employ a novel approach by using PubMed literature co-occurrences to estimate the boundary distinguishing between synergistic drug pairs and additive pairs.

Methods

For each of the 14 input drugs, we extracted a list of differentially expressed genes, relative to both media and DMSO samples using the Significance Analysis for Microarrays (SAM)[1] tool (False Discovery Rate<0.01), removing genes that were

Nature Biotechnology doi:10.1038/nbt.3052

differentially expressed when comparing between the media and DSMO samples. For Aclacinomycin A, we compared only to media, as none of the genes were differentially expressed compared to DMSO and media taken together.

We extracted drug targets for the input drugs from DrugBank [2], KEGG drug [3], TTD [4], SuperTarget [5] and Matador [5] databases and then used the ANAT tool [6] to construct the most probable pathways connecting the drug targets to the drug-induced differentially expressed genes via protein-protein and protein-DNA networks. Briefly, ANAT compromises between local (i.e. shortest paths) and global (i.e. Steiner tree) network approaches to extract the most probable sub-network connecting two sets of vertices (proteins). For drugs with no known targets, we constructed the most probable sub-network including only the differentially expressed genes, using the aforementioned tool.

For each pair of drugs, we computed a Jaccard score based on the gene co-occurrences in their drug-induced pathways (pathway overlap score). In order to differentiate between synergy vs. inhibition, we also scored each drug pair based on the agreement between the direction of the genes included in each drug-induced gene expression signature (i.e. up or down regulation) by computing the ratio between the number of common genes regulated in same directions and the number of genes regulated in opposite directions (regulation score). Thus, drug pairs with regulation score lower than one were considered inhibitory and were ranked below drug pairs with regulation score higher than one. Each of the groups (inhibitory vs. non-inhibitory) where then ordered according to decreasing pathway overlap score.

Finally, we extracted the frequency of drug name co-occurrences in PubMed and PubMed Central abstracts and full papers to compute the drug pairs that were prevalently co-mentioned in the literature (relative to their single name statistics).

Finding good agreement between drug pairs with high pathway overlap and drug with high co-mentioning, we set a literature co-occurrence threshold based on the score distribution as a proxy for synergistic effect between drugs, enabling us to set a threshold differentiating between synergistic and additive drugs.

Implementation was done in Matlab.

Conclusion/Discussion

The novelty in this work lies in the use of literature co-occurrence scores to set a threshold on pathway co-occurrence score. It is reassuring that these two scores agree (Pearson correlation between the two = 0.54, $p<4e^{-8}$), suggesting this integrated approach should be further explored.

References

1. Tusher, V.G., Tibshirani, R. & Chu, G. Significance analysis of microarrays applied to the ionizing radiation response. *Proceedings of the National Academy of Sciences* **98**, 5116-5121 (2001).

Nature Biotechnology doi:10.1038/nbt.3052

2. Wishart, D.S. et al. DrugBank: a knowledgebase for drugs, drug actions and drug targets. *Nucleic Acids Res* **36**, D901-906 (2008).
3. Kanehisa, M., Goto, S., Furumichi, M., Tanabe, M. & Hirakawa, M. KEGG for representation and analysis of molecular networks involving diseases and drugs. *Nucleic Acids Res* **38**, D355-360 (2010).
4. Zhu, F. et al. Update of TTD: Therapeutic Target Database. *Nucleic Acids Res* **38**, D787-791 (2010).
5. Gunther, S. et al. SuperTarget and Matador: resources for exploring drug-target relationships. *Nucleic Acids Res* **36**, D919-922 (2008).
6. Yosef, N. et al. Anat: A tool for constructing and analyzing functional protein networks. *Science Signalling* **4**, pl1 (2011).

RANK 15

Weighted Euclidean Distance for Predicting the Activity of Compound Combinations

Summary Sentence: A weighted Euclidean distance method was used to predict the activity of the pairs of compounds.

Background/Introduction

A weighted Euclidean distance was used to calculate the similarity between the time series profiles. We assume that the more similar or closer any given two compounds are, the more similar their response and hence their time series profiles. Euclidean distance has long been used to calculate similarities between different profiles and has been shown to achieve reasonable results as compared to more advanced methods (e.g., non-linear methods) in time series applications [1, 2]. The weight of every compound represents a "measure of importance" which is computed based on the individual compound activity of the 14 drugs provided in this challenge.

Methods

The data is partitioned into 14 groups; each group contains the time series profile of a single drug compound. Each drug compound is assigned a weight according to its rank based on its respective activity. Therefore, drug compounds with higher activity are assigned higher weights. For instance, the drug with the highest compound activity is assigned the highest weight of 14, while the drug with the lowest compound activity is assigned the lowest weight of 1.

$$Weight_i = Rank_{Drug_i} \; where \; i = 1 \ldots 14$$

Next, the weighted distance between all pairs of compounds is computed to obtain 91 similarity measures; where each similarity measure represents the distance between two different compounds across the different time points.

Nature Biotechnology doi:10.1038/nbt.3052

$$Distance(Drug_i, Drug_j) = \sqrt{\sum_{k=1}^{n}(Weight_i * Drug_{i,k} - Weight_j * Drug_{j,k})^2} \; where \; i \neq j$$

The 91 similarity measures were ranked from the most similar to the most dissimilar (e.g., from the most synergistic to the most antagonistic) to provide a ranked list in terms of efficacy of all the pairs of compounds in the DLBCL LY3 cell line.

Conclusion/Discussion

The weighted Euclidean distance provides a simplistic approach to calculating the similarity between the different profiles to predict the efficacy of all pairs of drug combinations. Therefore, the more similar two compounds are, the more alike their response should be and thus the more efficacious they should be. A disadvantage of this method is that it only accounts for linear relationships and does not capture non-linear dependence. Therefore, in future using a different distance function that accounts for non-linear relationships could improve the results (e.g., Dynamic Time Warping).

References

1. Ding, H., Trajcevski, G., Scheuermann, P., Wang, X. & Keogh, E. Querying and mining of time series data: experimental comparison of representations and distance measures. *VLDB*, 1542-1552 (2008).
2. Lu, Y. & Han J. Cancer classification using gene expression data. *Inform. Syst.*, 28243–268 (2003).

RANK 16

2-stage Drug Combination Efficacy Prediction

Summary Sentence: The method simulates the use of multiple compounds by first predicting the gene expression levels of each gene, which are then used to predict the viability reduction.

Background/Introduction

We approached the problem as two separate sub-problems. The first sub-problem is to predict the gene expression level of each gene, at each time-point and for both dosages for a given combination of compounds. In the challenge, only results of combinations of two drugs are requested, but in general multiple drugs could be used. The second sub-problem is then to use those gene expression levels in the construction of a model to predict the induced viability reduction *v*. This implicitly assumes that *v* is conditionally independent of the used compounds given the measured gene expressions of all genes. However, this may not hold in general since the compound may affect other quantities, which again may influence the viability reduction. Figure 1 shows a graphical representation of our approach.

A vital issue in the second sub-problem is that it requires data samples where *v* is measured, and has at least some variance. In the provided data however, *v* is either zero or 20% by design. But, as we noticed in the titration curves, the used drug concentrations

Nature Biotechnology doi:10.1038/nbt.3052

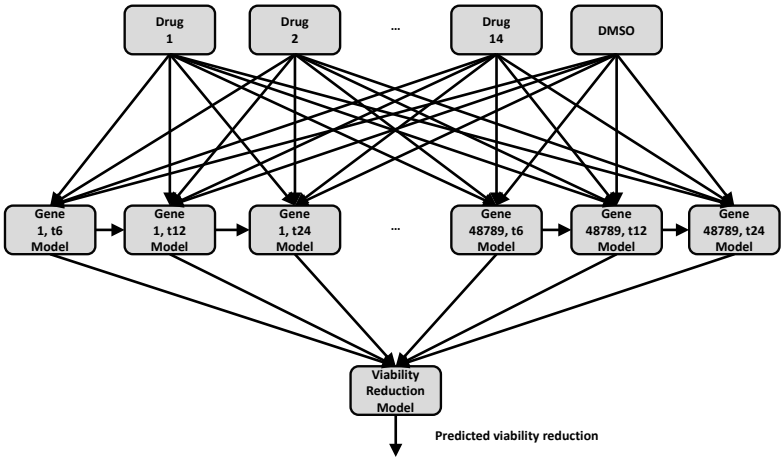

Figure 1: An overview of our approach. This model can simulate the effect of different

did not always correspond to a 20% viability reduction. It is thus plausible to use the real (estimated by the fitted curves) viability reduction value for each compound instead. Unfortunately, the fitted models were not provided and we had to estimate them from the titration curve plots. Additionally, since we had two concentrations for each drug, we used them to estimate the viability reduction after both 24 and 48 hours, effectively doubling the number of data samples. Specifically, if the IC_{20} of drug X is d_{24} μM and d_{48} μM for the 24 and 48 hour cases respectively, we estimated four viability reduction values: two for X after 24 hours, with d_{24} μM and d_{48} μM, and two for X after 48 hours, again with d_{24} μM and d_{48} μM.

In addition to the provided data, one could also use any other prior knowledge or available data. We did not use any other data sources; our method uses only data as provided in the competition.

Methods

The first sub-problem is to create models that are able to predict the gene expression level for each gene, at each time-point and for both concentrations. The available data are 2 replicates with growth media, 8 replicates with DMSO and growth media and 3 replicates for each compound with DMSO, for 3 different time points. The drug compound data were provided for two different dosages. Since sample size is low, we chose to fit linear models. Also, we chose to use the original gene expression values (not the logarithms) to train the models. The models are:

$$gene_{j,c,t_6} = w_{0,t_6} + w_{dmso,t_6} \cdot dmso + \sum_{i=1}^{14} w_{drug_i,t_6} \cdot drug_i$$

$$gene_{j,c,t_{12}} = w_{0,t_{12}} + w_{dmso,t_{12}} \cdot dmso + w_{t_6}.gene_{j,c,t_6} + \sum_{i=1}^{14} w_{drug_i,t_{12}} \cdot drug_i$$

$$gene_{j,c,t_{24}} = w_{0,t_{24}} + w_{dmso,t_{24}} \cdot dmso + w_{t_{12}}.gene_{j,c,t_{12}} + \sum_{i=1}^{14} w_{drug_i,t_{24}} \cdot drug_i$$

where j denotes the j-th gene and c the concentration. The variables dmso and $drug_i$ take values in {0,1}, taking the value 0 if not used in the specific data sample and 1 otherwise. The coefficients are different for each gene, but we used the same names for brevity. Also, we assumed that the value of each gene depends also on its value at the previous time-point.

Nature Biotechnology doi:10.1038/nbt.3052

After training all models, we used them to create two datasets, one for each concentration, as follows: for each gene and each time-point, we predicted the expression levels of each drug individually, with DMSO set to 1. We did this to deal with the multiple replicates. The new datasets contain $48789 \cdot 3 = 146367$ variables, where 48789 is the number of genes and 3 the number of different time-points, and 14 data samples, one for each drug. We used the log values of the data for the next step. Recall that we have two response values for each drug, one for each concentration. We concatenated the previously generated datasets into one dataset, containing the gene expressions for all genes at all time-points.

The next step is to train models that predict the viability reduction after 24 hours and after 48 hours. To avoid overfitting, we used nested-cross-validation, using the R^2 performance measure, and leaving one drug out at each step, i.e., leaving both samples corresponding to a drug out instead of leaving one sample out, since that could bias the results. We employed the following methods and parameters:

a) nu-SVR with polynomial kernel, degree 1, gamma set to 1, with nu varied in {0.01 0.015 0.02 0.03 0.05 0.1 0.15 … 0.9 0.95 1},
b) nu-SVR with radial basis kernel and gamma set to 1,
c) nu-SVR with sigmoid kernel and gamma set to 1,
d) epsilon-SVR with polynomial kernel, degree in {1,2}, and epsilon varied in {0.001 0.002 0.005 0.01 0.02 0.05 0.1 0.15 0.25 0.5},
e) tree-bagging, ensemble size varied in {5, 10, 20, 50, 100}, and minimum number of observations per leaf in {3,5},
f) least-squares boosting with trees, learning rate set to 0.1 and ensemble size in {100, 200, 500}.

Unless specified otherwise, all parameters are set to their default values. We used LIBSVM (Chang & Lin, 2011) for the SVM based methods, and the MATLAB implementations of bagging and boosting. We also performed feature selection using the following methods:

a) Univariate filtering (using the p-value of the Pearson correlation), with the α threshold varied in {0.0001, 0.0005, 0.001, 0.005, 0.01, 0.15, 0.2}
b) Lasso, with lambda varied in {0, 0.1, 0.5, 1, 10, 100}
c) MMPC (Tsamardinos, Brown, & Aliferis, 2006), with maxk (size of the maximum conditioning set) set to 1, and α (p-value threshold) set to {0.0001, 0.001}, and Fisher's z-transform of the partial correlation as the conditional independence test in MMPC.

We trained two models, one for predicting the viability reduction after 24 hours and one after 48 hours. To rank the combinations of drugs, we simulated the gene expression values for each gene and each combination, and used our models to predict the viability reduction. However, because the initial viability reduction of each drug was not always 20%, we scaled the results to estimate the case where both drugs were given with an IC_{20} concentration, as: $v_{scaled} = 0.36 \cdot \frac{v_{predicted}}{v_{additive}}$

Nature Biotechnology doi:10.1038/nbt.3052

We chose to submit the results of the first model (i.e. the effect after 24 hours), since they seemed more realistic. Alternatively, one could use a combination of both.

References

1. Chang, C.-C., & Lin, C.-J. (2011). LIBSVM: A library for support vector machines. *ACM Transactions on Intelligent Systems and Technology* , 27:1--27:27.
2. Tsamardinos, I., Brown, L. E., & Aliferis, C. F. (2006). The max-min hill-climbing Bayesian network structure learning algorithm. *Machine Learning* , 31--78.

RANK 18

Proteochemometric approaches for predicting cell line drug sensitivity

Summary Sentence: Pareto-ranking based on chemical & target similarity and potency.

Background/Introduction

- When looking at combinations of drugs, in an ideal situation one would like to have compounds that have a synergistic effect and are potent. Drugs are usually synergistic if they are both diverse in terms of chemical similarity as well as target similarity (the targets they are active on). Potency of the drugs was provided as the IC_{20} values.
- The method that was used was Pareto ranking based on the different features.
- To account for the target similarity in an indirect way, the Chembl-db[1] was included.

Methods

Because no potency of the combinations was known we applied a Pareto ranking strategy (Pipeline Pilot [2]; NSGA-II Pareto sorting algorithm).
For this ranking 6 properties were derived to perform an optimization strategy:

1. Chemical similarity calculated by converting the molecules to FCFP_6 fingerprints and using Tanimoto similarity (in Pipeline Pilot). This property was minimized (the higher the similarity the more likely 2 compounds will act in a similar fashion.)
2. IC^{ratio}, the ratio between IC_{20} - 48/ IC_{20} - 24 added for both drugs.
   This property was maximized.

3. IC_{20}-24, the IC_{20} at 24 hours of both drugs, this property was minimized.
4. IC_{20} 48, the IC_{20} at 48 hours of both drugs, this property was minimized.
5. Distance of the probe cell responses. Using a python script, the average of all three samples was taken and the media (baseline response) was subtracted. Then the Euclidean distance was calculated between two drugs and summed up for all the different hours. This property was maximized.
6. Chembl-db target similarity, the chembl-14[1] database was mined for activity values of the different compounds. Drugs were compared with each other on the different

Nature Biotechnology doi:10.1038/nbt.3052

targets using a python script. When two drugs shared a similar activity value on the same target (cutoff 25%) it was counted as 1. When they did not it was counted as 0. In this way the similarity could be calculated:

$$\frac{Actives}{Total} * (\log(total1)/\log(total2)) \; or \; \log(total2)/\log(total1))$$

Where total is the total number of activities for compound 1 or 2. If compound 1 had more activities then compound 2 the totals were switched. More activities usually means more confidence and in this way it is accounted for. This property was minimized. Based on the different properties a Pareto- sorting algorithm was applied on the different combinations. In this way combinations of compounds with a low IC_{20}, target and chemical similarity and a high probe cell response distance were sorted.

Conclusion/Discussion

Based on the methodology the ranking of compounds was obtained. When the compounds were only sorted on the distance of the probe cell responses it showed two drugs that shared a similar effect. This compound pair is not deemed to have a significant synergistic effect. These were Doxorubicin and Aclacinomycin A; interestingly enough they are chemically the most similar and share a similar substructure.

Usually however synergistic effects are not accounted for only by chemical diversity but also by the physicochemical properties that lead to activity on several targets or target classes. This was done by using the Chembl-DB and mining for activities of these compounds. In an ideal situation one would like to link the “systems chemistry” to the systems biology. Methods like the Similarity ensemble approach (SEA) [3,4, 5] relate the ligand similarity to the target poly- pharmacology; in this way a combination could have been chosen that was both chemically and pharmacologically diverse.

The method presented here to account for target similarity, by means of compounds that targets share, is relatively simple. In the future more sophisticated implementations should be considered.

References

1. Gaulton, A; et al. (2011). "ChEMBL: a large-scale bioactivity database for drug discovery". *Nucleic Acids Research*.
2. *Accelrys Software Inc, Pipeline Pilot, Scitegic*.
3. Keiser MJ, Roth BL, Armbruster BN, Ernsberger P, Irwin JJ, Shoichet BK. Relating protein pharmacology by ligand chemistry. *Nat Biotech* **25** (2), 197-206 (2007).
4. Lin, H., Sassano, M. F., Roth, B. L., & Shoichet, B. K. (2013). A pharmacological organization of G protein-coupled receptors. *Nature methods*
5. van Westen , G.J.P, Overington J.P (2013). A ligand's-eye view of protein similarity *Nature Methods*

Nature Biotechnology doi:10.1038/nbt.3052

RANK 19

Pathway guided synergy/antagonism scoring

Summary Sentence: Combined synergy and antagonism scores constructed from association of the drugs' gene effects, as measured over selected cellular signaling pathways

Introduction

This challenging task to predict the response of cells to drug pairs was structurally different from the training/test paradigm in part because learning was essentially unsupervised. Nevertheless we reasoned that benefit would follow from reducing complexity of the high-dimensional genomic data. We focused on genes within 15 core signaling pathways (apoptosis, base excision repair, cell cycle, MAPK, Notch, etc. Eng et al.) whose regulation is central to cell stasis and whose dysregulation is associated with cancer. After preprocessing gene-level data, we scored each pathway and drug pair on the aggregate agreement between effects these two drugs had on genes in the pathway. With very limited information, we reasoned that two drugs that affect the cell in opposite ways might be candidates for an antagonistic response, since effectively the two drugs would be canceling each other out. Similarly, drugs that affect the cell in the same ways might be candidates for an additive response, since, from the cell's perspective, having the two drugs is like having a double dose of either one. Finally, a synergistic response might be predicted if the drugs have more or less disjoint effects. Thus we constructed two metrics, one for synergy and one for antagonism, and then ranked lines by the difference. Aspects of the growth curves themselves were considered but not incorporated into the final ranking.

Methods

We reasoned that primary genomic signals would appear most readily at the 6 hours after treatment time point, and so we standardized expression data at that time by centering and scaling according to features of the matched DMSO control samples, yielding standardized gene/drug scores z [drug,gene] (for the 14 drugs and for genes within the 15 core signaling pathways). Seeking further noise reduction, we discretized these standardized effects:

$$\text{score[drug,gene]} = \begin{cases} -1 & \text{if } z[\text{drug,gene}] <= -1 \\ +1 & \text{if } z[\text{drug,gene}] >= +1 \\ 0 & \text{otherwise} \end{cases}$$

From these drug/gene scores we computed pathway statistics for the 15 core signaling pathways. In doing so, we said that drugs j and k agree at gene g if score[j,g]=score[k,g], and that a drug j affects gene g if score[j,g] is different from zero. Then pathway, drug-pair scores were derived as follows, for drugs j and k and pathway p:

$$\text{score}[p,j,k] = \{A[p,j,k] - B[p,j,k]\}/C[p,j,k]$$

Nature Biotechnology doi:10.1038/nbt.3052

where C[p,j,k] counts the number of genes in pathway p that are affected by either drug j or drug k, A[p,j,k] is the number of genes that are affected by both j and k and that agree, and B[p,j,k] is the number of genes where j and k disagree. These pathway drug -pair scores lie in [-1,1], like correlation, and have the similar property that +1 means the complete agreement in drug effects within pathway, zero means no association of effects, and -1 means completely opposite effects within pathway.

Two drugs that affect the cell in opposite ways might be candidates for an antagonistic response, since effectively the two drugs would be canceling each other out. Similarly, drugs that affect the cell in the same ways might be candidates for an additive response, since, from the cell's perspective, having the two drugs might be like having a double dose of either one. Finally, a synergistic response might be predicted if the drugs have more or less disjoint effects. Thus we constructed two metrics, one for synergy and one for antagonism, and then ranked lines by the difference:

$$\text{Synergy}[p,j,k] = C[p,j,k] * [\, 1 - \text{abs}(\, \text{score}[p,j,k] \,) \,]$$

$$\text{Antagonism}[p,j,k] = C[p,j,k] * [\, -\text{score}[p,j,k] \,]$$

$$\text{Overall}[j,k] = \text{sum\_}\{\text{paths } p\} \; \{ \, \text{Synergy}[p,j,k] - \text{Antagonism}[p,j,k] \, \}$$

Aspects of the growth curves themselves were considered but not incorporated into the final ranking.

Conclusion

The ranking of drug-pair effects on cell lines based on single drug data is extremely challenging. Success would seem depend on technical aspects of the drug-response measurements as well as detailed molecular effects of individual drugs, neither of which the present analysis explores more than superficially. Our scoring is based on conjectures (models) of the drug-interaction effects on the cell. In further work it would be interesting to test the suitability of these modeling assumptions by assessing them in the context of molecular signatures from pair-treated cells.

References

1. Eng, K., Wang, S, Bradley, W, Rader, J, and Kendziorski, C. 2012. Pathway-index models for construction of patient-specific risk profiles. *Statistics in Medicine*. doi: 10.1002/sim.5641 [Epub ahead of print].

RANK 20

Prediction of synergistic effect from transcriptome perturbation by single compound

Summary Sentence: For each pair of compounds, we design a cooperative score so that it is larger if these two compounds influence different set of transcripts (hence more likely to be synergistic) and it is smaller if these two compounds influence the same set of transcripts with reverse effect (hence more likely to be antagonistic).

Background/Introduction

This is a very challenging problem of predicting interaction effect while the data only provide marginal effect. Cancer is a complex genetic disease. Multiple pathways or gene sets are involved in cancer development [1], thus cancer treatment may require multiple compounds to simultaneously target multiple pathways or multiple genes in a pathway to completely stop tumor cell proliferation. Motivated by this consideration, we design a cooperative score for each compound pair to reflect the tendency that this pair of compounds has synergistic (larger cooperative score) or antagonistic effect (smaller cooperative score). We predict a synergistic effect if two compounds target different groups of transcripts; and we predict an antagonistic effect if two compounds target the same group of transcripts, but the effects are at different directions, e.g., if compound A increase the expression of a group of transcripts, while B decreases the expression of this group of transcripts, then the compound pair (A, B) has antagonistic effect.

Methods

Our method includes three steps. (1) Transcript filtering, to remove transcripts with low variation with respect to compound treatment. (2) Identify the transcripts that response to the treatment of each compound. (3) Calculate cooperative scores and rank compound pairs based on this score.

Gene Filtering

First, we identified the transcripts that had differential expression for at least one compound perturbation. Specifically, for each compound, we conducted a two-way ANOVA analysis of the expression of each transcript vs. time (6h, 12h, and 24h) and compound concentration (0, IC_{20} at 48 hrs, and IC_{20} at 24hrs), where the concentration 0 corresponded to the DMSO treatment. Each transcript had 14 ANOVA p-values corresponding to 14 compounds. We selected the 31,786 transcripts that had at least one p-value less than 0.01 for the following analysis.

Identify the transcripts that response to the treatment of each compound

Second, for a given compound concentration and for each transcript filtered by the previous step, we conducted three linear models tests to assess the compound treatment effect on the three time points. Then we combined the three t statistics by weighting them in the following way:

$$Wt_{concentration}=(2t_{6h}+2^{1/2}t_{12h}+t_{24h})/(4+2+1)^{1/2}$$

The weights were chosen so that those shorter-term responses had higher weights and those longer-term responses had lower weights. We used the 95% percentile for t-distribution with degree of freedom of 9 as a cutoff to select the transcripts whose expression were significantly perturbed by the compound treatment.

Nature Biotechnology doi:10.1038/nbt.3052

Calculate cooperative scores and rank compound pairs

Finally, we calculated the cooperative scores for each compound pair at each concentration. Specifically, for compounds A and B at concentration IC_{20} at 48hrs, we defined the following notations:

- n_A: the number of transcripts whose expression were significantly perturbed by compound A.
- n_B: the number of transcripts whose expression were significantly perturbed by compound B.
- n_{AB}: the number of transcripts whose expression were significantly perturbed by compounds A and B.
- r_{AB}: the correlation of weighted t statistics across all transcripts filtered by the first step.
- ρ_{AB}: the correlation of weighted t statistics across the transcripts whose expression were significantly perturbed by both compounds A and B.

Then the cooperative score for compounds A and B at concentration IC_{20} at 48hrs was

$$2(1 - n_{AB} / n_A) + 2(1 - n_{AB} / n_B) + r_{AB} + \rho_{AB} (n_{AB} / n_A + n_{AB} / n_B).$$

The first part of this cooperative score: $2(1 - n_{AB} / n_A) + 2(1 - n_{AB} / n_B)$ reflected the notion that the compound pairs that targeted different genes should have higher score. The later part of this cooperative score: $r_{AB} + \rho_{AB} (n_{AB} / n_A + n_{AB} / n_B)$ reflected the notion that the compound pairs with reverse effect were likely to be antagonistic and should have lower scores.

Similarly, we obtained the cooperative score at concentration IC_{20} at 24hrs by the same formula, and the final cooperative score was the average of cooperative scores at IC_{20} at 48hrs and IC_{20} at 24hrs. Finally, we assigned the ranks of compound pairs by the final scores in decreasing order; i.e., the compound pair with highest final score was given rank 1.

Conclusion/Discussion

The performance of our method can be improved by incorporating gene functional category or pathway information. For example, the expression change of some transcripts may have larger impact on cell survival because those transcripts encode proteins on the rate-limiting steps of cancer-related pathways.

References

1. Hanahan D, Weinberg RA. Hallmarks of cancer: the next generation. Cell. 2011 Mar 4;144(5):646-74.

Nature Biotechnology doi:10.1038/nbt.3052

RANK 21

Drug Combinatorial Effect Prediction by Consistently Differentially Expressed Genes

Summary Sentence: Calculate the similarity of drugs based on the consistently differentially expressed genes and then combine it with drug response curves to predict synergistic score.

Introduction

The basic assumption is that the combinatorial effect of drug pairs can be at least partly predicted by their similarity. Drug response curve can reveal the result if two same drugs are combined. Then the similarity between two drugs can help to build a model to calculate synergy score. We believe the genes consistently differentially expressed through three time points are the most informative data to estimate the similarity score between two drugs.

Methods

We applied linear regression model to the gene expression data for each drug and estimated p-values for differential expression for each gene. We applied a cutoff of 10% false discovery rate (FDR) to identify consistently differentially expressed across all three time points and took them as the cell-response-related key genes (CRK genes).

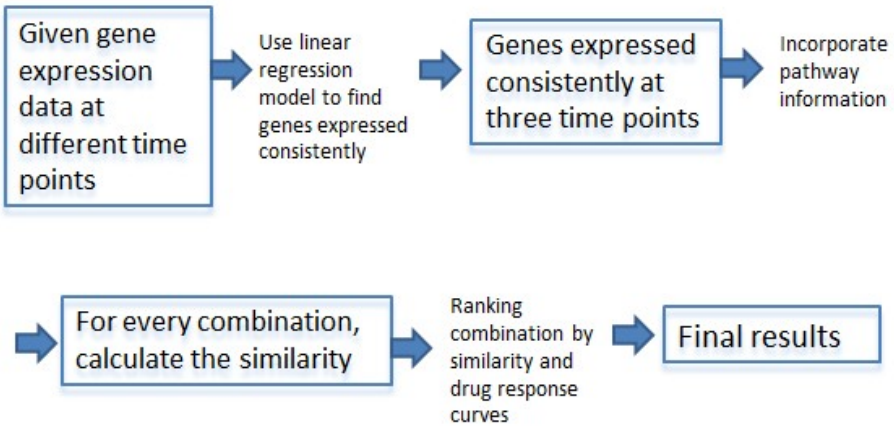

Figure 1: Work flow.

If two CRK genes target same pathway, we call them the same target genes. Then we find out those same target genes for each drug pair to calculate the similarity between the drugs. We predicted the effects of the combined treatment by considering the drug similarities and the drug response curve of each single drug. Particularly, we think if two drugs are more similar, the combinatorial effect will be closer to the effect of double doses of single drug. For each drug pair, we estimated its combinatorial effect by:

$$score = s * (X + Y)/2$$

Nature Biotechnology doi:10.1038/nbt.3052

Where *X* equals the percentage at which the cells were killed by two doses of drug A, *Y* equals the percentage at which the cells were killed by two doses of drug B. *s* is the similarity score. Finally, we calculated the synergistic index and rank the drug combinations (as shown in Figure 1).

Conclusion

The synergistic effect prediction is a challenging task. The combinatorial effect may come from either the similarity part of two drugs or different part of two drugs. Here we tried to calculate the similarity of two drugs based on the consistently differentially expressed genes and then applied it to derive the synergistic score by combining with drug response curve. The relatively poor performance indicates we may fail to find the underlying connection between drug response curve and gene expression profiles.

RANK 22

Predicting drug-drug interactions using bagged regression trees

Summary Sentence: Used bagged regression trees to build a machine-learning model to predict synergistic/additive/antagonistic drug interactions between pairs of drugs.

Introduction

Drug-drug similarities based on chemical structure of the drugs, sequences of the targeted proteins, or proximity of related proteins in the protein interaction network (PPI) have been successfully used in predicting drug–drug interactions [1, 2]. The current similarity-based approaches can predict interactions between drugs but cannot differentiate between a synergistic and an antagonistic interaction. So, we developed a more specific prediction model for specifically predicting synergistic, additive, or antagonistic interactions between drugs.

Data collection

Data for pairwise drug similarities features were collected from the following databases. Canonical simplified molecular input line entry specification (SMILES)[3] of the drugs was downloaded from DrugBank [4]. Drug targets were obtained from DrugBank [4], Matador [5], KEGG DRUG databases [6] and STITCH [7]. Protein sequences and Gene Ontology (GO) annotations were downloaded from National Center for Biotechnology Information (NCBI) database. A human PPI network was constructed from the BIOGRID database [8]. MeSH descriptor scores were obtained from Metab2MeSH database [9]. In total, we collected 124,301pairwise similarity features between 506 drugs.

We constructed a training set of 50 synergistic and 89 antagonistic drug pairs, so that we could apply supervised machine learning tools to this problem. These known drug interaction pairs were filtered from a much larger set of drug relations in the DrugBank [4] based on the description of the type of drug-drug interactions. Given that the drug interactions are rare [10], the rest of the drugs pairs between 506 drugs were considered additive interactions for this study.

Nature Biotechnology doi:10.1038/nbt.3052

Similarity measures
We calculated four drug–drug similarity metrics according to Gottlieb *et al.* [11]. Three of the drug–drug similarities are based on the drug targets (protein-related) obtained from DrugBank, KEGG drug and STITCH. All the similarity measures were normalized to be in the range (0, 1).

(1) Chemical structure based: Canonical SMILES [3] of the drug molecules were downloaded from DrugBank [4]. Hashed fingerprints were computed using the Chemical Development Kit with default parameters [12]. The similarity score between two drugs is computed based on their fingerprints according to the two - dimensional Tanimoto score [13], which is equivalent to the Jaccard score [14] of their fingerprints, i.e. the size of the intersection over the union when viewing each fingerprint as specifying a set of elements.

(2) Sequence based: This similarity metric is based on a Smith–Waterman sequence alignment score [15] between the drug-related genes for the pair of drugs. Following the normalization suggested in Bleakley and Yamanishi [16], we divide the Smith–Waterman score by the geometric mean of the scores obtained from aligning each sequence against itself.

(3) Closeness in a PPI network: The distances between each pair of drug-related genes were calculated on their corresponding proteins using an all-pairs shortest paths algorithm on the human PPI network. Distances were transformed to similarity values using the formula described in Perlman *et al.* [17]: Sp1,p2=Ae-bD(p1,p2), where S(p1,p2) is the computed similarity value between two proteins, D(p1,p2) is the shortest path between these proteins in the PPI network and A, b were chosen according to [17]to be 0.9 × e and 1, respectively. Self-similarity was assigned a value of 1.

(4) GO based: Semantic similarity scores between drug-related genes were calculated according to [18], using the csbl.go R package selecting the option to use all three ontologies [19].

(5) MeSH based: MeSH descriptor scores were used to produce compound-compound similarity scores based on Pearson correlation between profiles. The MeSH descriptors used fell under all possible MeSH headings in the database [9].

Regression tree modeling
We used regression trees to build a machine learning model using drug similarity features (see Similarity measures) to predict synergistic, additive, or antagonistic interactions between pairs of drugs given in the NCI-DREAM data. Regression values 1, 0 and -1 were assigned to synergistic, additive and antagonistic drug pairs respectively. To generate a robust prediction model, we used bootstrapping on two levels. The first level was to subsample the classes to reflect the expected prevalence of synergistic/antagonistic drug-drug interactions (we assumed 4–10% of all drug pairs [10]). Our training data contains 50 synergistic, 89 antagonistic, and 100,597 unknown (assumed to be additive [10]) drug pairs. We constructed 100 sets of training data, each

Nature Biotechnology doi:10.1038/nbt.3052

of which contained all synergistic/antagonistic interactions along with 1,250 additive interactions which were randomly chosen from the pool of 100,597 unknown interactions. For each training dataset created, we used a second level of bootstrapping, training 200 classifiers each based on a different subsampling (~63%) of the training samples. For any drug pair in the test data, we made 200 predictions using the generated 200 classifiers, and then aggregated them by taking the median prediction. We used the same aggregation strategy for the predictions from 100 different training datasets.

To determine the rank cutoff where the synergistic/antagonistic interactions are no longer significant, we evaluated the predictive models based on their performance on the held out 37% of training data for each second level run. The median of the predictions on the held-out training data across 200 runs was used for evaluation. More specifically, the cutoffs for synergistic and antagonistic interactions were selected based on receiver operating characteristic (ROC) curves. For the antagonistic interaction, we achieved a true positive rate of about 97% at a false positive rate of less than 0.05%. For synergistic interaction, the best true positive rate we obtained was about 68% at a false positive rate of around 0.05%.

We predicted the regression scores for the 91 drug pairs using the prediction model described above and ranked them from highest to lowest. The least rank where the interaction is no longer significantly synergistic is 21 and the maximum rank where the interaction is no longer antagonistic is 75. The additive cutoff score was determined by the significant synergistic interaction cutoff score from the training. That means we consider pairs from Ranks 1 to Rank 20 as synergistic interactions, and pairs from Rank 76 to 91 as antagonistic interactions.

Conclusion and discussion

Beyond the statistical evaluation of predictions for held-out examples described above, we manually examined evaluated our predictions for the 91 drug pairs and found many of them were supported by literature. For example, Doxorubicin and Etoposide has been found antagonistic in vitro activity of paclitaxel [20] and this drug pair is ranked 88th on our list. Another drug pair, Vincristine and Etoposide, is ranked 1st and [21] reported Vincristine as a supporting agent that may be coadministered with Etoposide during the cancer chemotherapies. However, drug-drug interactions are certainly cell-type specific and sensitive to environmental or experimental context. To improve the prediction performance, a list of gold standard drug-drug interactions derived from the same cell line and under the same experimental conditions may be beneficial. Furthermore, our approach has not used the genome-wide profiling data for this cell line, which could also be a fruitful direction for further improvement.

References

1. Assaf Gottlieb, G.Y.S., Yoram Oron, Eytan Ruppin, Roded Sharan, *INDI: a computational framework for inferring drug interactions and their associated recommendations.* Molecular Systems Biology, 2012. **8:592**.
2. Santiago Vilar, R.H., Eugenio Uriarte, Lourdes Santana, Raul Rabadan, Carol Friedman, *Drug–drug interaction through molecular structure similarity analysis.*

Nature Biotechnology doi:10.1038/nbt.3052

Journal of the American Medical Informatics Association, 2012.
3. Weininger, D., *SMILES, a chemical language and information system. 1. Introduction to methodology and encoding rules.* Journal of Chemical Information and Computer Sciences, 1988.
4. Knox, C., et al., *DrugBank 3.0: a comprehensive resource for 'omics' research on drugs.* Nucleic Acids Res, 2011. **39**(Database issue): p. D1035-41.
5. Gunther, S., et al., *SuperTarget and Matador: resources for exploring drug-target relationships.* Nucleic Acids Res, 2008. **36**(Database issue): p. D919-22.
6. Kanehisa, M. and S. Goto, *KEGG: kyoto encyclopedia of genes and genomes.* Nucleic Acids Res, 2000. **28**(1): p. 27-30.
7. Kuhn, M., et al., *STITCH: interaction networks of chemicals and proteins.* Nucleic Acids Res, 2008. **36**(Database issue): p. D684-8.
8. Stark, C., et al., *The BioGRID Interaction Database: 2011 update.* Nucleic Acids Res, 2011. **39**(Database issue): p. D698-704.
9. Metab2MeSH. Available from: http://ws.ncibi.org.
10. Cokol, M., et al., *Systematic exploration of synergistic drug pairs.* Mol Syst Biol, 2011. **7**: p. 544.
11. Gottlieb, A., et al., *PREDICT: a method for inferring novel drug indications with application to personalized medicine.* Mol Syst Biol, 2011. **7**: p. 496.
12. Steinbeck, C., et al., *Recent developments of the chemistry development kit (CDK) - an open-source java library for chemo- and bioinformatics.* Curr Pharm Des, 2006. **12**(17): p. 2111-20.
13. Tanimoto, T., *IBM Internal Report 17th Nov.* 1957.
14. P, J., *Nouvelles recherches sur la distribution florale.* Bul Soc Vaudoise Sci Nat, 1908. **44: 223–270**.
15. Smith, T.F., M.S. Waterman, and C. Burks, *The statistical distribution of nucleic acid similarities.* Nucleic Acids Res, 1985. **13**(2): p. 645-56.
16. Bleakley, K. and Y. Yamanishi, *Supervised prediction of drug-target interactions using bipartite local models.* Bioinformatics, 2009. **25**(18): p. 2397-403.
17. Perlman, L., et al., *Combining drug and gene similarity measures for drug-target elucidation.* J Comput Biol, 2011. **18**(2): p. 133-45.
18. P, R., *Semantic similarity in a taxonomy: an information-based measure and its application to problems of ambiguity in natural language.* J Artif Intell Res, 1999. **11: 95–130**
19. Ovaska, K., M. Laakso, and S. Hautaniemi, *Fast gene ontology based clustering for microarray experiments.* BioData Min, 2008. **1**(1): p. 11.
20. Viallet J, T.M., Gallant G., *Etoposide and doxorubicin antagonize the in vitro activity of paclitaxel in human non-small cell lung cancer cell lines.* Lung Cancer, 1996. **15**(1).
21. Takashi Kawashiro, K.Y., Xue-Jun Zhao, Eriko Koyama, Masayoshi Tani, Kan Chiba, Takashi Ishizaki, *A Study on the Metabolism of Etoposide and Possible Interactions with Antitumor or Supporting Agents by Human Liver Microsomes.* The Journal of Pharmacology and Experimental Therapeutics, 1998. **286**(3): p. 1294-1300

RANK 24

Predicting Drug Synergy by Analyzing Up/Down Regulated Genes in Multicomponent Therapeutics

Summary Sentence: First identify gene sets targeted by individual agents and then analyze pair-wise combination of these sets to determine drug synergism, antagonism, or additivism for pairs of drugs.

Background/Introduction:
The rationale behind our approach is as follows.

Two drugs will have an antagonistic effect if the set of genes up-regulated by one of the drugs significantly overlaps with the set of genes down-regulated by the other drug.

Two drugs will have an additive effect if the set of genes up/down-regulated by one of the drugs significantly overlaps with the set of genes up/down-regulated by the other drug.

Two drugs will have a synergistic effect if the set of genes up/down-regulated by one of the drugs does not significantly overlap with the set of genes up/down-regulated by the other drug. In other words two active drugs will have a synergistic effect when they are targeting genes associated with different biological pathways.

Methods
Each gene expression level for DMSO is compared against that of DMSO + drug using a t-test. We performed right- and left-tail tests to find out if the gene expression level perturbed by the drug + DMSO combination is statistically higher or lower than the gene expression level perturbed by the DMSO alone. If there is statistical significance ($p=0.0001$) then we considered that gene as a hit for that drug. If the drug + DMSO value is higher than that of DMSO alone we assumed that the gene is up-regulated by the drug. If the drug + DMSO value is lower than that of the DMSO alone we assume that the gene is down-regulated by the drug. We performed this analysis at each time point (6, 12, 24 hours) and for each dose level (IC_{20} at 24 and 48 hours) and merged the set of hits to obtain a combined set of up-regulated and down-regulated genes for each drug.

Once the sets of up- or down-regulated genes are obtained for each individual drug we compared these sets pair-wise to identify the degree of overlap between them.
The overlap between two sets is measured by the ratio of the number of genes in the intersection to the number of genes in the union of these two sets. For each pair of drugs two such measures are obtained. The first is the additive score that measures the overlap between genes regulated in the same direction by both drugs. The second is the antagonistic score that measures the overlap between genes regulated in the reverse direction by both drugs. These two values are assessed to rank drug pairs from most synergistic to most antagonistic.

Nature Biotechnology doi:10.1038/nbt.3052

Conclusion/Discussion
When the ranking of drug pairs obtained by this approach was compared against the experimentally-determined gold standard the results were found not statistically significant. We believe a more viable approach would require mapping hits onto known pathways and using this information to derive scores for drug synergism.

RANK 25

Over-representation of Genes With Respect to Function is a Very Weak Sign of Synergy

Summary Sentence: Modeled based on assumption that two drugs will act in a synergistic fashion if they perturb different genes with similar functionality.

Background/Introduction
We assumed that synergy would come from multiple drugs affecting different genes with similar function as these would then complement each other rather than be independent perturbations (Léhar et al., 2007; Yeh et al., 2009).

In order to detect this class of situations, we first detected a set of perturbed genes. We then mapped these to GO terms to obtain a set of perturbed GO terms. For any pair of drugs, we can measure the similarity between their perturbed GO term sets and predict the similarity in genes sets. If the actual similarity in genes is lower than predicted, then this pair is assumed to be synergistic.

Methods
As a first step, the media and DMSO data was used to determine a baseline variation and genes were considered disturbed if they moved more than 1.5 standard deviations away from the mean at any time point. This is a noisy measurement, but it will only be used very indirectly. We had tried stricter measures (e.g., 1.5 std. deviations on multiple time-points) but those led to a very small number of perturbed genes on some drugs (including no perturbation).

We applied the same procedure after grouping genes by GO terms. This grouping was performed by assigning to each GO term and condition the sum of all the expression value of all genes that are associated with this term. After filtering as above, we obtained a set of GO terms. Only the molecular function vocabulary was used for submission.

Each drug was thus characterized by two signatures:

1. A set of disturbed genes, represented as a binary vector,$\overrightarrow{g_i}$.
2. A set of disturbed molecular function GO terms, equally represented as a binary vector, $\overrightarrow{t_i}$.

Nature Biotechnology doi:10.1038/nbt.3052

For each pair of drugs, we computed the Pearson correlation of the gene perturbation vectors, $c(\overrightarrow{g_i}, \overrightarrow{g_j})$, and its GO terms perturbation vector, $c(\overrightarrow{t_i}, \overrightarrow{t_j})$. There is a roughly linear correlation between these two values, $c(\overrightarrow{g_i}, \overrightarrow{g_j}) \approx \alpha c(\overrightarrow{t_i}, \overrightarrow{t_j}) + \beta$,as can be seen in Figure 1.

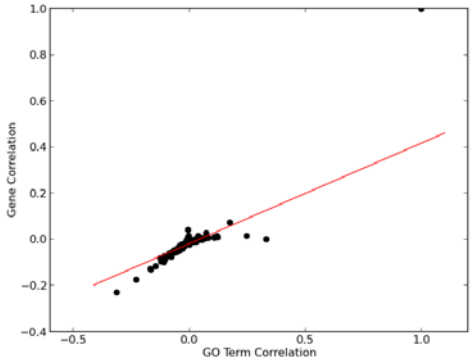

Figure 1: Gene correlations as a function of GO term correlations. Each circle represents a drug pair, the straight line is the best least-squares fit.

However, this is not perfect. The distance to the regression line is our measure of synergy. Drugs pairs for which the genes are less correlated than predicted by the correlation at the GO term were predicted to be synergistic.

Conclusion/Discussion

This method was very simple and it obtained only mediocre results. With the benefit of the testing data, which was not available at the time of the competition, we can test a few variations and measure whether they would have been better than the submission. In particular, the restriction to the Molecular Function vocabulary was somewhat arbitrary and we can test other GO vocabularies. In total, there are 6 possible combinations of vocabularies. The best result is the combination of the molecular function and the biological process vocabularies, but the p-value is 16%. The best single vocabulary is not molecular function, but biological process. In retrospect, this may have been a better embodiment of the idea that was underlying this method, but the result is still of limited value, as the resulting p-value is 21%.

Another variation results from reversing the prediction and predict GO term correlation based on gene correlation, with synergy being again measured as the deviation from prediction. The best results are obtained with the molecular function, or the biological process vocabularies, or both combined. These three combinations all result in p-values of 16% or 17%.

We thus conclude that fundamentally, this model was of limited value and a richer model would have been necessary for adequate prediction.

References

Nature Biotechnology doi:10.1038/nbt.3052

1. Cokol, Murat, Hon Nian Chua, Murat Tasan, Beste Mutlu, Zohar B. Weinstein, Yo Suzuki, Mehmet E. Nergiz et al. "Systematic exploration of synergistic drug pairs." *Molecular systems biology* 7, no. 1 (2011).
2. Yeh PJ, Hegreness MJ, Aiden AP, Kishony R (2009) Drug interactions and the evolution of antibiotic resistance. *Nat Rev Microbiol* **7**: 460–466
3. Lehár, Joseph, et al. "Chemical combination effects predict connectivity in biological systems." *Molecular systems biology* 3.1 (2007).

RANK 26

Adhoc inference of commonly targeted pathways

Summary Sentence: Inferred whether two drugs are targeting the same pathway, based on gene expression patterns, and then estimate the amount of synergy between the drugs, based on their targeting similar or different pathways.

Background/Introduction

The analysis was based on the following general assumptions:

- The effect of combined drug treatment on cells should be related to the individual IC_{20} of the two drugs separately. So, a drug that is more potent in the single treatment should be more potent in the combination treatment.
- If two different drugs are targeting the same pathway or process in cells, the gene expression profiles induced after treatment of the one drug should be similar to that of the other drug. If the two drugs are targeting different pathways, the two drug-inducible gene expression profiles should be more distinct from each other.
- Combination treatment with two drugs, where each targets a different pathway, ought to have more of a “synergistic” or more potent effect, than would two drugs that target the same pathway. In the former case, the cancer could be impacted in at least two different ways, versus targeting a single pathway or process.
- By 6 hours of treatment, early transcriptional effects induced by drug treatment should be observable. By 24 hours and later, more off-target and indirect effects would be observable in the expression data, such as any impact on cell cycle and cell proliferation. (This would be in line with observations made in other studies, such as those regarding estrogen or IGF treatment of breast cancer cells, and this would be the reason for focusing on the expression data from the 6h time point.)
- Without more complete information, one may not be able to make precise predictions of drug synergy, using the genomic data alone, but one might be able to make reasonable “ball park” estimates based on the above assumptions.

Methods

Nature Biotechnology doi:10.1038/nbt.3052

For each two drugs combination pair, the following equation was used to score the pair as an estimate for the potency:

$$(X + Y) + Z*(X + Y)$$

where

- X equals the relative $-\log(IC_{20})$ of the first drug (the $-\log(IC_{20})$'s of all the drugs being first centered so that the drug with the lowest $-\log(IC_{20})$ has a sensitive score of 0).
- Y equals the relative $-\log(IC_{20})$ of the second drug
- Z equals 0, if the drugs are inferred (using transcriptomic data) to target similar pathways, and 1, if the drugs are inferred to target different pathways from each other

Using the above, a combination would score highest, if both drugs individually had low IC_{20}'s (i.e. high $-\log(IC_{20})$'s) and if the two drugs were inferred to target separate pathways. A combination would score lowest, if both drugs individually had high IC_{20}'s and if the two drugs targeted the same pathway.

The determination of whether two drugs might target the same pathway ("Z" in the above equation) was determined in the following manner. For each drug, the gene expression profiles from the 6h treated group were compared with those from the DMSO 6h group (by student's t-test of the log-transformed data). Using all the genes represented in the dataset, for two given drugs, the (Pearson's) correlation was computed between the corresponding set of t-statistics (expressed as Pearson's r-values) from the treated versus untreated comparison. If this correlation r-value between the t-statistics was greater than 0.2, the two drug-induced expression profiles were deemed to be highly similar, and Z was set to 0; otherwise, Z was set to 1. The choice of r=0.2 for the cut-off was rather arbitrary. There were no strong anti-correlations observed between drug-inducible patterns; otherwise, in such a case, we might have penalized the combined score even further, if the two drugs were deemed to have antagonistic effects (e.g. set Z equal to -1).

"Camptothecin & Geldanamycin" was the pair put forth has having the additive effect, as that pair scored highest according to the above.

Conclusion/Discussion

The method did not perform well overall, and in fact gave significant predictions in the wrong direction. In terms of any benefit of our knowing what approaches did *not* work, this analysis description might be helpful.

RANK 27

A combined Bayesian and Cosine Distance Based Analysis of Time-Series Drug Response Data

Nature Biotechnology doi:10.1038/nbt.3052

Summary Sentence: BETR-NTP based analysis of time series drug response data.

Background/Introduction

In order to determine combination therapies that are effective, we developed an algorithm based on the following assumptions:

1. Cancer cell lines have distinct population of cells with different transcriptome profiles. Among the distinct population of cells, there are drug-resistant and -sensitive populations that can be identified after exposure to drug.
2. There are a population of cancer cells (probably cancer stem cells; CSC) that are intrinsically resistant to drug treatments whereas other population of cells (dubbed as non-CSC) are sensitive to the same treatment.
3. The change in transcriptome profiles is predominantly the result of a dominant population of CSC cells that are resistant to treatment.

Time-series drug response and molecular data provided in this challenge can be used to identify transcriptome profiles of CSC and non-CSC subpopulations of cells. We reasoned that combinations of two drugs that affect one way or the other both the populations of CSC and non-CSC cells are an effective pair. Our method did not use SNP profiles or IC_{20} values.

Methods

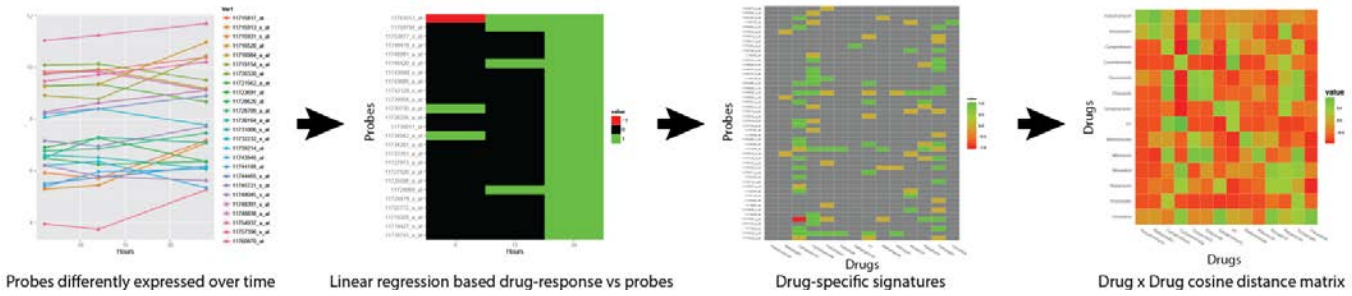

Figure 1: Summary of the methodology.

Identification of differentially expressed genes

The time-series transcriptome data provide the advantage to improve the sensitivity of detecting the changes over time, while noisy signals sustains across time point and can be removed. Common static gene expression analysis methods are not useful for these data. On the other hand, bayesian estimation of temporal regulation (BETR) correlates transcriptiome data and identifies genes that are differentially expressed between two consecutive time points[1]. R based BETR package[1] was used to select probes with differential expression for each drug against DMSO with a confidence of >95%.

Filtering of probes for each time point

In order to select the most relevant probes for each drug, we assumed that there is a linear correlation between drug dosage (0, IC_{20} at 48 hrs and IC_{20} at 24 hrs) and a subset of

Nature Biotechnology doi:10.1038/nbt.3052

probes. Linear regression for each probe was performed at a given time and the quality of the fitted model was determined by one-way ANOVA.

Identification of drug-response specific signatures
For a given drug and a time point, probes were clustered into two signatures depending on the sign of the slope. In total, 84 signatures were obtained (14 drugs x 3 time points x 2 up/down probes). The down-regulated genes were considered as representative of the drug effect (drug-effect signature, ***DES***) whereas up-regulated genes were considered as representative of the compensatory mechanisms that the tumor cells used to survive (drug-surviving signature, ***DSS***).

Derivation of the drug-drug interaction matrix
Nearest Template Prediction (NTP) algorithm[2] with cosine distance metric was used to associate all the samples that were treated with a particular drug (eg., drug A) to either DES or DSS of another drug (eg., drug B). Only those associations with Benjamini and Hochberg (BH) false discovery rate greater than 0.05 after NTP analysis were considered. A single score of cosine distance (*CD*) was calculated as below:

$$CD_x = \frac{1}{n}\left(\sum_i CD^i_{DSS} - \sum_j CD^j_{DES}\right)$$

where, CD_{DSS} and CD_{DES} represent distance (cosine distance) for each sample that were treated with drug A to that of the DSS and DES, respectively, from drug B. $n=i+j$, where i represents number of samples associated DSS and j represents the number of samples associated with DES.

Furthermore, the weighted (arbitrary weights) sum of the *CD* scoring across 3 time points was performed as below:

$$CD = CD_6 x(4/7) + CD_{12} x(2/7) + CD_{24} x(1/7)$$

where, CD_6 represents *CD* scoring for 6 h time point, CD_{12} for 12 h and CD_{24} for 24 h. This entire scoring system was repeated for all possible drug combinations leading to a final 14x14 interaction matrix. A final score was calculated as below:

$$S = CD_{AB} + CD_{BA}$$

Where CD_{AB} represents *CD* for drug A and the association of its samples with DSS and DES of drug B where CD_{BA} represents *CD* for drug B and the association of its samples with DSS and DES of drug A. The drug combination was considered synergistic if *S* is greater than $CD_{AA} + CD_{BB}$, and otherwise, additive.

Discussion

	BETR	Linear drug-gene at 6h	Linear drug-gene at 12h	Linear drug-gene at 24h

Nature Biotechnology doi:10.1038/nbt.3052

	# Probe	DES	DSS	DES	DSS	DES	DSS
Aclacinomycin	633	0	52	0	346	0	6
Blebbistatin	6519	0	413	5	1910	0	294
Camptothecin	14701	51	6240	1	5231	71	4177
Cycloheximide	18177	16	4671	2	4329	421	5602
Doxorubicin	10211	3	1439	27	2408	2	2779
Etoposide	2761	0	701	2	621	3	636
Geldanamycin	2460	1	958	0	597	7	520
H7	13368	9	3772	5	3017	50	759
Methotrexate	2912	17	166	2	270	12	1511
Mitomycin	2656	0	218	0	268	27	554
Monastrol	9334	1	1190	6	2160	178	2035
Rapamycin	8850	9	1515	2	1975	8	1217
Trichostatin	17440	7	5557	2	4982	1012	2404
Vincristine	573	0	59	0	189	0	105

Table 1: A summary of probes (DSS and DES) that were selected for each drug at different time points.

We observed that there was significantly less number of genes in DES compared to DSS in all the drugs, and this could have affected algorithm. In this case, logistic model may be suitable for the dose-response relationship. In addition, the association study using NTP algorithm could be improved by comparing transcriptome data of each drug to that of the other drugs.

Conclusion

Our ability to understand tumor response offers the possibility to anticipate the escape mechanism that tumors use.

References

1. Aryee, M.J., Gutierrez-Pabello, J.A., Kramnik, I., Maiti, T. & Quackenbush, J. An improved empirical bayes approach to estimating differential gene expression in microarray time-course data: BETR (Bayesian Estimation of Temporal Regulation). *BMC bioinformatics* **10**, 409 (2009).
2. Hoshida, Y. Nearest template prediction: a single-sample-based flexible class prediction with confidence assessment. *PloS one* **5**, e15543 (2010).

Nature Biotechnology doi:10.1038/nbt.3052

RANK 28

Predicting the synergistic effects of compound combinations from gene expression profiles after treatments of individual compounds

Summary Sentence: Build a model to predict the cell viability from a gene expression profile and then predict the expression profile of the cell line treated with the combined compounds based on the expression profiles after the treatments of individual compounds.

Background/Introduction

One of the most crucial aspects of a cellular state is its gene expression[1]. Previous studies have demonstrated that the gene expression pattern is very informative for inferring the phenotypic effect of cells such as drug response[2-4]. Therefore, one way to predict the synergistic effect of a compound combination on cell viability is to build predictive models from the gene expression profile of the cell line after the compound-combination treatment. However, due to the combinatorial complexity and experimental costs, the gene expression profiles for the compound combinations in this challenge are not available, and only the expression profiles after the treatments of individual compounds are available. Therefore, we used a two-step computational approach to predict the activity of a compound combination (Fig.1): (i) build a model to predict the cell viability from a gene expression profile; (ii) predict the expression profile of the cell line treated with the combined compounds based on the expression profiles obtained after the treatments of individual compounds.

Methods

1. Predict the cell viability from gene expression

In this challenge, a set of gene expression profiles of the LY3 cell line exposed to individual compounds, DMSO and media at three time points were provided. In addition, for each compound, we acquired the cell viabilities corresponding to the treatments of IC_{20}-24h and IC_{20}-48h from the given compound response curve of 24h. With the gene expression profiles and their corresponding cell viabilities, the main task here is to build a function f to predict the viability V of the cells based on their expression profile E (Fig. 1B). Then this task can be defined as a standard machine learning problem, i.e., we treated the cell viability as a response variable and gene expression at a time point (or expression difference between two time points or treatments) as independent variables (features). We used ANOVA to select genes that are significantly associated with the activity of a compound treatment. Significant genes were selected as candidate features (p-value < 0.0001). We then applied three machine-learning methods: random forest, support vector machine (SVM), and linear regression; and we used LASSO for feature selection. Based on the best performance of leave-one-out cross-validation, the model from SVM was chosen in which the expression differences of 13 genes between two treatment conditions (media and IC_{20} at 24h) were selected as the features. Then we used the obtained model to predict the cell viability treated with a compound combination.

Nature Biotechnology doi:10.1038/nbt.3052

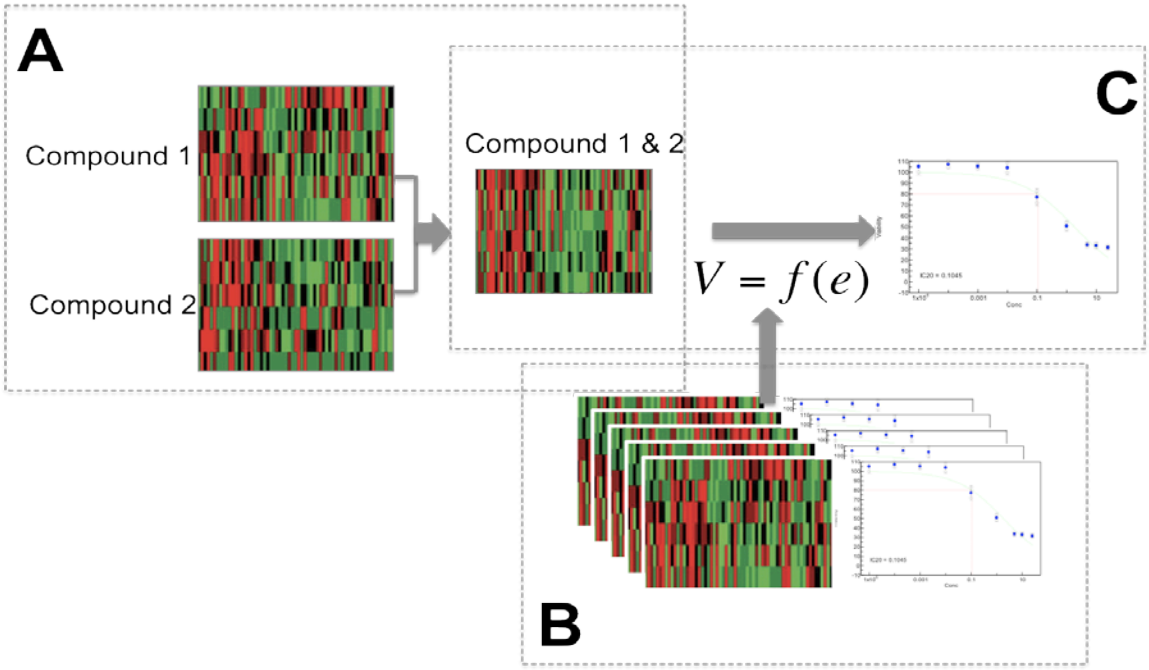

Figure 1: The analytic scheme for predicting the synergistic effects of compound combinations in a DLBCL cell line. (A) Predict the expression profile of the cell line treated with Compound 1 and Compound 2 based on those expression profiles after the treatments of individual compounds. (B) Construct a predictive model $V = f(e)$ using machine-learning methods, which takes the expression data as the input and the cell viability as the output. (C) The viability of the cell line treated with Compound 1 & 2 can be predicted based on the expression profile predicted in (A) and the model $V = f(e)$ built in (B).

2. Predict the gene expression profile after the treatment of a compound combination

To predict the cell viability from the model *V* obtained above, we need to predict the expression profiles of the selected genes for each compound combination (Fig. 1A). For each gene of interest, with the expression data at different time points and given different treatments (media, DMSO, compounds in different concentrations), we used an ANOVA-based linear regression model to decompose the gene expression profiles into several effects: the time effect, the compound effect and their interaction effect (if the item appears to be significant). Then we used the formula below to calculate the gene expression given a compound combination of "a" and "b".

$$E(a,b,t) = T_t + D_a + D_b + T_t : D_a + T_t : D_b$$

Here E is a function, where "a" and "b" are two compounds in some concentration, t represents a certain time point. T_t, D_a, D_b, $T_t : D_a$ and $T_t : D_b$ are decomposed expressions for a certain time, compound and interaction of the time and compound derived from the model. The interaction items were included only when they were statistically significant (*p*-value < 0.05). With the predicted expression profile of a compound combination, we then calculated the cell viabilities after the treatments using the model $V = f(e)$ built in the first step (Fig. 1C). Finally, we ranked the synergistic effects of all the compound pairs.

Nature Biotechnology doi:10.1038/nbt.3052

Conclusion
In this study, we proposed a novel method for predicting the synergistic effect of a compound combination. The main idea is to construct a model that links gene expression with the observed cell viability. The gene expression profile after a compound-combination treatment was predicted based on decomposed expression inferred by ANOVA. However, this approach may have some limitations. First, the expression profile is a complicated consequence involving many biological factors. Thus, the ANOVA linear model we used may not be able to predict the gene expression after the combination treatment accurately. Second, in this challenge, we had a very limited number of data points for cell viability, so the model *V* obtained by machine learning cannot well capture the complex relationships between gene expression and cell viability. In future, incorporating other biological profiling data may further improve the performance of the predictive models.

References

1. Rockman, M.V. & Kruglyak, L. Genetics of global gene expression. *Nat Rev Genet* **7**, 862-872 (2006).
2. Prins, R.M. et al. Gene expression profile correlates with T-cell infiltration and relative survival in glioblastoma patients vaccinated with dendritic cell immunotherapy. *Clinical cancer research : an official journal of the American Association for Cancer Research* **17**, 1603-1615 (2011).
3. van't Veer, L.J. & Bernards, R. Enabling personalized cancer medicine through analysis of gene-expression patterns. *Nature* **452**, 564-570 (2008).
4. Emilsson, V. et al. Genetics of gene expression and its effect on disease. *Nature* **452**, 423-428 (2008).

RANK 29

Synergy Prediction by Interpolation of Drug Response Curve

Summary Sentence: Predict drug synergism via drug response interpolation based on gene expression patterns.

Introduction
The similarity between two drugs was calculated to predict synergistic effect. Furthermore, we think the drug response curve can provide information to indicate whether the similarity will lead to synergistic or antagonistic. For example, we can directly read how many cells will be killed from the drug response curve if two drugs are exactly same.

Methods
The method includes steps are as follows,

1. Gene expression data pre-processing: Normalized the gene expression data against DMSO samples.

Nature Biotechnology doi:10.1038/nbt.3052

2. Only select gene expression data at 24hr because it is closer to the time point when gold standard is calculated.
3. Use fold change to find differentially expressed genes.
4. Find the differentially expressed genes overlapping between each drug pair and use it to estimate the similarity for each pair.
5. Use similarity as the coefficient to do linear interpolation between two dose points on each drug response curve.
6. Take the interpolation result as the contribution for each drug and then calculate the synergistic score.

Conclusion

The performance of this method is poor. There are several possible reasons: 1) only considering the overlap between the differentially expressed genes may be not enough to get similarity score between two drugs. Different gene targets within same pathway may provide similar treatment effect and contribute to the similarity between two drugs. 2) Simple interpolation formula may be not suitable in such a complex biological environment.

RANK 31

Responses to individual drugs vs. Response of their combination

Summary Sentence: Measure drug similarity by computing correlation between gene expression profiles of drug treated samples and use this similarity to induce an ordering of drug combinations.

Background/Introduction

We tested whether similarity between responses to two individual drugs can predict effect of their combination, synergistic or antagonistic. For example, we wanted to know that if two drugs lead to similar response, do they tend to be antagonistic or synergistic? Similarly, if two drugs lead to different responses, do they tend to be synergistic or antagonistic?

Methods

The method we used is described in the following:

1. Normalize expression data against DMSO

   We normalize the treatment expression data with respect to the DMSO data. Basically, for each drug, each concentration and each time point, we find the corresponding time point in DMSO condition, and compute the difference between the mean of the 3 replicates of the treated samples and the mean of the 8 replicates of DMSO.

   After normalization, the data for each drug and each concentration becomes a 3-column matrix whose size is the number of genes * 3 time points. These data represent the expression deviation of treated time series with respect to the DMSO time series.

2. Select features

Nature Biotechnology doi:10.1038/nbt.3052

We take all normalized data (a matrix with 14*2*3 columns), compute the sum of absolute value of the normalized data for each gene, and select the top 3000 genes that show maximum deviation between treatment and DMSO.

3. Evaluate similarity between each pair of drugs

To evaluate the similarity for each pair of drugs, we used the expression data for selected 3000 genes to compute correlations. For two drugs, we computed the correlation between the 6hr-3000gene-data of the two drugs, which is the similarity of those two drugs at 6hr. We also computed the same correlation for the other time point. After that, we obtained two values between that pair of drugs, and then took the sum of the two correlation values. The sum represented one overall similarity score between the two drugs. This calculation is performed for each pair of drugs. For final submission, we rank-ordered all the drug combinations according to this score. According to the evaluation score, drugs that induce similar expression change tend to be antagonistic, whereas drugs that induce different expression change tend to be synergistic.

Conclusion/Discussion

After the gold standard and scores were released, we noticed that our prediction scored poorly. Therefore, the conclusion here is: the effective of a drug combination cannot be predicted by simply looking at the similarity of responses to individual drugs.

SynGen

SynGen: Inferring synergistic interaction by prediction of complementary regulatory mechanisms implementing cell toxicity

Mariano J. Alvarez, Yao Shen, Andrea Califano

Summary Sentence: SynGen Algorithm: Regulatory network-based inference of compounds implementing a given phenotypic outcome through complementary regulatory mechanisms.

Background

Cell regulatory networks propagate changes in the activity of a few regulatory proteins into specific differential gene expression profile (GEP) signatures. Conversely, we have shown that interrogation of cell specific regulatory networks with GEP signatures representative of specific biological phenotypes allows systematic inference of master regulator (MR) genes causally associated with their implementation (1,2).

Given a specific cellular context, suppose that a GEP signature associated with cell death were implemented by a specific MR activity pattern. Then, it is reasonable to expect that any small molecule whose perturbation recapitulates the same MR pattern should also induce cell viability reduction. The SynGen algorithm extends this simple concept to predict compound combinations that synergistically induce loss of cell viability by implementing distinct yet complementary subsets of a given cell death MR activity pattern.

Nature Biotechnology doi:10.1038/nbt.3052

Method

Given a specific cellular context, suppose that a gene expression signature *CD* associated with cell death were implemented by a specific MR activity pattern $MR_{CD} = \{MR_1^R \downarrow, MR_2^R \downarrow, \dots, MR_M^R \downarrow, \dots, MR_1^A \uparrow, MR_2^A \uparrow, \dots, MR_N^A \uparrow\}$. Then, it is reasonable to expect that any small molecule, whose perturbation recapitulates the same MR pattern, should also induce cell viability reduction. By trivial extrapolation of this concept, two compounds, C_1 and C_2, whose individual perturbations induce distinct but complementary MR activation patterns MR_{C1} and MR_{C2}, such that $MR_{C1+C2} = (MR_{C1} + MR_{C2})/2$ recapitulates the *CD* signature more closely than the compounds C_1 and C_2 in isolation, should likely induce synergistic cell death. As a result, we need a metric to evaluate the complementarity of the MR activity pattern induced by two compounds as well as one to evaluate the similarity of the compound induced MR activity patterns with the desired one. We propose the following metric:

$$Z = \mathrm{ES}(MR_{CD}, (MR_{C1} + MR_{C2})/2) - \max\big(\mathrm{ES}(MR_{CD}, MR_{C1}), \mathrm{ES}(MR_{CD}, MR_{C2})\big)$$

Here, ES is the enrichment score representing the similarity between two MR activity patterns using a two-way two-tail enrichment analysis method (3,4). For example, $ES(MR_{CD}, MR_{C1})$ is the similarity between the targeted MR_{CD} and the compound induced MR_{C1}. To compute this score, we divided the query gene set into two subsets: a positive subset containing the 50 most activated regulators in the query signature (MR_{C1}), and a negative subset encompassing the 50 most inactivated regulators in the query signature. The target signature (MR_{CD}) was then sorted from the most activated to the most inactivated regulator (signature A) and the rank positions for the positive query subset were computed. The rank positions for the negative subset were computed from the target signature, but this time sorted from the most inactivated to the most activated regulator (signature B). The enrichment score (ES) was computed as described (10), using the computed rank positions for the positive and negative subsets, but taking the score values only from signature A. The normalized enrichment score (NES) was estimated by uniformly permuting the query signature ranks 10,000 times. Reciprocally, we computed the enrichment score ($ES_{C1,CD}$). Finally, we define ES(MR_{CD}, MR_{C1}) as the average of $ES_{CD,C1}$ and $ES_{C1,CD}$, representing how similar the targeted MR_{CD} and the compound induced MR_{C1} are. If the average of the two compounds implementing a MR activity pattern is more similar to MR_{CD} than any of the two individual compounds, we would get a score Z > 0 indicating synergistic effect.

To compute the MR activity pattern of a specific signature, either associated with a desired outcome phenotype (e.g. viability reduction) or with a drug perturbation phenotype, we use the MARINA algorithm (1). Briefly, we reconstructed a B-cell interactome generated by ARACNE (5,6) using *in-vivo* B-cell tumor samples (GSE16131 (7), GSE4475 (8)) to represent the regulatory mechanisms in DLBCL Ly3 cell line. Given this specific regulatory model and the compound perturbation gene expression signature, MARINA determines the MRs whose activation or inactivation is most likely to have contributed to the signature implementation.

So now the remaining question is how to chose appropriate toxicity signatures inducing cell death.

Nature Biotechnology doi:10.1038/nbt.3052

For the inference of compound that synergistically induce cell viability reduction in a specific line, we propose using two relatively orthogonal gene expression signatures: (a) a ***generic toxicity signature*** (GTS), directly associated with cell viability reduction induced by chemotoxic compounds; and (b) an ***oncogene addiction signature*** (OAS) based on the broadly accepted observation that inhibition of the master regulators that are responsible for maintaining the oncogenic state of the cell elicits oncogene addiction and thus cell viability reduction. SynGen integrates the predictions based on both cell death signatures by taking the maximum synergistic score: $\max(Z_{GTS}, Z_{OAS})$.

To define the GTS, we used the molecular profile obtained following perturbations with compounds that induced toxic response in the Ly3 cell line, as reported by the compendium of toxicity profiles of the individual compounds in the DREAM dataset. Specifically, there are two different concentrations at which each compound in this study was profiled: one corresponding to the IC_{20} viability, as measured at 24h, and the other to the IC_{20} viability, as measured at 48h. We reasoned that for any toxic compound, the difference of the MRs' activities between the high and low concentration of the same compound mainly represents the toxicity signature elicited by the compound. We thus obtained the GTS by averaging the toxicity profiles across all the 14 compounds.

Then, we generated the OAS by inferring the master regulators driving the phenotypic difference between 5 Germinal Center B-Cell (GCB-subtype) DLBCL cell lines (Ly1, Ly7, Ly8, Ly18 and SUDHL5) and the Activated B-Cell (ABC-subtype) DLBCL Ly3 cell line (9) by the MARINA algorithm. We found 9 out of 14 drugs from the DREAM dataset that significantly reversed this ABC-DLBCL subtype-specific signature, suggesting their preferential activity on the Ly3 cell line compared with the other GCB-subtype DLBCL cell lines.

Conclusion and Discussion

The heatmap in Fig.1 (left) shows the results of our synergy analysis using both signatures. As shown in the ROC curve in Fig.1 (right), based on comparison of these predictions with assays validating each of the 91 candidate combinations of 1 individual compounds, the approach was highly effective in inferring bona fide synergistic compound interactions. Specifically, 69% of the experimentally validated synergistic compound pairs were identified among the top 20% of the predictions (11 out of 16 validated predictions).

Nature Biotechnology doi:10.1038/nbt.3052

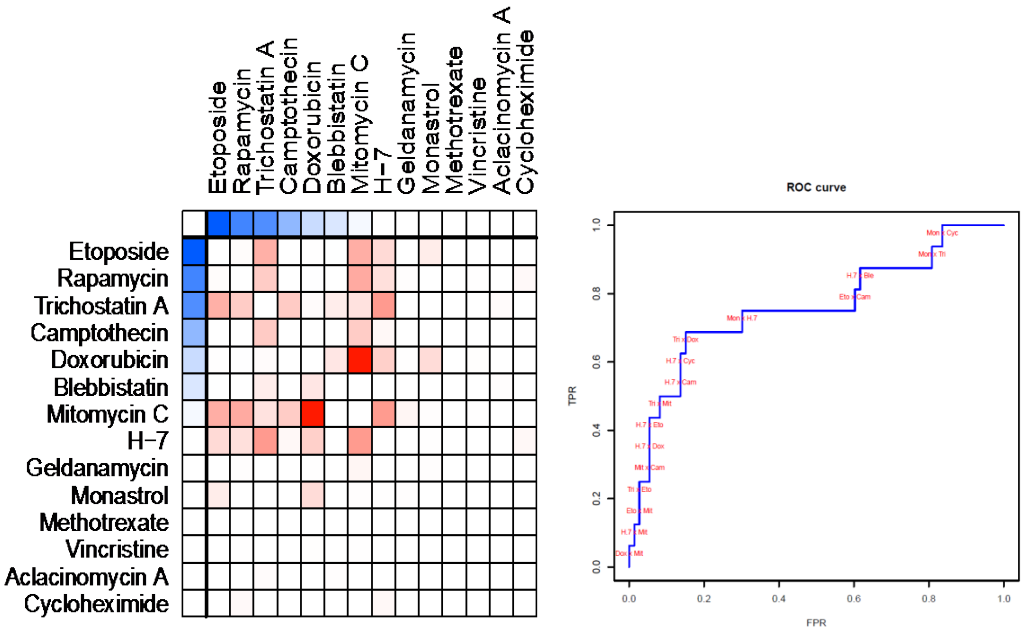

Figure 1: (Left) Heatmap showing the predicted synergy score for all combinations among the 1 compounds (shown in red), and the average enrichment of each compound TF activity signature on the target TF activity signatures (shown in blue). (Right) Receiver operating characteristic curve showing the prediction of synergistic interaction for all combinations of the 1 assessed compounds. Indicated are the 16 compound pairs found by Bliss to be synergistic.

Notably, the SynGen algorithm is only designed to predict synergy and is not effective in predicting antagonism. As a result, we used a purely synergy based metric for evaluation, different from that of the DREAM challenge, which evaluates both the ability to predict synergistic and antagonistic interactions. This has the added benefit of preventing any direct comparison between SynGen and the algorithms used in the DREAM challenge, which would be unfair, since the latter were tested in truly blind fashion, while SynGen was tested using the standard predict-and-validate methodology. Notably, since SynGen is not based on machine learning but rather on model based prediction from first principle, there are virtually no parameters that could be tuned or changed to improve the algorithm performance. Indeed, the regulatory model was previously published, the signatures are generated directly from experimental data, and the MRs were inferred using the published MARINA algorithm, using standard parameters.

References:

1. Lefebvre C, Rajbhandari P, Alvarez MJ, Bandaru P, Lim WK, Sato M, et al. A human B-cell interactome identifies MYB and FOXM1 as master regulators of proliferation in germinal centers. Mol Syst Biol. 2010; 6:377
2. Carro MS, Lim WK, Alvarez MJ, Bollo RJ, Zhao X, Snyder EY, et al. The transcriptional network for mesenchymal transformation of brain tumours. Nature. 2010;463(7279):318-25.

Nature Biotechnology doi:10.1038/nbt.3052

3. Lim WK, Lyashenko E, Califano A. Master regulators used as breast cancer metastasis classifier. Pac Symp Biocomput. 2009:504-15.
4. Kruithof-de Julio M, Alvarez MJ, Galli A, Chu J, Price SM, Califano A, Shen MM. Regulation of extra-embryonic endoderm stem cell differentiation by Nodal and Cripto signaling. Development. 2011;138(18): 3885–3895.
5. Margolin AA, Nemenman I, Basso K, Wiggins C, Stolovitzky G, Dalla Favera R, et al. ARACNE: an algorithm for the reconstruction of gene regulatory networks in a mammalian cellular context. BMC bioinformatics. 2006;7 Suppl 1:S7.
6. Basso K, Margolin AA, Stolovitzky G, Klein U, Dalla-Favera R, Califano A. Reverse engineering of regulatory networks in human B cells. Nat Genet. 2005;37(4):382-90.
7. Leich E, Salaverria I, Bea S, Zettl A, Wright G, Moreno V, Gascoyne RD, Chan WC, Braziel RM, Rimsza LM, Weisenburger DD, Delabie J, Jaffe ES,Lister A, Fitzgibbon J, Staudt LM, Hartmann EM, Mueller-Hermelink HK, Campo E, Ott G, Rosenwald A. Follicular lymphomas with and without translocation t(14;18) differ in gene expression profiles and genetic alterations. Blood. 2009;114(4):826-34.
8. Hummel M, Bentink S, Berger H, Klapper W, Wessendorf S, Barth TF, Bernd HW, Cogliatti SB, Dierlamm J, Feller AC, Hansmann ML, Haralambieva E, Harder L, Hasenclever D, Kühn M, Lenze D, Lichter P, Martin-Subero JI, Möller P, Müller-Hermelink HK, Ott G, Parwaresch RM, Pott C, Rosenwald A, Rosolowski M, Schwaenen C, Stürzenhofecker B, Szczepanowski M, Trautmann H, Wacker HH, Spang R, Loeffler M, Trümper L, Stein H, Siebert R. A biologic definition of Burkitt's lymphoma from transcriptional and genomic profiling. N Engl J Med. 2006;354(23):2419-30.
9. Bea S, Zettl A, Wright G, Salaverria I, Jehn P, Moreno V, Burek C, Ott G, Puig X, Yang L, Lopez-Guillermo A, Chan WC, Greiner TC, Weisenburger DD,Armitage JO, Gascoyne RD, Connors JM, Grogan TM, Braziel R, Fisher RI, Smeland EB, Kvaloy S, Holte H, Delabie J, Simon R, Powell J, Wilson WH,Jaffe ES, Montserrat E, Muller-Hermelink HK, Staudt LM, Campo E, Rosenwald A. Diffuse large B-cell lymphoma subgroups have distinct genetic profiles that influence tumor biology and improve gene-expression-based survival prediction. Blood. 2005;106(9):3183-90.
10. Subramanian, A. et al. Gene set enrichment analysis: a knowledge-based approach for interpreting genome-wide expression profiles. Proc. Nat. Acad. Sci. USA 102, 15545–50 (2005).

Supplementary Figures

A community computational challenge to predict the activity of pairs of compounds

Mukesh Bansal[1,2,18], Jichen Yang[3,18], Charles Karan[4,18], Michael P Menden[5], James C Costello[6,61], Hao Tang[3], Guanghua Xiao[3], Yajuan Li[7], Jeffrey Allen[3,7], Rui Zhong[3], Beibei Chen[3], Minsoo Kim[3,8], Tao Wang[3], Laura M Heiser[9], Ronald Realubit[4], Michela Mattioli[10], Mariano J Alvarez[1,2], Yao Shen[1,2], NCI-DREAM community[11], Daniel Gallahan[12], Dinah Singer[12], Julio Saez-Rodriguez[5], Yang Xie[3,8], Gustavo Stolovitzky[13] & Andrea Califano[1,2,14–17]

[1]Department of Systems Biology, Columbia University, New York, New York, USA. [2]Center for Computational Biology and Bioinformatics, Columbia University, New York, New York, USA. [3]Quantitative Biomedical Research Center, Department of Clinical Sciences, University of Texas Southwestern Medical Center, Dallas, Texas, USA. [4]Columbia Genome Center, High Throughput Screening Facility, Columbia University, New York, New York, USA. [5]European Molecular Biology Laboratory, European Bioinformatics Institute, UK. Wellcome Trust Genome Campus, Hinxton, Cambridge, UK. [6]Howard Hughes Medical Institute, Department of Biomedical Engineering and Center of Synthetic Biology, Boston University, Boston, Massachusetts, USA. [7]Department of Immunology, University of Texas, Texas, USA. [8]Simmons Comprehensive Cancer Center, University of Texas Southwestern Medical Center, Texas, USA. [9]Department of Biomedical Engineering, Oregon Health and Science University, Portland, Oregon, USA. [10]Center for Genomic Science of IIT@SEMM, Fondazione Istituto Italiano di Tecnologia (IIT), Milan, Italy. [11]Full lists of members and affiliations appear below.. [12]Division of Cancer Biology, National Cancer Institute, Bethesda, Maryland, USA. [13]IBM Computational Biology Center, IBM, T.J. Watson Research Center, Yorktown Heights, New York, USA. [14]Department of Biomedical Informatics, Columbia University, New York, New York, USA. [15]Department of Biochemistry and Molecular Biophysics, Columbia University, New York, New York, USA. [16]Institute for Cancer Genetics, Columbia University, New York, New York, USA. [17]Herbert Irving Comprehensive Cancer Center, Columbia University, New York, New York, USA. [18]These authors contributed equally to the work

Supplementary Figure 1

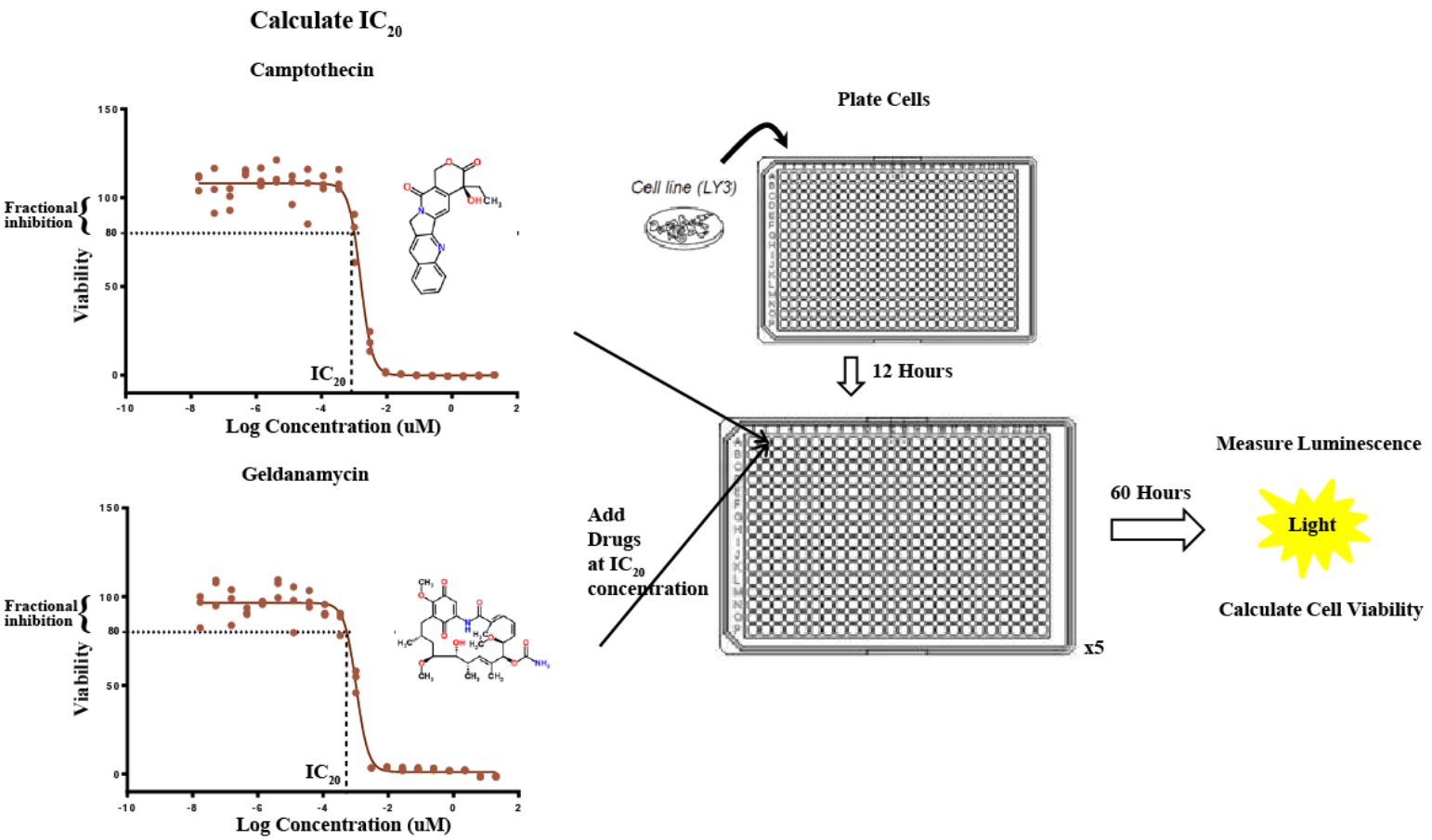

Supplementary Fig. 1: The IC_{20} of each of the 14 compounds were determined in a dose response assay. After the cells are plated and incubated for 12 hours, the compounds at their IC_{20} were added by sequential addition into the plated cells. The compound plates also included wells to test individual compound activity by combining the compounds with DMSO at the same percentage as the rest of the wells at 0.4%. After 60 hours, the assay plates were analyzed by CellTiter-Glo.

Supplementary Figure 2

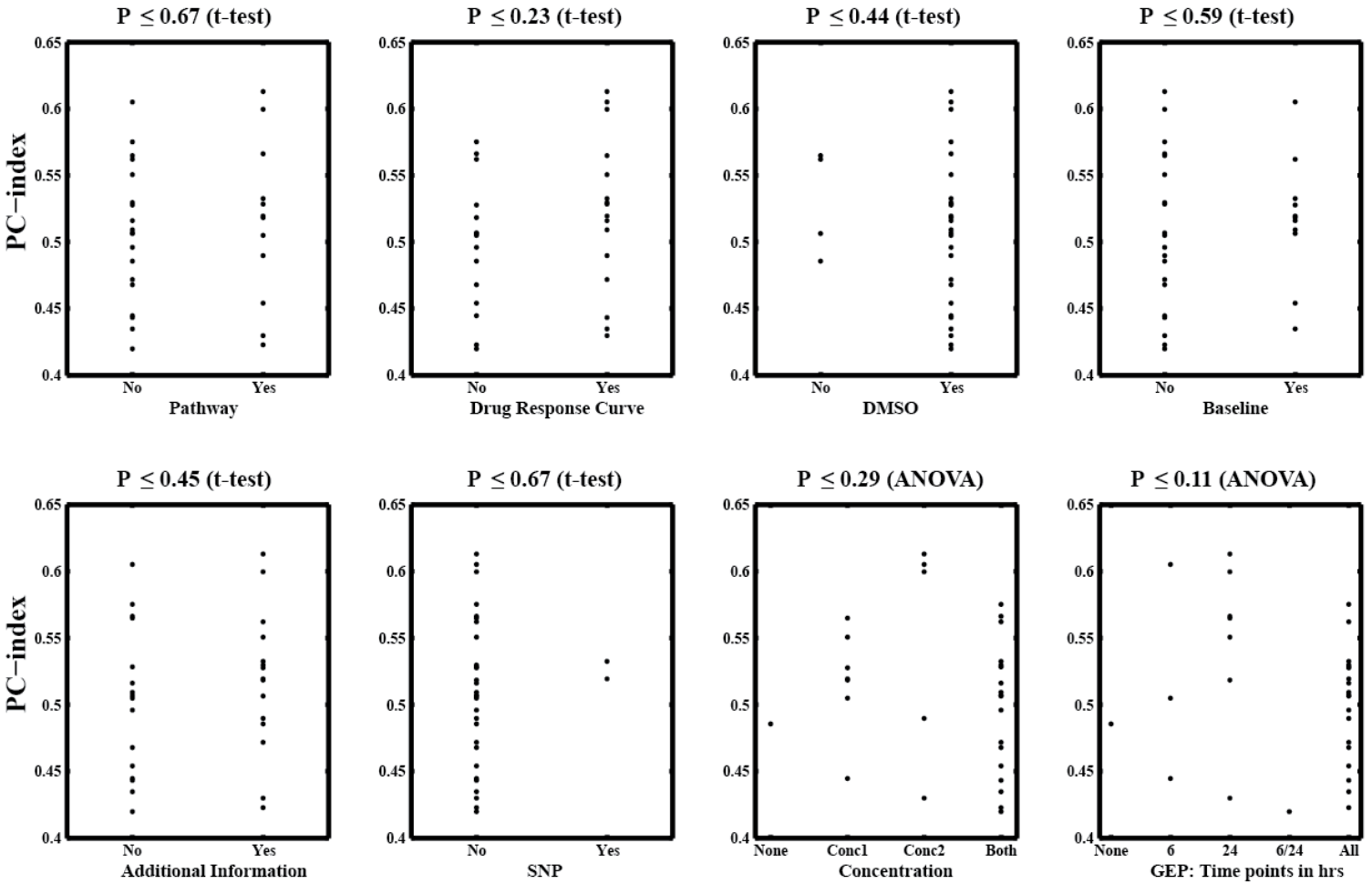

Supplementary Fig. 2: Performance of all teams in the challenge when a particular data type or information is used by any method. Conc1: IC_{20} at 24 hrs; Conc2: IC_{20} at 48 hrs. For each data or information, we reported p-value and the statistical test used to estimate that p-value to indicate the significance between the final score and the kind of data or information used.

.

Supplementary Figure 3

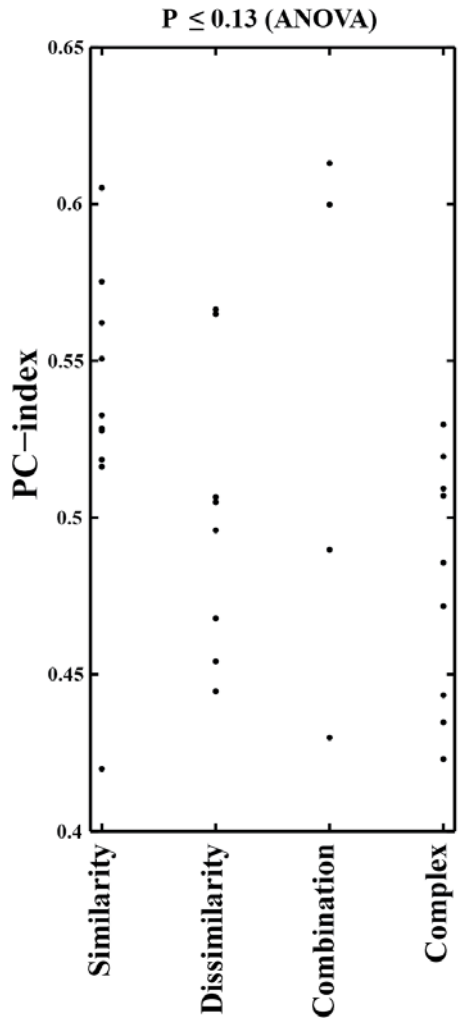

Supplementary Fig. 3: PC-index of all teams when different hypotheses are used in their model. Teams utilizing similarity hypothesis generally have higher PC-index than methods utilizing other hypotheses.

Supplementary Figure 4

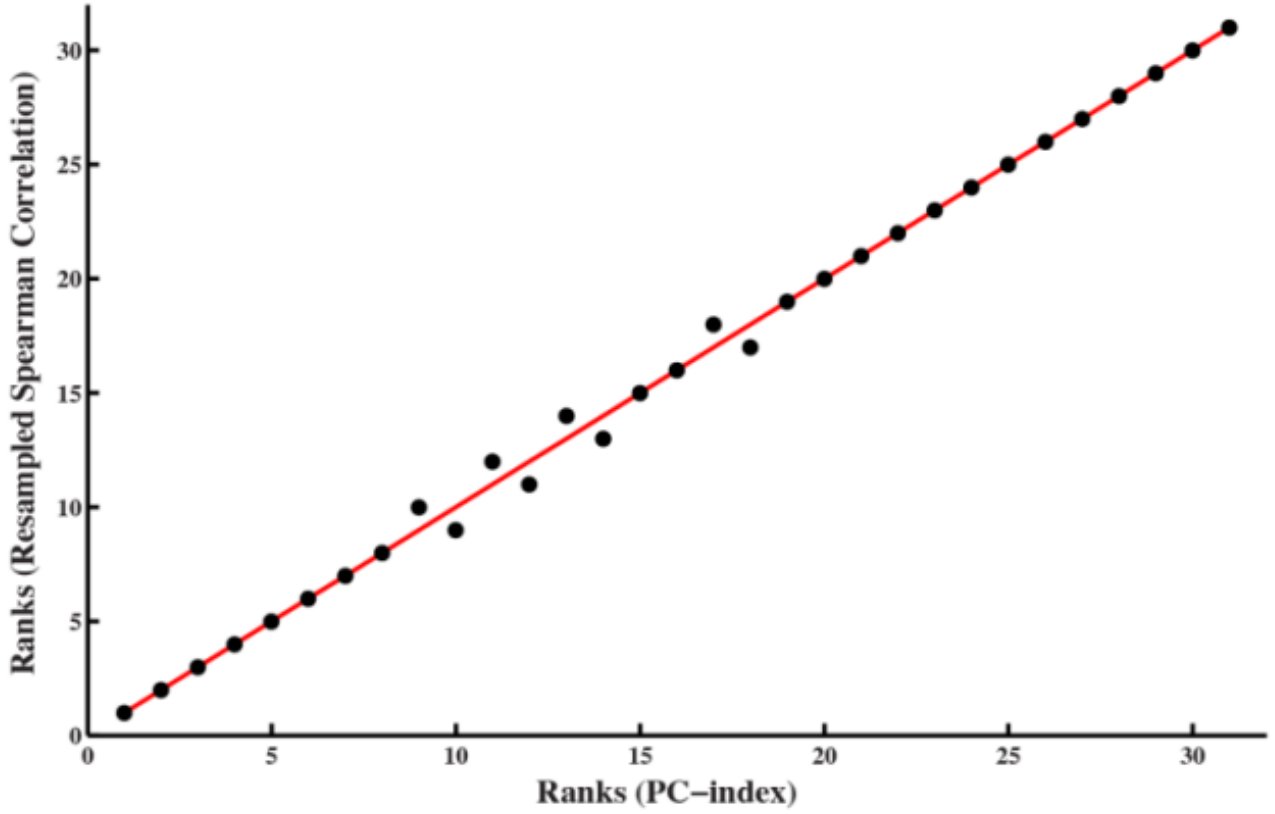

Supplementary Fig. 4: Plot comparing ranks of all teams obtained from PC-index (x-axis) and resampled Spearman correlation method (y-axis) showing a good agreement between the ranks of all teams using both methods.

Supplementary Figure 5

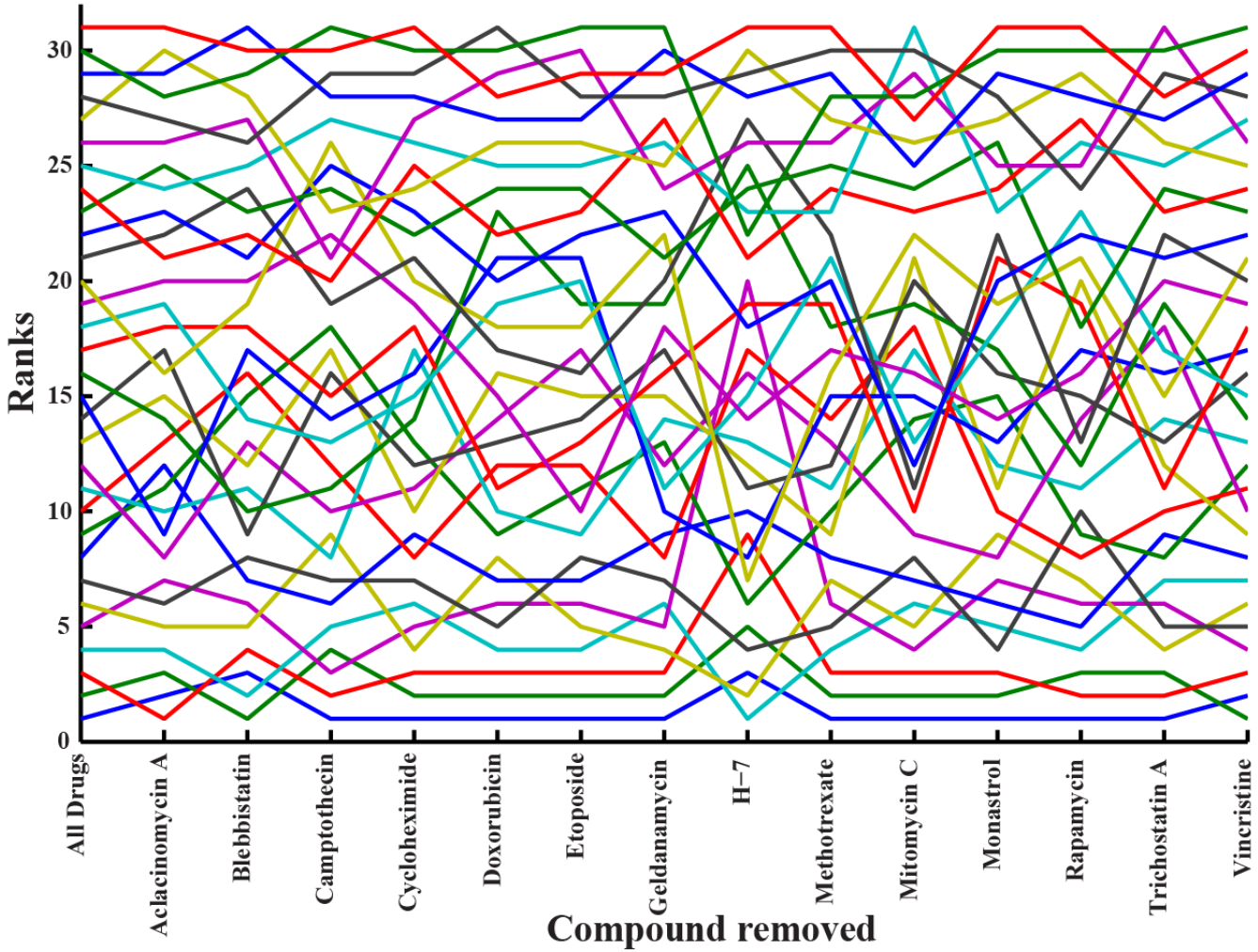

Supplementary Fig. 5: Ranks of teams in leave-one-out method when systematically one compound is removed and 13 are considered for performance evaluation. First point shows the rank when all 14 compounds are used for performance evaluation..

Supplementary Figure 6

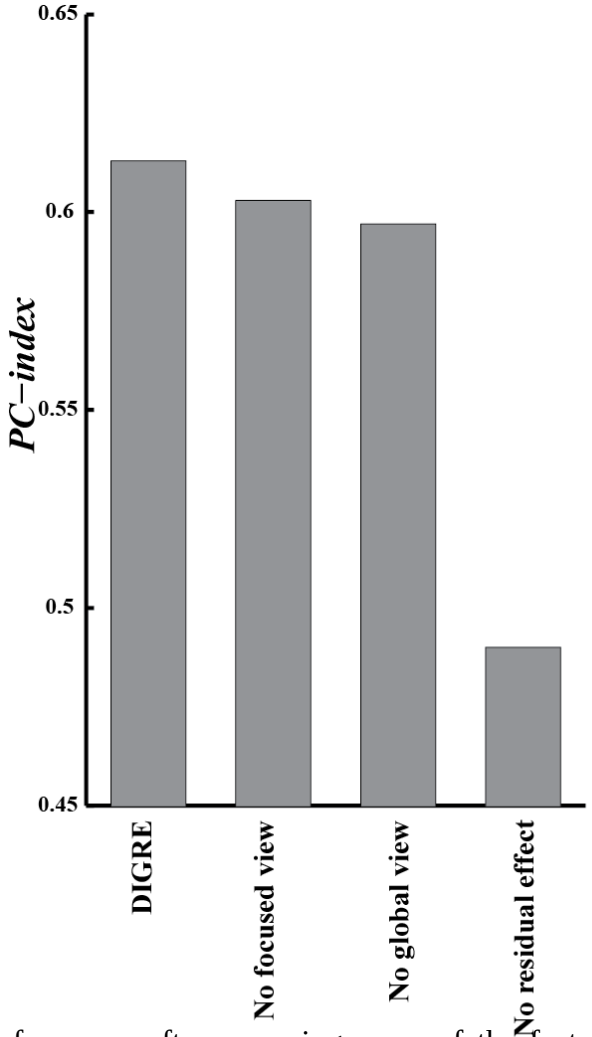

Supplementary Fig. 6: DIGRE's performance after removing some of the features from the method. Performance after removing other features could not be tested due to the implicit nature of those in the model.

Supplementary Figure 7

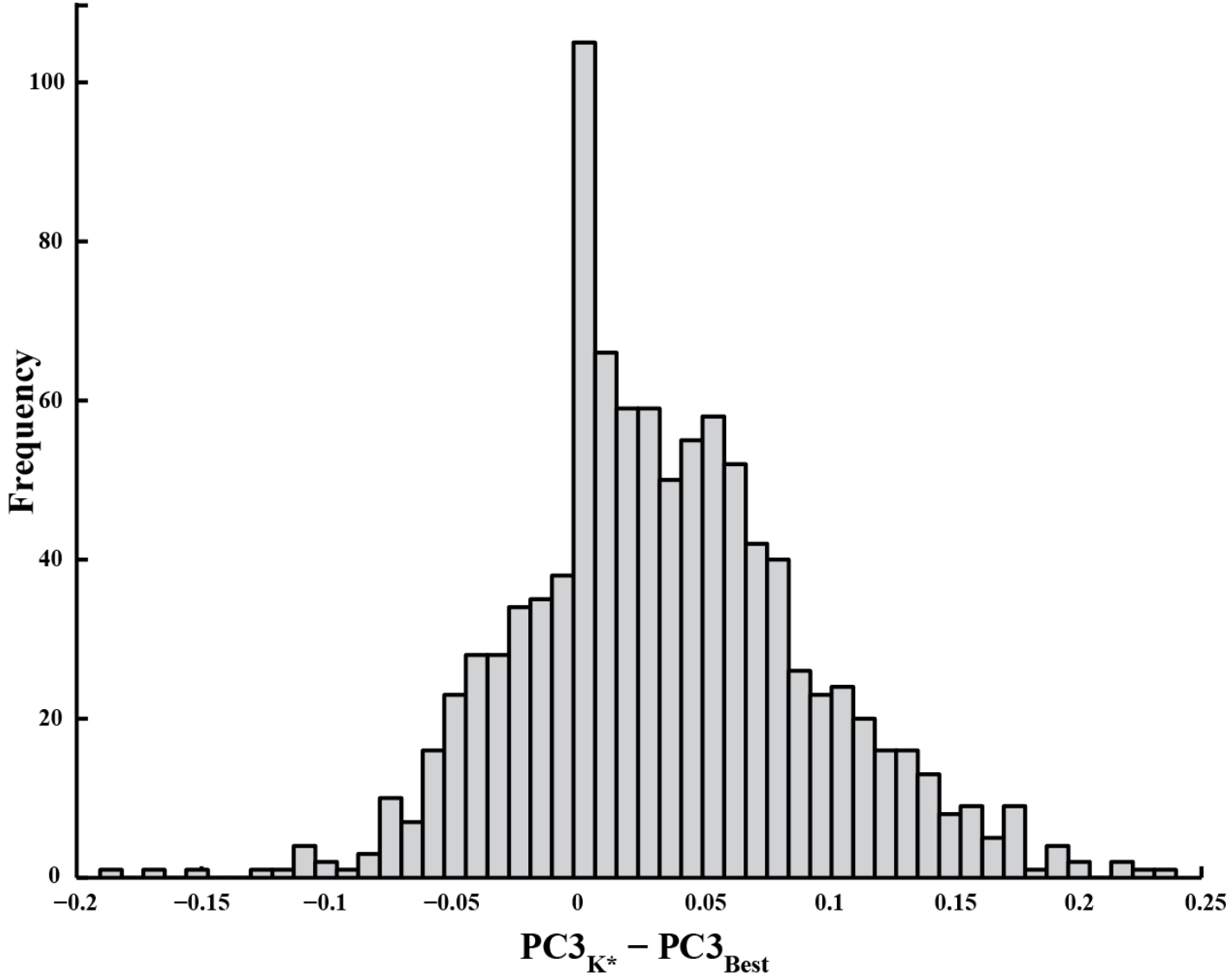

Supplementary Fig. 7: Distribution of the difference in PC-index between ensemble models ($PC3_{k*}$ with k* chosen using S2) and the PC-index of the single best model obtained from S1 ($PC3_{Best}$) when tested on S3 set, in 1000 independent splits of 91 compound pairs in 3 sets S1/S2/S3.

Supplementary Figure 8

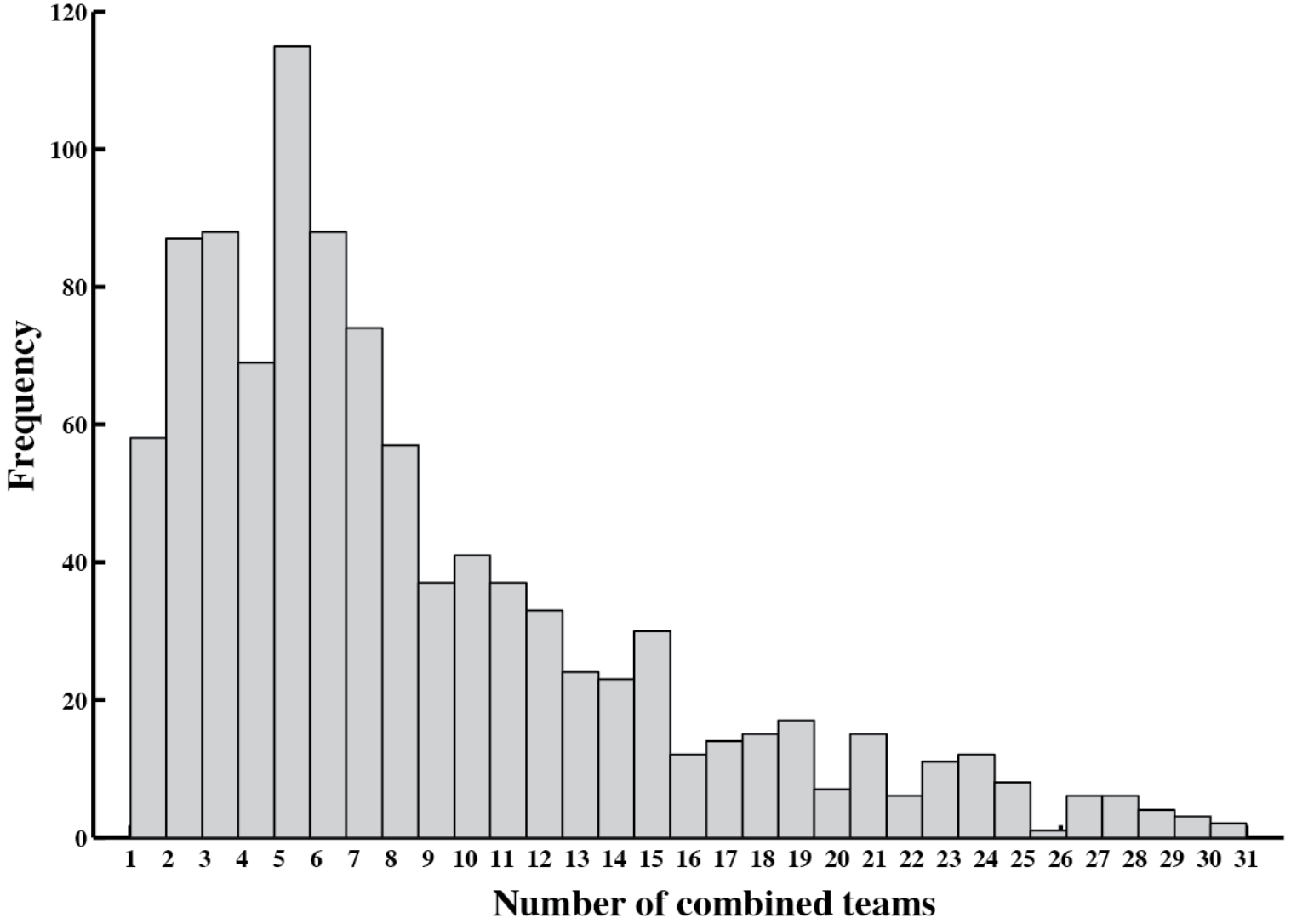

Supplementary Fig. 8: Distribution of number of methods needed to achieve the maximum performance in ensemble models obtained in 1000 independent splits. The mode of the distribution is at 5 models.

Supplementary Figure 9

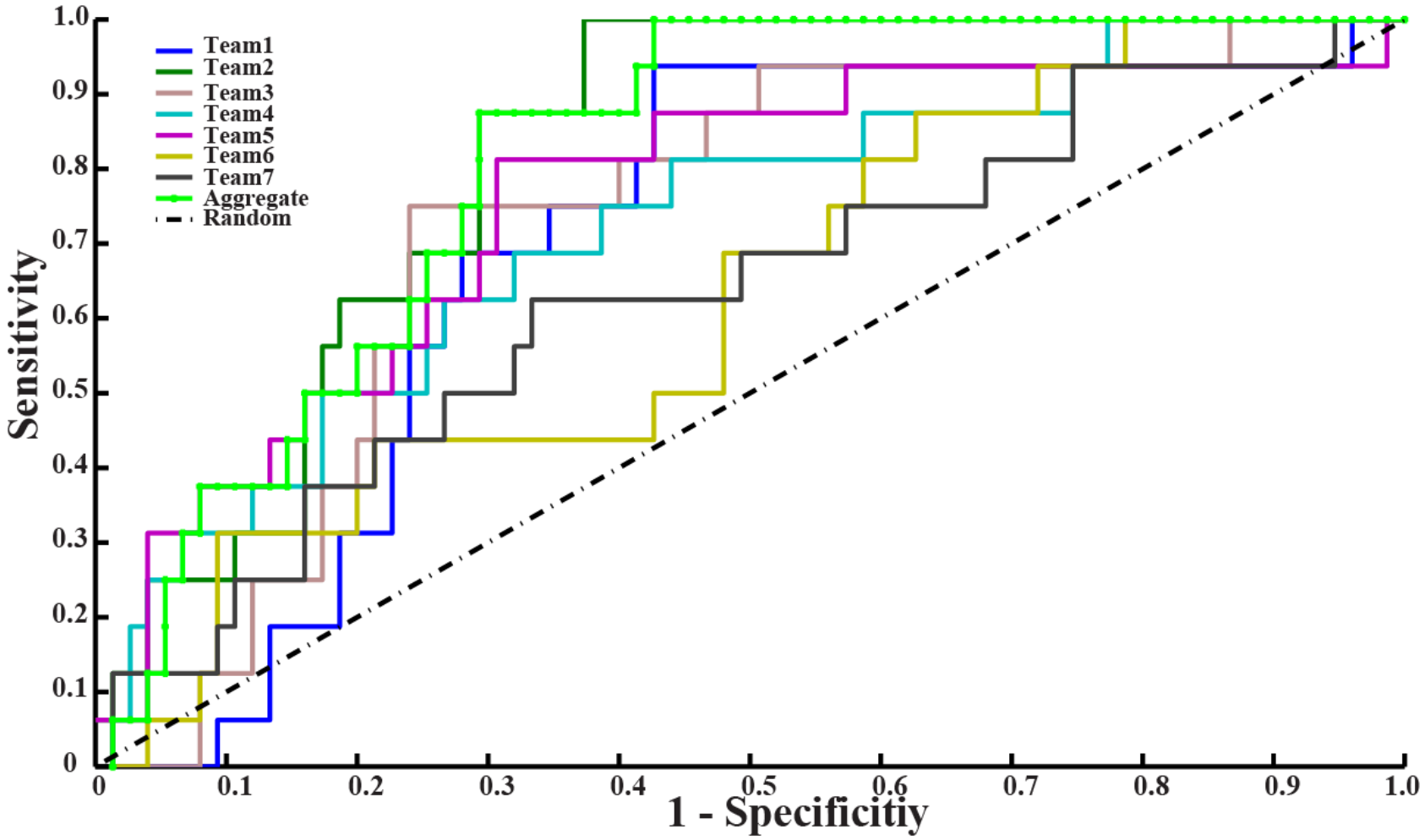

Supplementary Fig. 9: ROC curves of top performing methods and the aggregate of predictions from top 7 teams in predicting synergistic compound pairs. Dashed black line shows the average ROC curve for random prediction.

Supplementary Figure 10

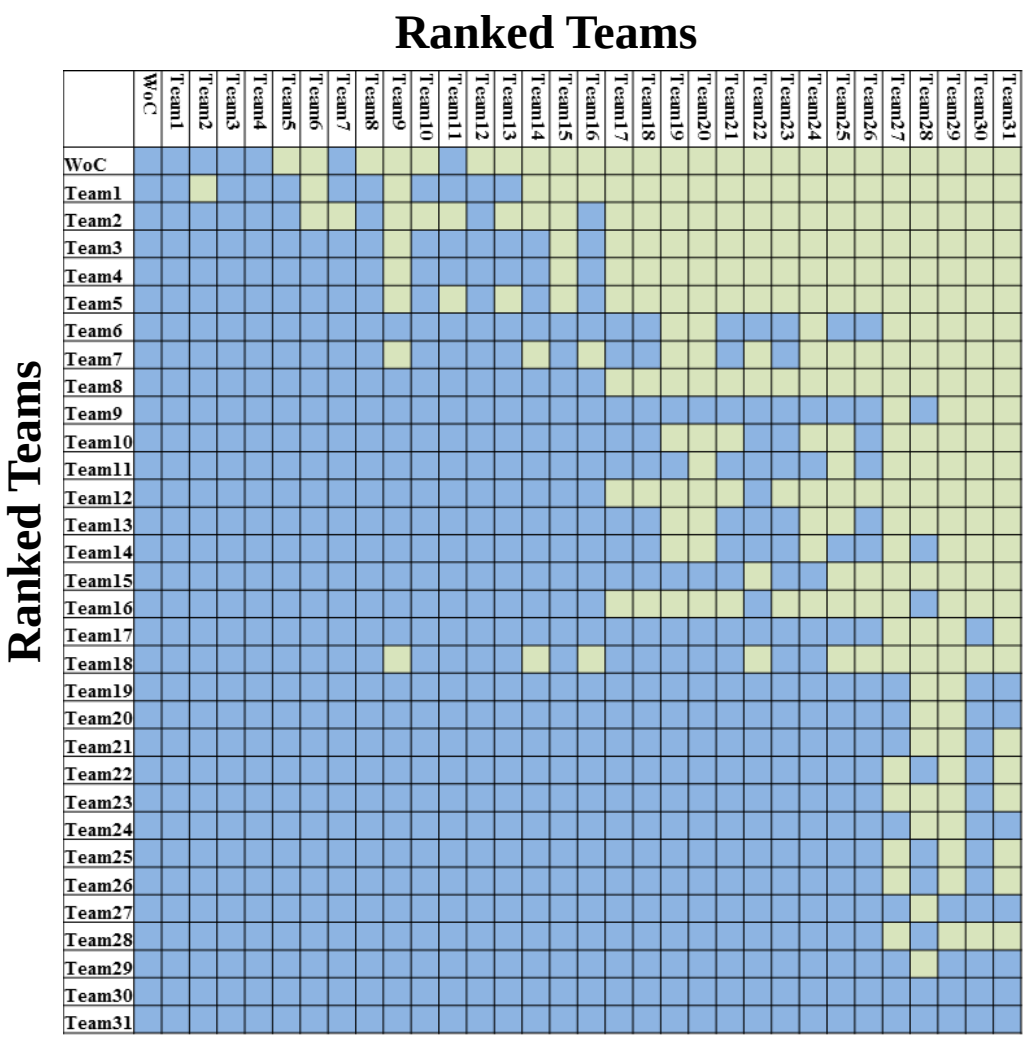

Supplementary Fig. 10: Pairwise comparison of all teams using difference in ROC curves for predicting synergistic and antagonistic compound pairs. A green square in position (*i*,*j*) indicates that AUROC of Team *i* is significantly better than Team *j* ($p \leq 0.05$) in predicting either synergistic or antagonistic compound pairs. A blue square in position (*i*,*j*) indicates that AUROC of Team *i* is neither better not worse than Team *j* and cannot be considered different ($p > 0.05$) neither in predicting synergistic nor in predicting antagonistic compound pairs.

Nature Biotechnology: doi:10.1038/nbt.3052

Supplementary Figure 11

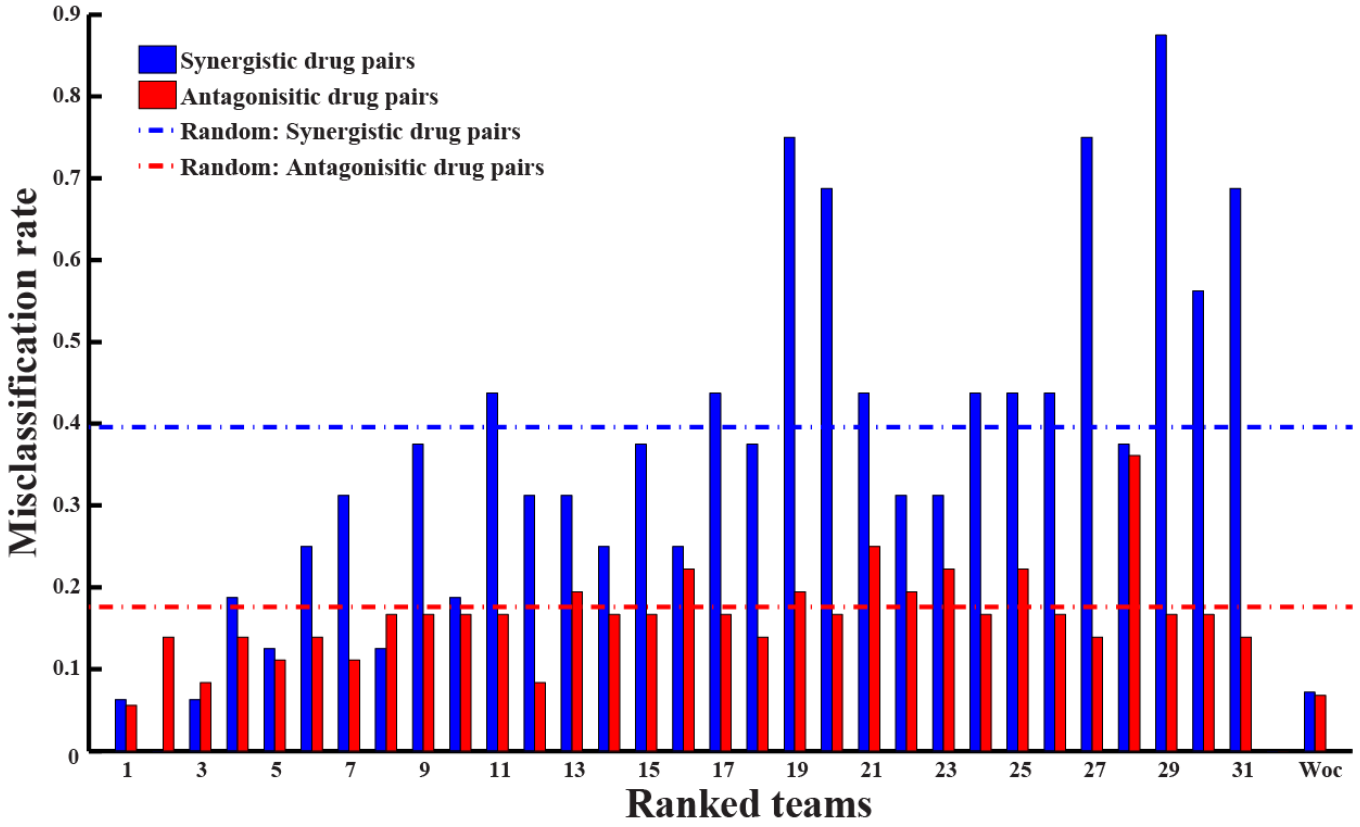

Supplementary Fig. 11: Misclassification rates for all methods. Fraction of synergistic compounds pairs misclassified as antagonistic (blue) and fraction of antagonistic compound pairs misclassified as synergistic (red). The horizontal lines in blue and red show the random expected rate of synergistic compound pairs misclassified as antagonistic and antagonistic compounds pairs misclassified as synergistic respectively. The misclassification rate for synergistic compound pairs is calculated as ratio between the number of synergistic compound pairs predicted to be antagonistic divided by the total number of synergistic compounds pairs; likewise, the misclassification rate for antagonistic compound pairs is calculated as the ratio of the number of antagonistic compound pairs predicted to be synergistic divided by total number of antagonistic compounds pairs. The bars labeled as WoC show the average misclassification rate for "wisdom of crowds" following the same average over partitions procedure described in the context of Figure 5.

Supplementary Figure 12

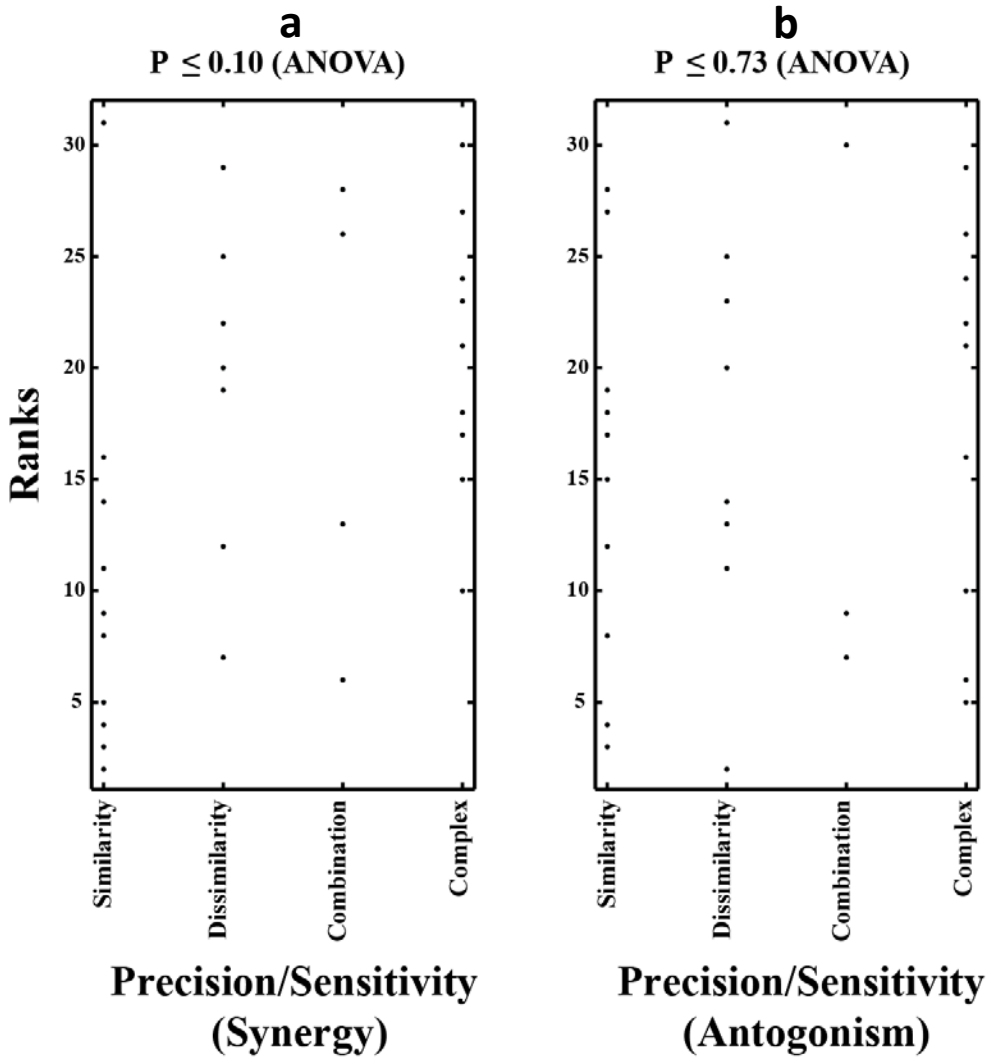

Supplementary Fig. 12: Rank of all teams when different hypotheses are used in their model. a) Teams utilizing similarity hypotheses generally rank better in predicting synergistic drug pairs (using precision/sensitivity analysis) b) but not for predicting antagonistic drug pairs as indicated by reported p-values. Since multiple methods have same precision, therefore to avoid overlapping points in the plot we used ranks instead of precision. However, ANOVA was performed using the precision value only.

Nature Biotechnology: doi:10.1038/nbt.3052

Supplementary Figure 13

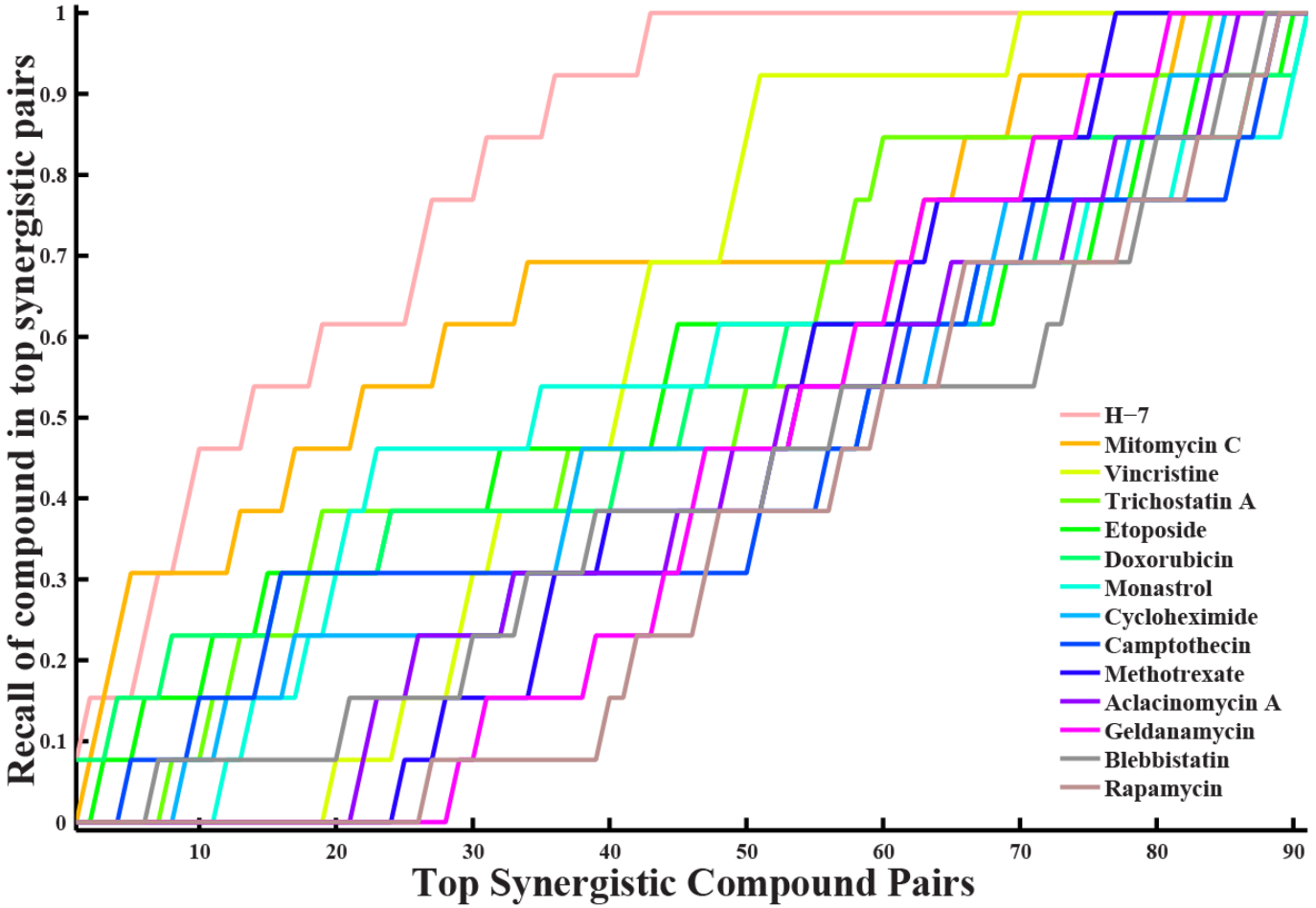

Supplementary Fig. 13: Recall curve for each compound to analyze their proclivity towards synergy or antagonism. Compounds are ranked with highest area under recall curve to lowest.

Supplementary Figure 14

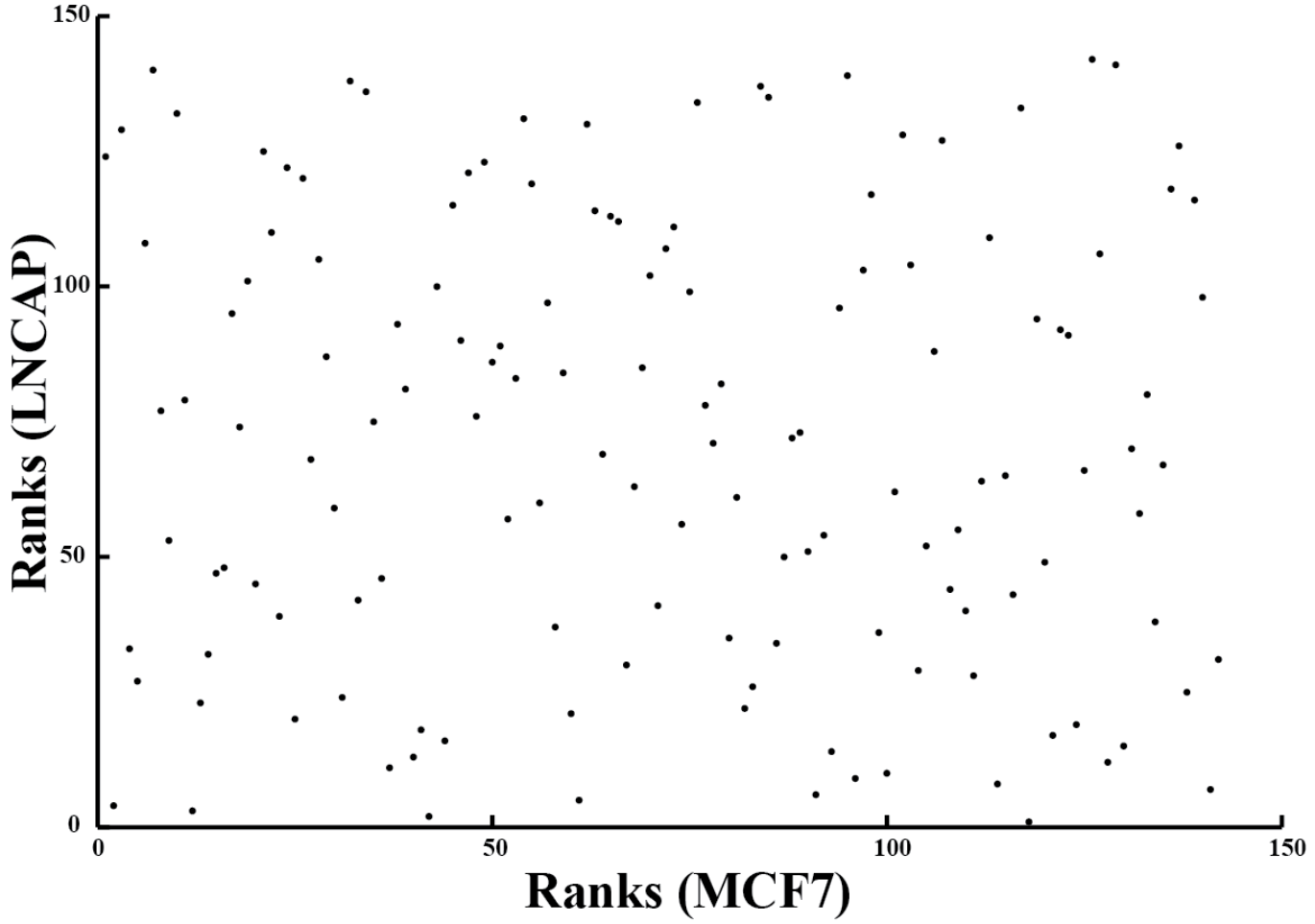

Supplementary Fig. 14: Scatter plot of the rank of compound 142 pairs obtained in the MCF7 and LNCAP cell lines showing no correlation between the activities of compound pairs obtained in different contexts.

Nature Biotechnology doi:10.1038/nbt.3052

Supplementary Figure 15

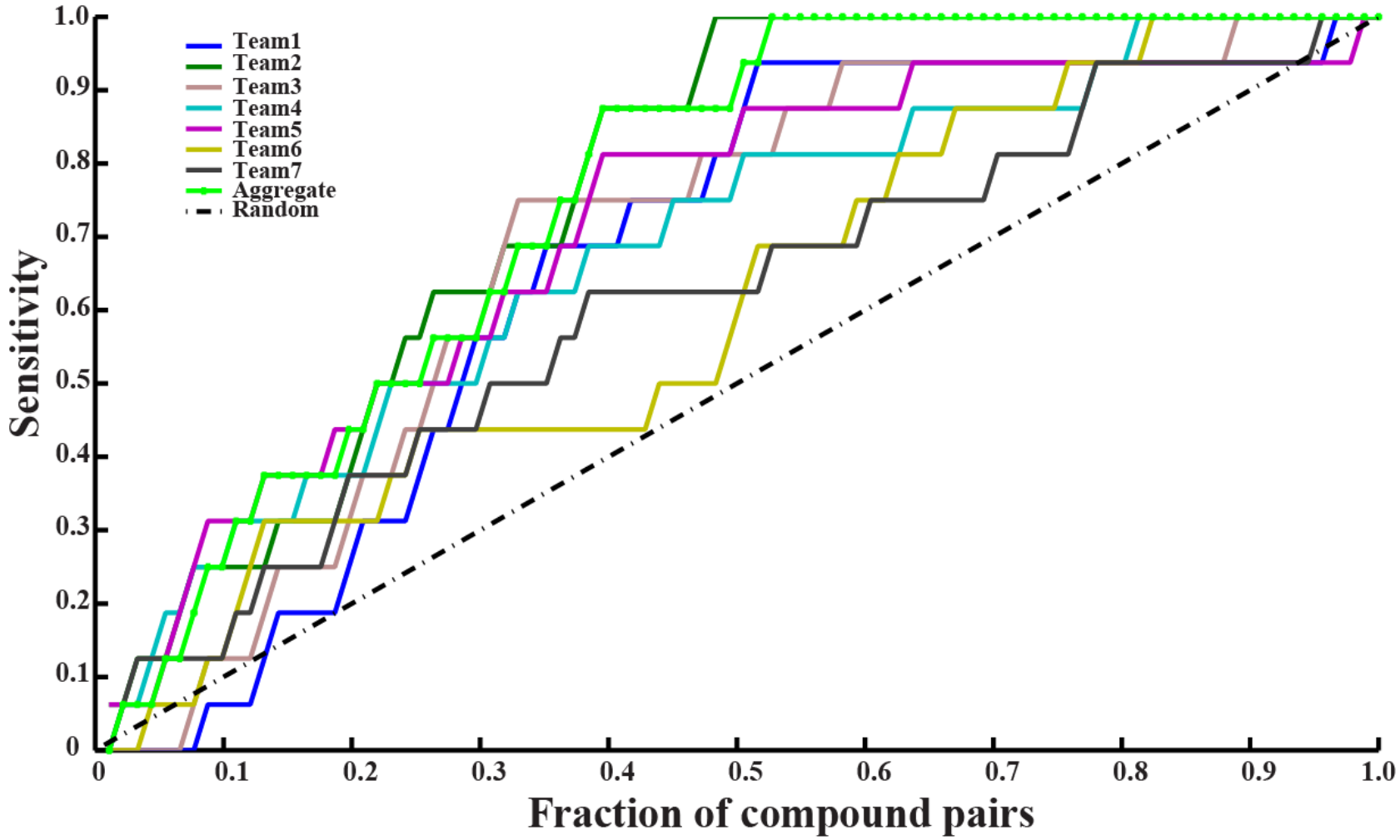

Supplementary Fig. 15: Sensitivity curve of top performing methods and the aggregate of predictions from top 7 teams in predicting synergistic compound pairs. The x-axis represents the fraction of top ranked compound pairs by each method. Dashed black line shows the sensitivity curve for random prediction.

Supplementary File

A community computational challenge to predict the activity of pairs of compounds

Mukesh Bansal[1,2,18], Jichen Yang[3,18], Charles Karan[4,18], Michael P Menden[5], James C Costello[6,61], Hao Tang[3], Guanghua Xiao[3], Yajuan Li[7], Jeffrey Allen[3,7], Rui Zhong[3], Beibei Chen[3], Minsoo Kim[3,8], Tao Wang[3], Laura M Heiser[9], Ronald Realubit[4], Michela Mattioli[10], Mariano J Alvarez[1,2], Yao Shen[1,2], NCI-DREAM community[11], Daniel Gallahan[12], Dinah Singer[12], Julio Saez-Rodriguez[5], Yang Xie[3,8], Gustavo Stolovitzky[13] & Andrea Califano[1,2,14–17]

[1]Department of Systems Biology, Columbia University, New York, New York, USA. [2]Center for Computational Biology and Bioinformatics, Columbia University, New York, New York, USA. [3]Quantitative Biomedical Research Center, Department of Clinical Sciences, University of Texas Southwestern Medical Center, Dallas, Texas, USA. [4]Columbia Genome Center, High Throughput Screening Facility, Columbia University, New York, New York, USA. [5]European Molecular Biology Laboratory, European Bioinformatics Institute, UK. Wellcome Trust Genome Campus, Hinxton, Cambridge, UK. [6]Howard Hughes Medical Institute, Department of Biomedical Engineering and Center of Synthetic Biology, Boston University, Boston, Massachusetts, USA. [7]Department of Immunology, University of Texas, Texas, USA. [8]Simmons Comprehensive Cancer Center, University of Texas Southwestern Medical Center, Texas, USA. [9]Department of Biomedical Engineering, Oregon Health and Science University, Portland, Oregon, USA. [10]Center for Genomic Science of IIT@SEMM, Fondazione Istituto Italiano di Tecnologia (IIT), Milan, Italy. [11]Full lists of members and affiliations appear below.. [12]Division of Cancer Biology, National Cancer Institute, Bethesda, Maryland, USA. [13]IBM Computational Biology Center, IBM, T.J. Watson Research Center, Yorktown Heights, New York, USA. [14]Department of Biomedical Informatics, Columbia University, New York, New York, USA. [15]Department of Biochemistry and Molecular Biophysics, Columbia University, New York, New York, USA. [16]Institute for Cancer Genetics, Columbia University, New York, New York, USA. [17]Herbert Irving Comprehensive Cancer Center, Columbia University, New York, New York, USA. [18]These authors contributed equally to the work

Aclacinomycin A

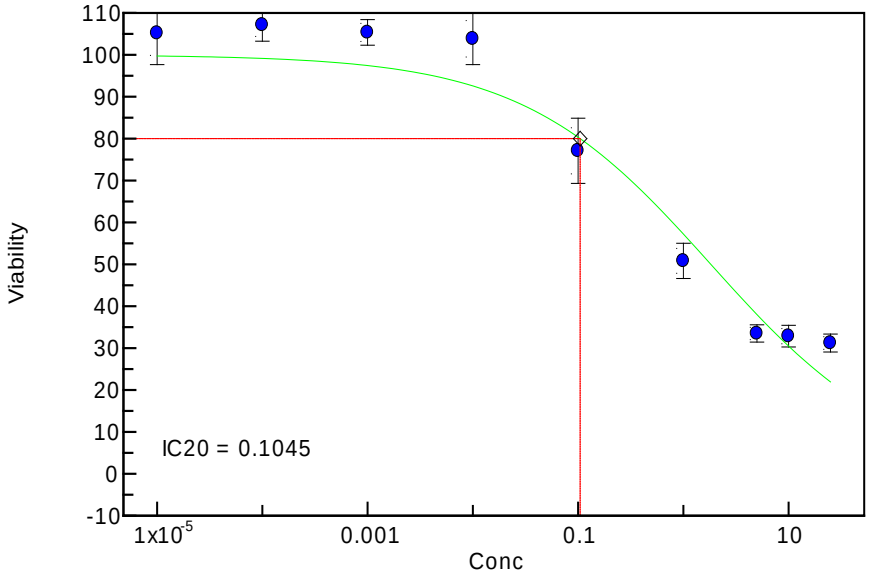

Drug response curve at 24hrs

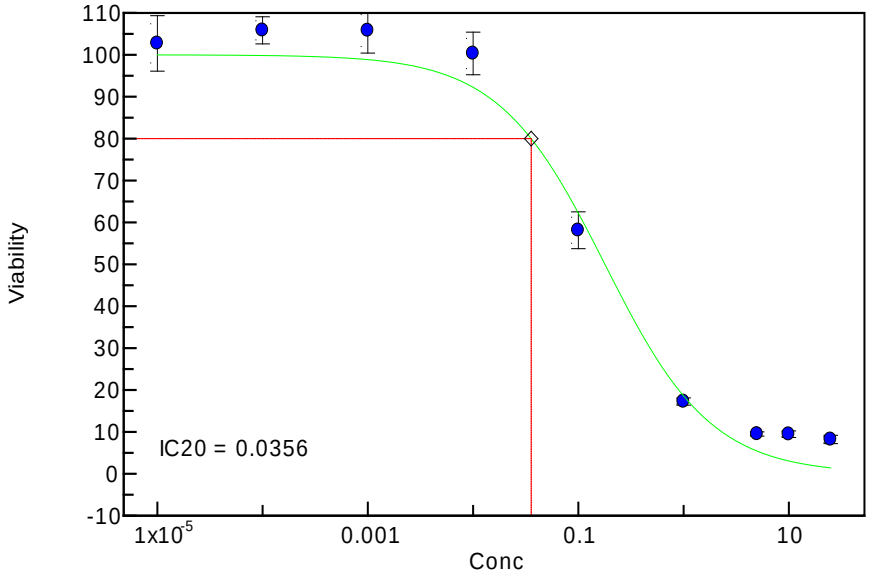

Drug response curve at 48hrs

Nature Biotechnology doi:10.1038/nbt.3052

Blebbistatin

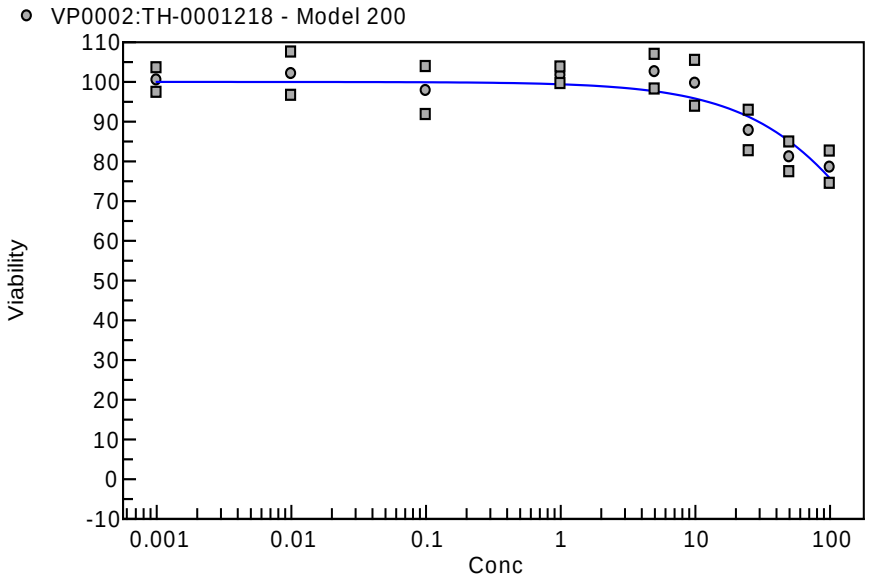

Drug response curve at 24hrs

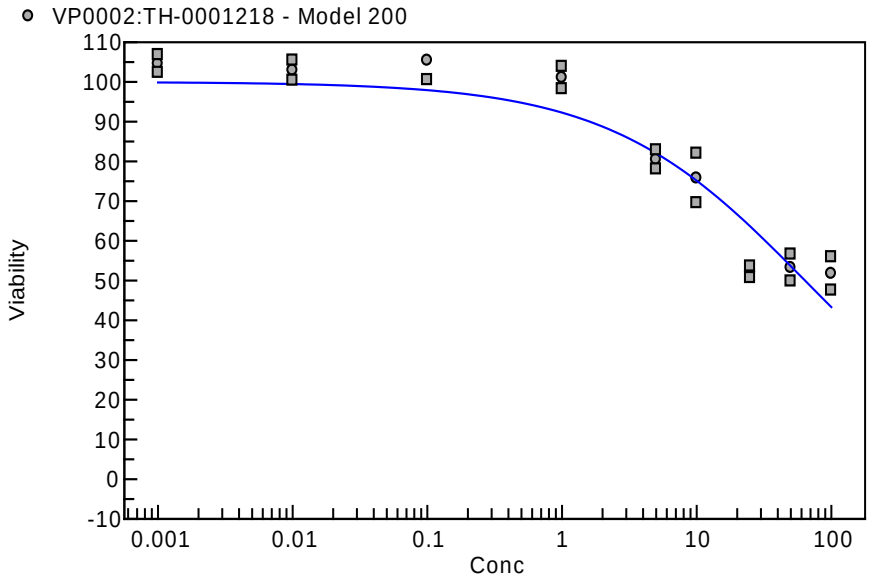

Drug response curve at 48hrs

Nature Biotechnology doi:10.1038/nbt.3052

Camptothecin

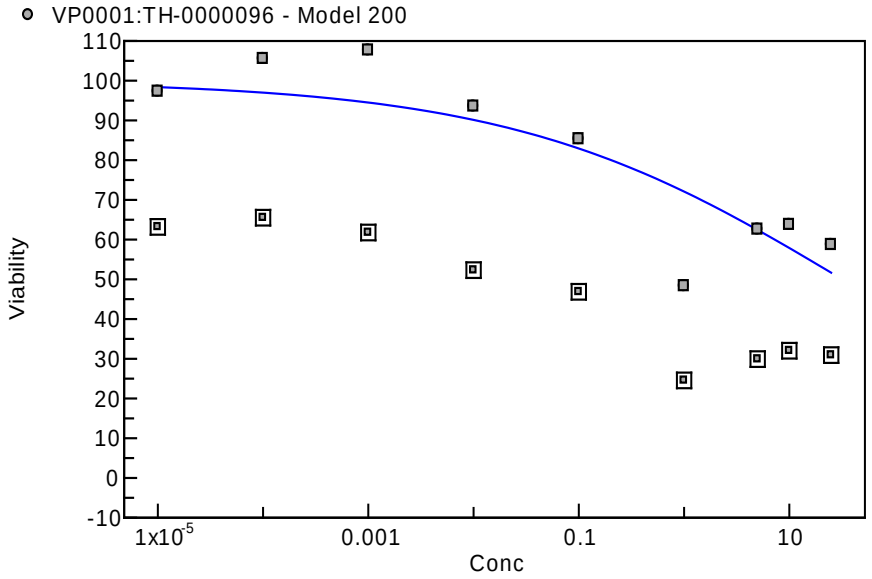

Drug response curve at 24hrs

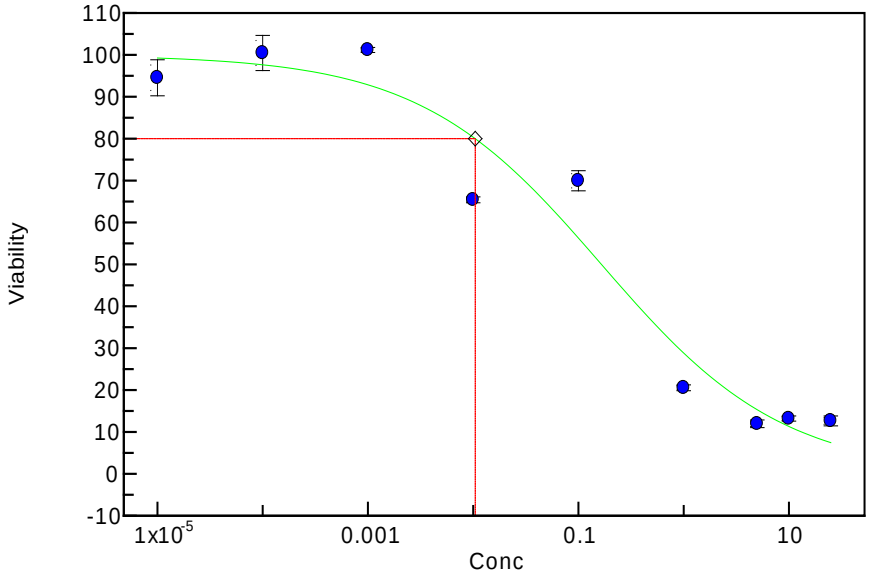

Drug response curve at 48hrs

Nature Biotechnology doi:10.1038/nbt.3052

Cycloheximide

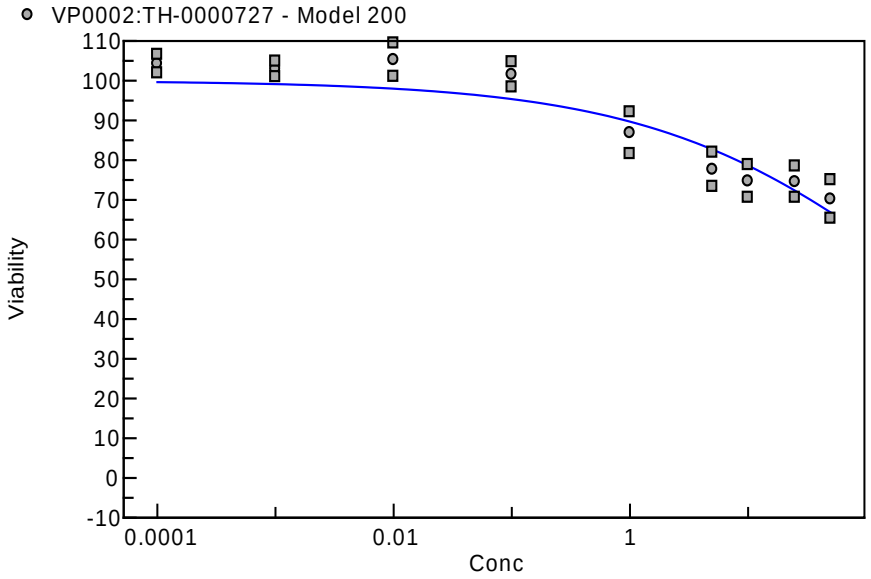

Drug response curve at 24hrs

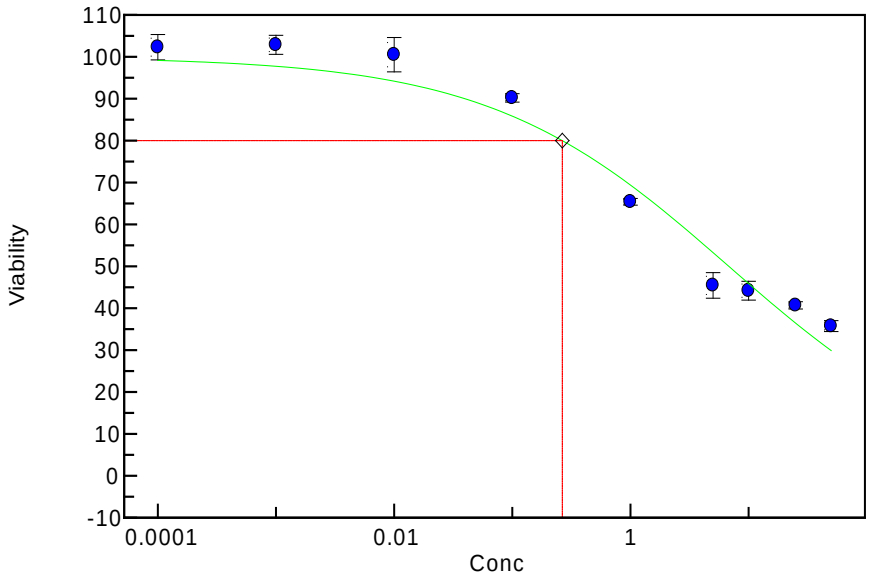

Drug response curve at 48hrs

Nature Biotechnology doi:10.1038/nbt.3052

Doxorubicin

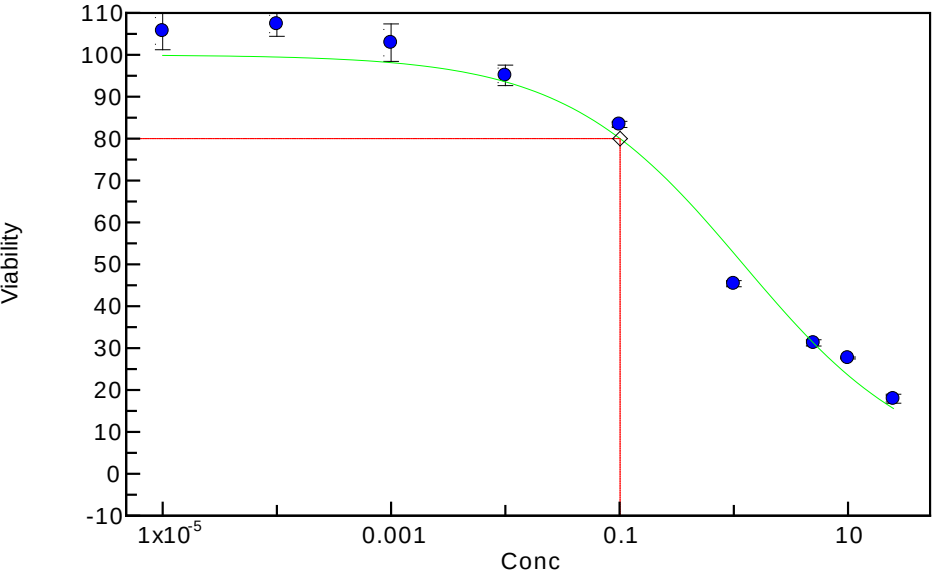

Drug response curve at 24hrs

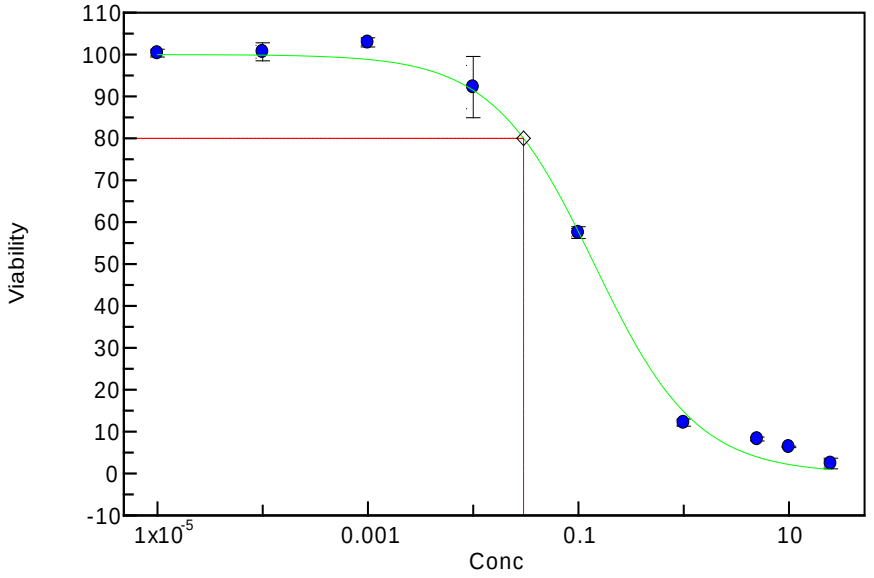

Drug response curve at 48hrs

Nature Biotechnology doi:10.1038/nbt.3052

Etoposide

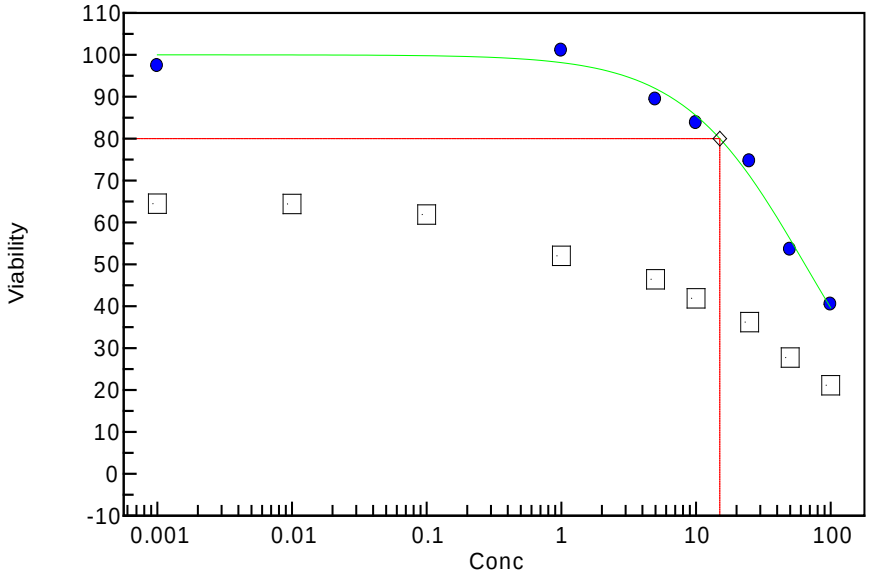

Drug response curve at 24hrs

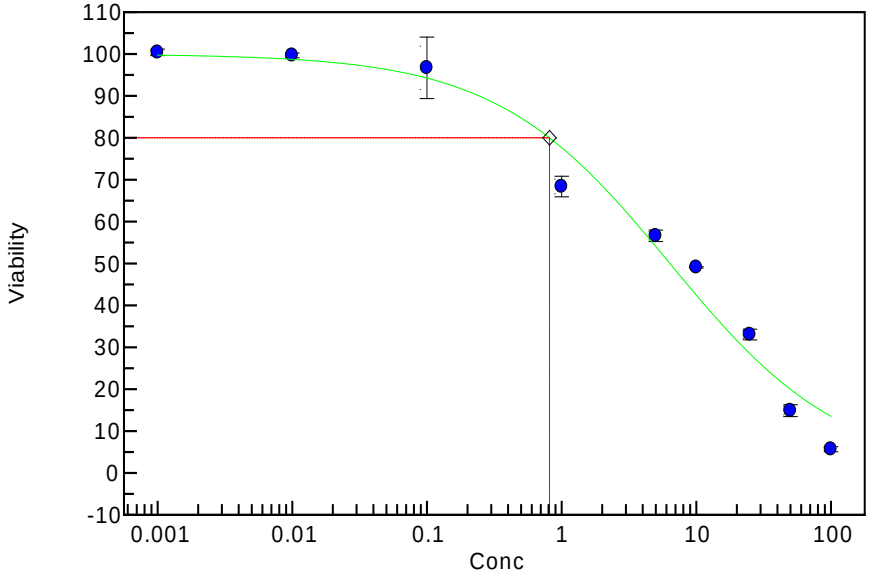

Drug response curve at 48hrs

Nature Biotechnology doi:10.1038/nbt.3052

Geldanamycin

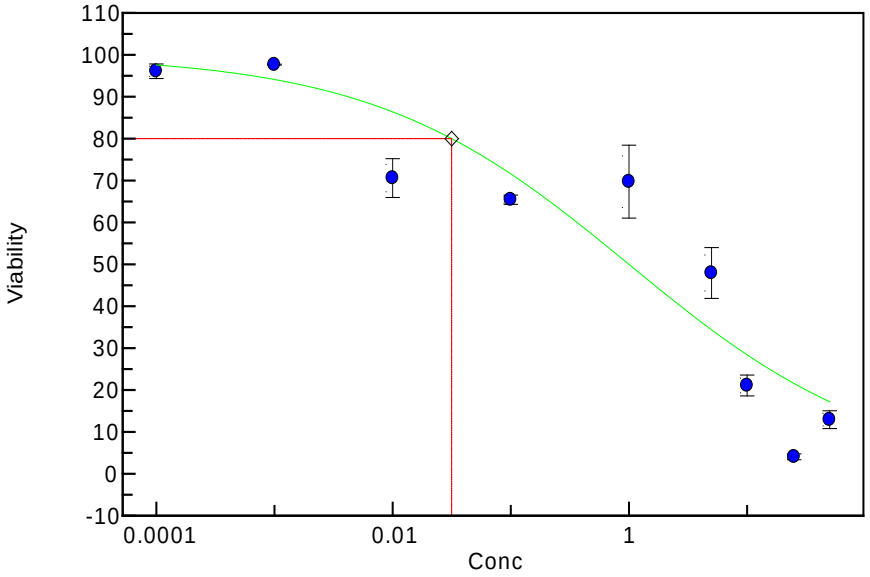

Drug response curve at 24hrs

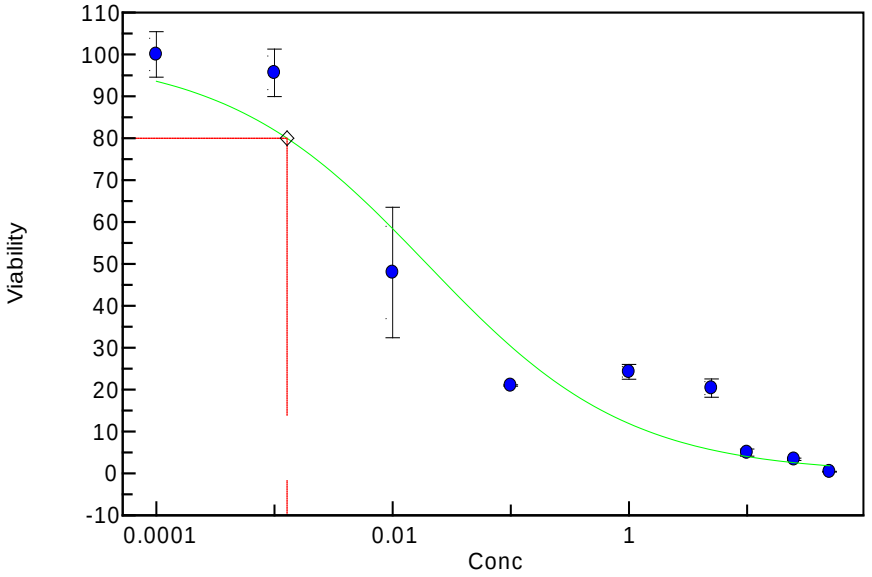

Drug response curve at 48hrs

Nature Biotechnology doi:10.1038/nbt.3052

H-7, Dihydrochloride

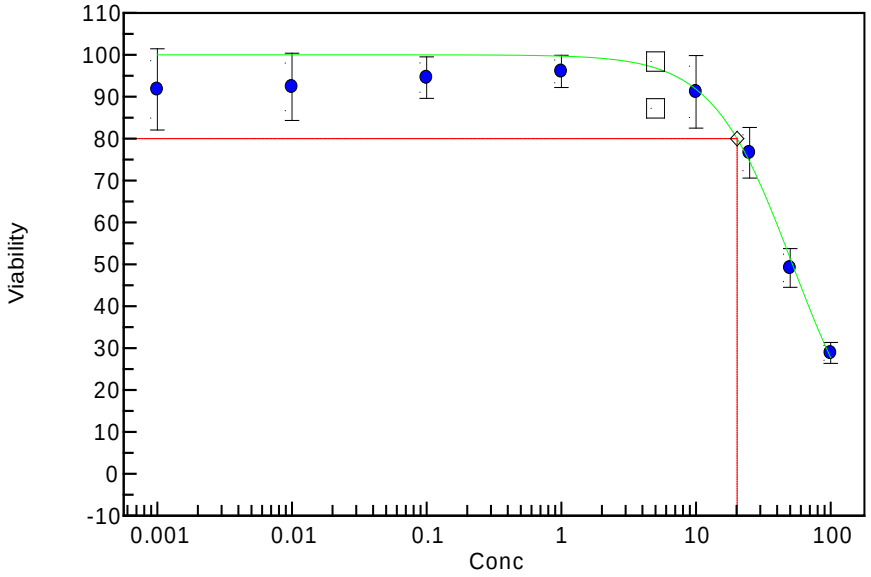

Drug response curve at 24hrs

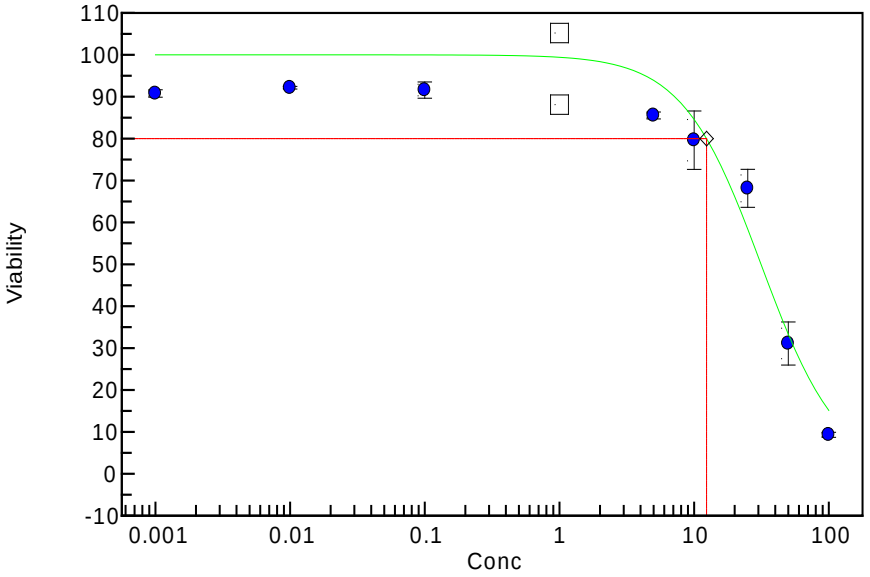

Drug response curve at 48hrs

Nature Biotechnology doi:10.1038/nbt.3052

Methotrexate

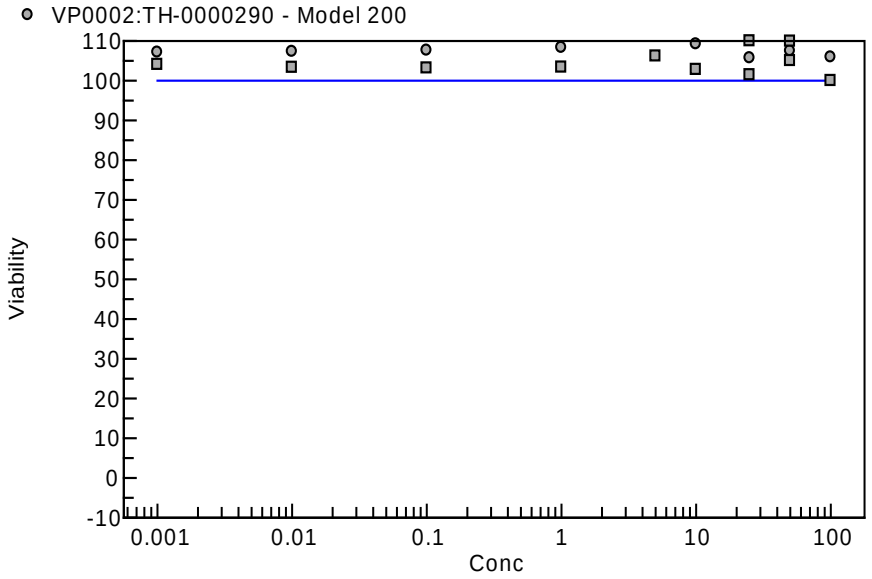

Drug response curve at 24hrs

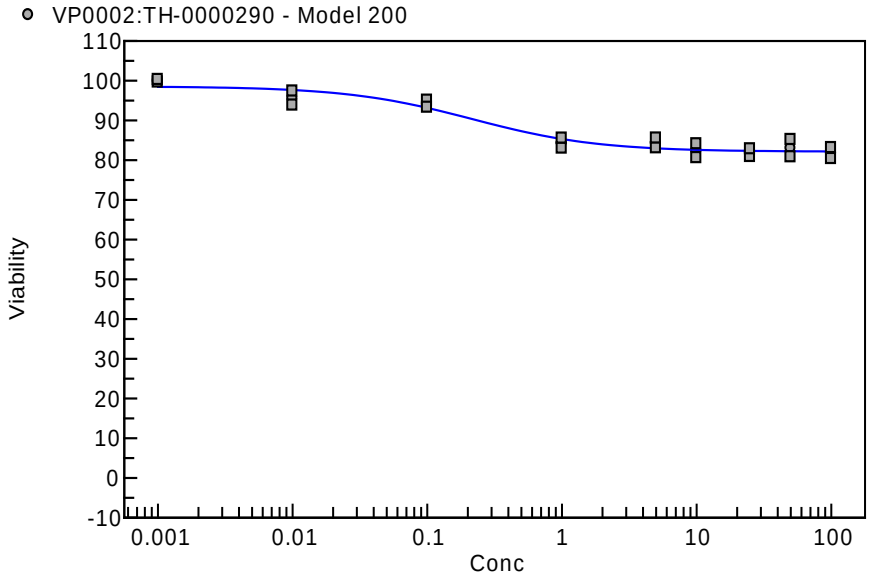

Drug response curve at 48hrs

Nature Biotechnology doi:10.1038/nbt.3052

Mitomycin C

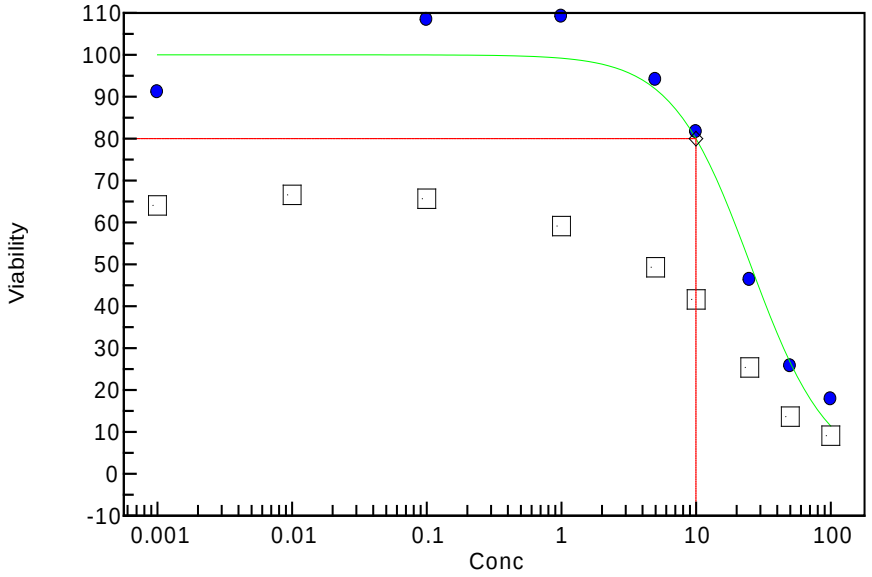

Drug response curve at 24hrs

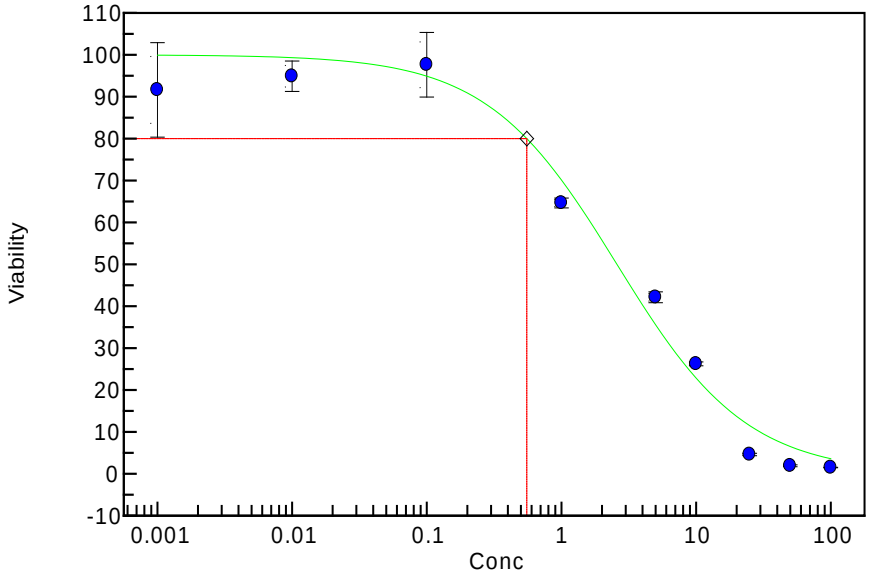

Drug response curve at 48hrs

Nature Biotechnology doi:10.1038/nbt.3052

Monastrol

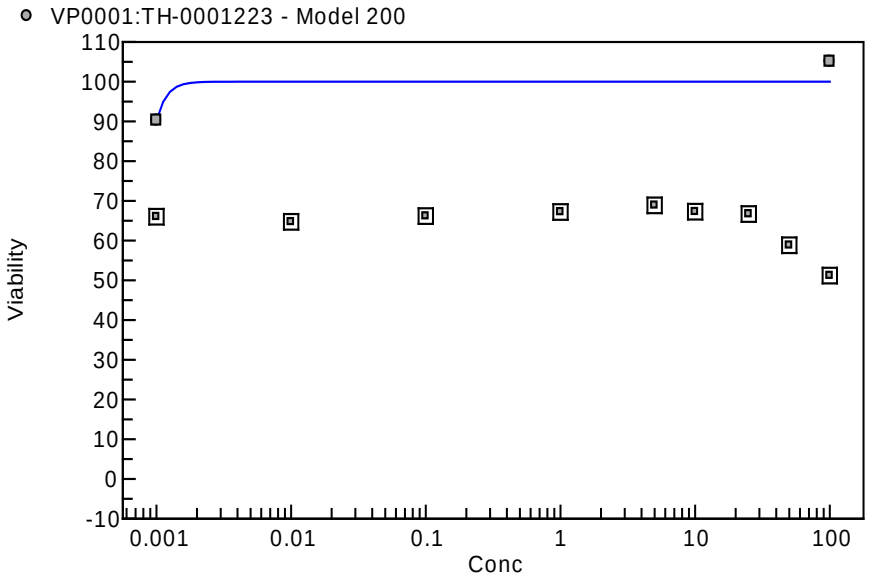

Drug response curve at 24hrs

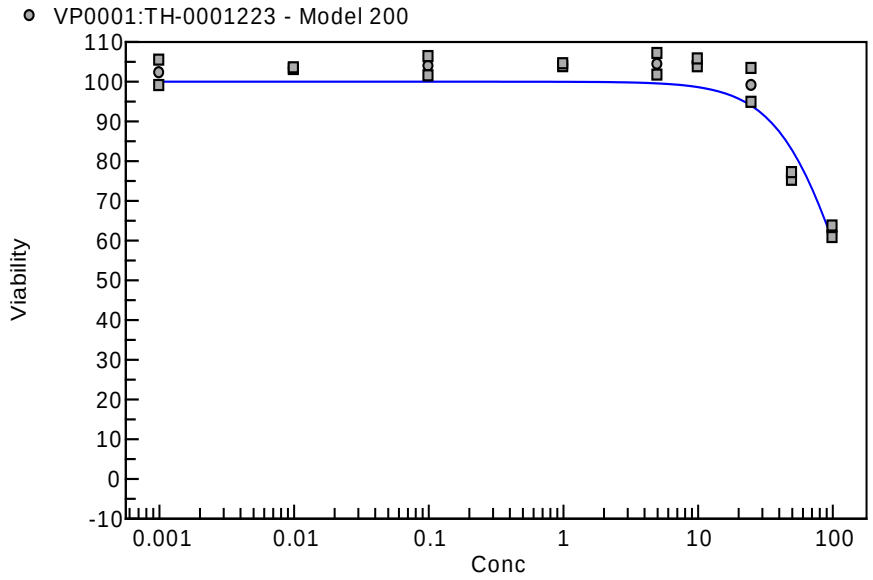

Drug response curve at 48hrs

Nature Biotechnology doi:10.1038/nbt.3052

Rapamycin

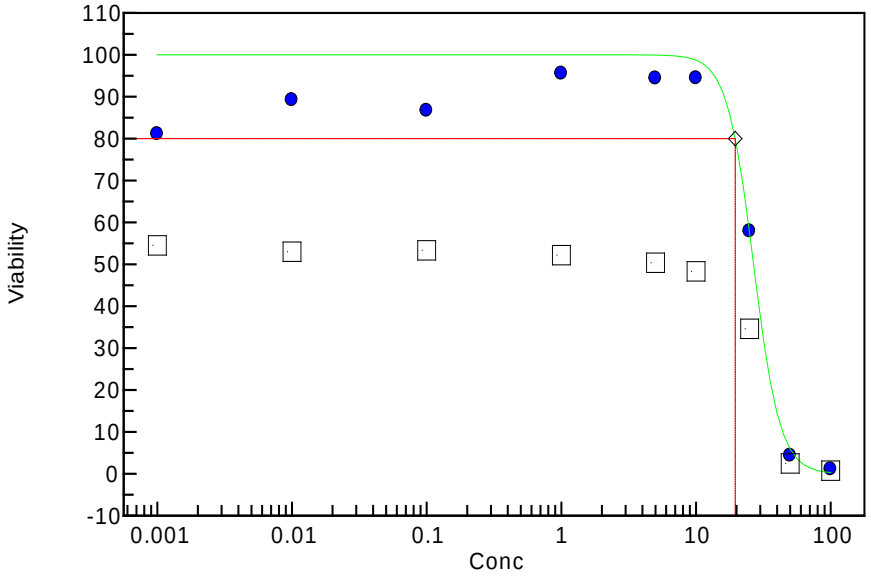

Drug response curve at 24hrs

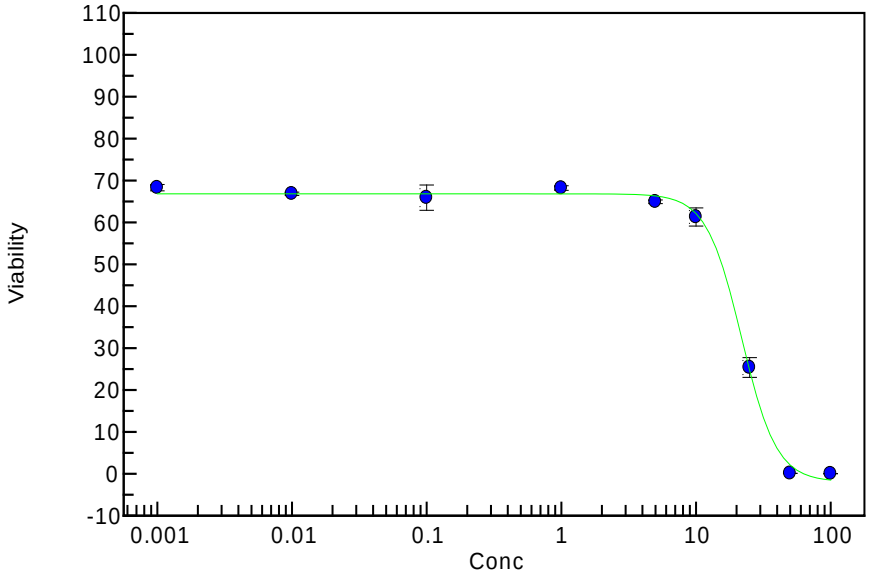

Drug response curve at 48hrs

Nature Biotechnology doi:10.1038/nbt.3052

Trichostatin A

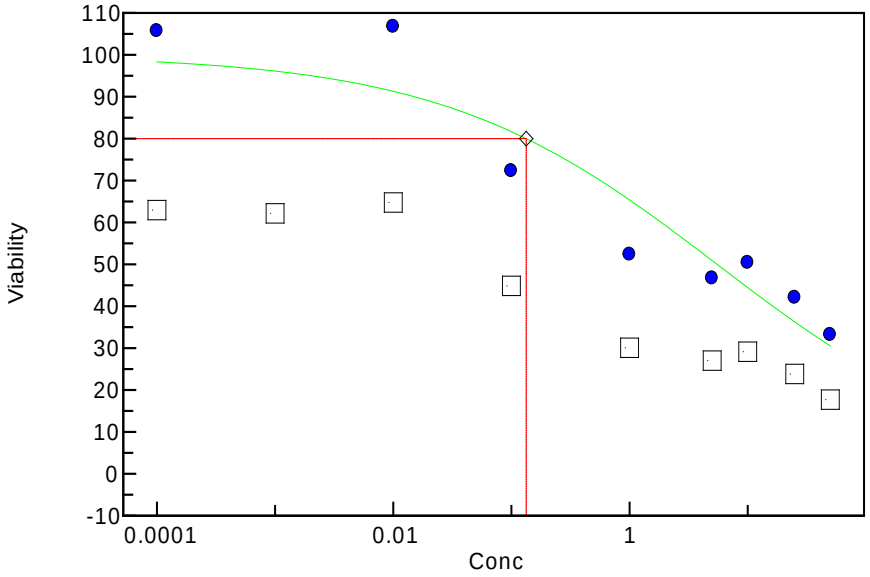

Drug response curve at 24hrs

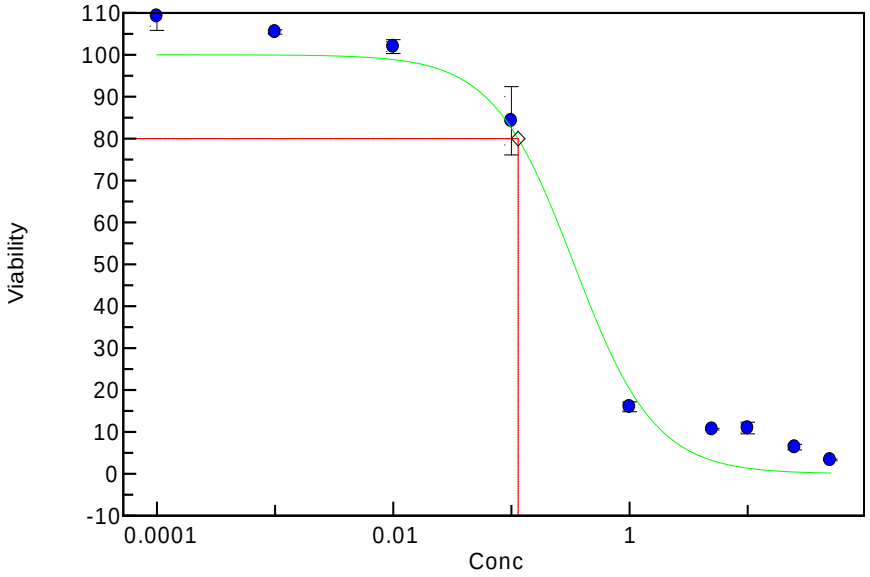

Drug response curve at 48hrs

Nature Biotechnology doi:10.1038/nbt.3052

Vincristine

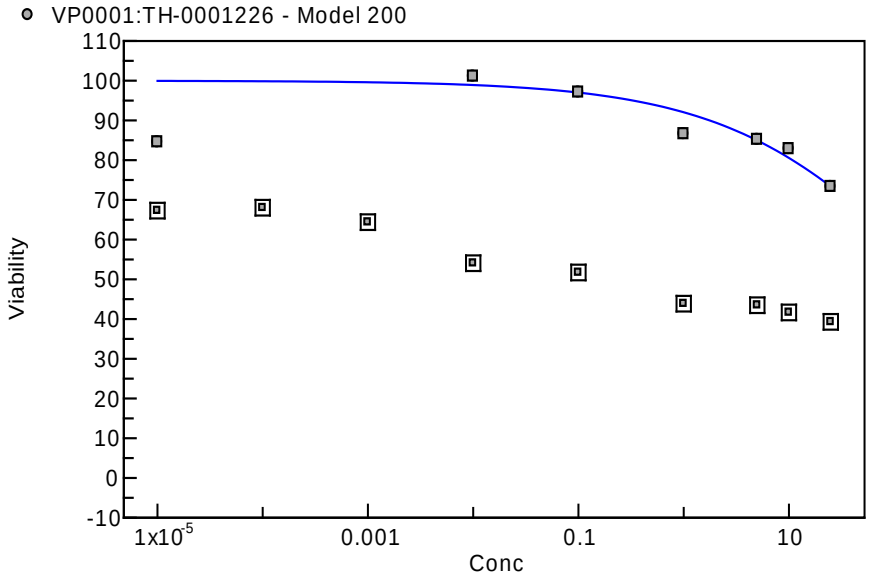

Drug response curve at 24hrs

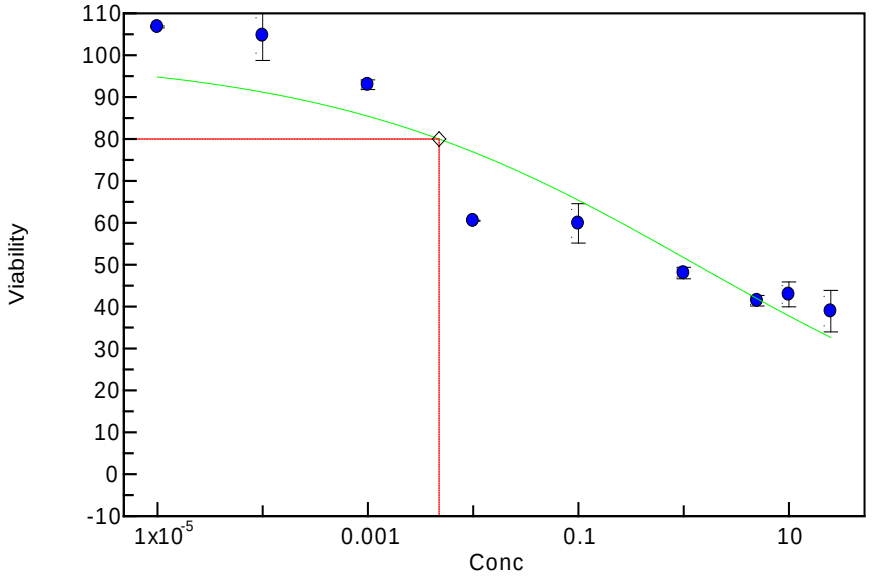

Drug response curve at 48hrs

Nature Biotechnology doi:10.1038/nbt.3052